VERIFICATION AND LOCAL CALIBRATION/VALIDATION OF THE MEPDG PERFORMANCE MODELS FOR USE IN GEORGIA

Validation of the MEPDG Transfer Functions Using the LTPP Test Sections in Georgia

Task 2 Interim Report

Submitted to:

Georgia Department of Transportation

Office of Research and Office of Materials Testing
15 Kennedy Drive
Forest Park, Georgia 30297

Submitted by:

Harold L. Von Quintus, P.E.
Michael I. Darter, P.E.
Jagannath Mallela
Biplab B. Bhattacharya, P.E.
Suri Sadasivam
Applied Research Associates, Inc.
100 Trade Center Drive, Suite 200
Champaign, IL, 61820

July 16, 2013

Notice

Quality Assurance Statement

TECHNICAL DOCUMENTATION PAGE

1. Report No. FHWA/GA-014-11-17	2. Government Accession No.	3. Recipient's Catalog No.
4. Title and Subtitle Validation of the MEPDG Transfer Functions Using the LTPP Test Sections in Georgia		5. Report Date July 16, 2013 6. Performing Organization Code
7. Author(s) Mr. Harold L. Von Quintus, P.E., Mr. Jagannath Mallela, Dr. Suri Sadasivam, P.E., and Dr. Michael I. Darter, P.E.		8. Performing Organization Report No.
9. Performing Organization Name and Address Applied Research Associates, Inc. 100 Trade Centre Blvd., Suite #200 Champaign, Illinois 61820		10. Work Unit No. (TRAIS) 11. Contract or Grant No. TOOMRPRO130020
12. Sponsoring Agency Name and Address Georgia Department of Transportation One Georgia Center, 19th Floor 600 West Peachtree Street, NW Atlanta, Georgia 30308		13. Type of Report and Period Covered Task 2 Interim Report – Task Order #1 14. Sponsoring Agency Code

15. Supplementary Notes
The Contracting Officer's Technical Representative (COTR) was Mr. Steve Pahno, P.E.

16. Abstract
The Georgia Department of Transportation (GDOT) is transitioning from empirical design procedures to the MEPDG procedure for designing new and rehabilitated highway pavements. GDOT currently uses the 1972 AASHTO Interim Guide for Design of Pavement Structures as the standard pavement design procedure. As a part of the implementation process, GDOT has undertaken a project to verify the MEPDG global distress models and locally calibrate these models for local field conditions of Georgia, if determined to be necessary by the verification process, using the Long-Term Pavement Performance (LTPP) and non-LTPP sections in Georgia.

One objective of this project is to verify or confirm that the MEPDG transfer functions and global calibration factors derived from NCHRP project 1-40D reasonably predict distresses and smoothness for the LTPP sites located in Georgia using proper design inputs. This report includes a comparison of the predicted and measured distress and International Roughness Index (IRI) values measured over time and between different projects, pavement design features, and/or site condition features. The confirmation process follows the procedure presented in the AASHTO MEPDG Local Calibration Guide (AASHTO, 2010). Specifically, this report documents use of the LTPP sites in Georgia to determine the bias and accuracy of the MEPDG transfer functions in predicting the distress and performance of those LTPP test sections.

In summary, the number of Georgia LTPP sites and levels of distress exhibited on the test sections are considered inadequate for the validation or confirmation process of the global calibration coefficients from a statistical perspective. More importantly, bias between the measured and predicted distress for some of the transfer functions of both flexible and rigid pavements were found. Thus, it is recommended that GDOT proceed with the next phase of the study and select projects to fill in the many key gaps so that the calibration process can be used to adjust the calibration coefficients for each distress.

17. Key Words Mechanistic-Empirical Pavement Design Guide, ME Design, Transfer Functions, Fatigue Cracking, Rutting, Thermal Cracking, Faulting, Mid-Slab Cracking, IRI.	18. Distribution Statement No restrictions.		
19. Security Classification of this report: Unclassified	20. Security Classification (of this page): Unclassified	21. No. of Pages 129	22. Price

Form DOT F 1700.7 (8-72) Reproduction of completed page authorized

SI* (MODERN METRIC) CONVERSION FACTORS

APPROXIMATE CONVERSIONS TO SI UNITS

Symbol	When You Know	Multiply By	To Find	Symbol
		LENGTH		
in	inches	25.4	millimeters	mm
ft	feet	0.305	meters	m
yd	yards	0.914	meters	m
mi	miles	1.61	kilometers	km
		AREA		
in^2	square inches	645.2	square millimeters	mm^2
ft^2	square feet	0.093	square meters	m^2
yd^2	square yard	0.836	square meters	m^2
ac	acres	0.405	hectares	ha
mi^2	square miles	2.59	square kilometers	km^2
		VOLUME		
fl oz	fluid ounces	29.57	milliliters	mL
gal	gallons	3.785	liters	L
ft^3	cubic feet	0.028	cubic meters	m^3
yd^3	cubic yards	0.765	cubic meters	m^3
		NOTE: volumes greater than 1000 L shall be shown in m^3		
		MASS		
oz	ounces	28.35	grams	g
lb	pounds	0.454	kilograms	kg
T	short tons (2000 lb)	0.907	megagrams (or "metric ton")	Mg (or "t")
		TEMPERATURE (exact degrees)		
^oF	Fahrenheit	5 (F-32)/9 or (F-32)/1.8	Celsius	^oC
		ILLUMINATION		
fc	foot-candles	10.76	lux	lx
fl	foot-Lamberts	3.426	candela/m^2	cd/m^2
		FORCE and PRESSURE or STRESS		
lbf	poundforce	4.45	newtons	N
lbf/in^2	poundforce per square inch	6.89	kilopascals	kPa

APPROXIMATE CONVERSIONS FROM SI UNITS

Symbol	When You Know	Multiply By	To Find	Symbol
		LENGTH		
mm	millimeters	0.039	inches	in
m	meters	3.28	feet	ft
m	meters	1.09	yards	yd
km	kilometers	0.621	miles	mi
		AREA		
mm^2	square millimeters	0.0016	square inches	in^2
m^2	square meters	10.764	square feet	ft^2
m^2	square meters	1.195	square yards	yd^2
ha	hectares	2.47	acres	ac
km^2	square kilometers	0.386	square miles	mi^2
		VOLUME		
mL	milliliters	0.034	fluid ounces	fl oz
L	liters	0.264	gallons	gal
m^3	cubic meters	35.314	cubic feet	ft^3
m^3	cubic meters	1.307	cubic yards	yd^3
		MASS		
g	grams	0.035	ounces	oz
kg	kilograms	2.202	pounds	lb
Mg (or "t")	megagrams (or "metric ton")	1.103	short tons (2000 lb)	T
		TEMPERATURE (exact degrees)		
^oC	Celsius	1.8C+32	Fahrenheit	^oF
		ILLUMINATION		
lx	lux	0.0929	foot-candles	fc
cd/m^2	candela/m^2	0.2919	foot-Lamberts	fl
		FORCE and PRESSURE or STRESS		
N	newtons	0.225	poundforce	lbf
kPa	kilopascals	0.145	poundforce per square inch	lbf/in^2

*SI is the symbol for the International System of Units. Appropriate rounding should be made to comply with Section 4 of ASTM E380. (Revised March 2003)

Table of Contents

Table of Contents - continued

List of Figures

List of Figures - continued

List of Tables

This page left blank intentionally.

Validation of the Mechanistic-Empirical Pavement Design Guide in Georgia Using the LTPP Test Sections

I. INTRODUCTION

1.1 Background

Many highway agencies, including the Georgia Department of Transportation (GDOT), are transitioning from empirical design procedures to the new Mechanistic-Empirical Pavement Design Guide (MEDPG) procedure for designing new and rehabilitated pavements. The new design procedure is a part of the American Association of State Highway and Transportation Officials (AASHTO) software *Pavement M-E Design* and uses mechanistic-empirical (M-E) principles. This procedure is a significant departure from the existing empirical procedures (such as the 1993 AASHTO procedure). GDOT currently uses the 1972 AASHTO Interim Guide for Design of Pavement Structures as its standard pavement design procedure.

To facilitate a seamless transition from the current pavement design methodology to a M-E approach, it is important that user agencies begin to assess their needs in terms of the MEPDG design inputs (traffic, materials and environment). Equally important is the validation of the distress prediction models with local data. Accordingly, the overall objective of the local implementation process is to validate and re-calibrate, if necessary, and streamline a design process and performance/distress prediction models that will enable GDOT to use the MEPDG for new and rehabilitation pavement design.

The MEPDG distress transfer functions and prediction methodology were calibrated using data from the Long Term Pavement Performance (LTPP) program under National Cooperative Highway Research Program (NCHRP) projects 1-37A and 1-40D. The global calibration effort, however, cannot be expected to consider all potential factors that can occur throughout all agencies, materials, design strategies, and climates found in North America. For example, factors such as maintenance strategies, construction specifications, aggregate and binder type, mixture design procedures, and material specifications can result in performance differences – all other factors being equal. In fact, small differences in some of the above factors can cause large differences in performance.

It is essential to determine the proper inputs and validate the prediction models to GDOT's operational policies, material and construction specifications, truck traffic, and climate. Thus, GDOT initiated an implementation study to ensure that all of the input procedures are acceptable and practical, and the distress and smoothness prediction models or transfer functions accurately represent the performance of GDOT roadways. A transfer function is defined as a mathematical relationship that transfers computed pavement responses (stresses, strains, and/or deflections) into what is observed or measured on the pavement surface. The proposed work plan to implement the MEPDG into GDOT's procedures consists of seven tasks:

- Task 1 Literature Search/ Synthesis and Two Draft Verification Work Plans
- Task 2 Verification using LTPP Test Sections located in Georgia
- Task 3 Non-LTPP Verification Sites
- Task 4 Calibration of the Distress Transfer Functions
- Task 5 Validation of the Distress Transfer Functions
- Task 6 Design Manual
- Task 7 Final Report

This report addresses Task 2 using the LTPP test sections located in Georgia to verify or confirm the global calibration parameters of the distress transfer function included in the MEPDG software and Manual of Practice (AASHTO, 2008).

1.2 Study Objective

The objective of task 2 is to verify or confirm that the MEPDG transfer functions and global calibration factors reasonably predict distresses and smoothness for the LTPP sites located in Georgia using proper design inputs.

Task 2 includes a comparison of the predicted and measured distress and International Roughness Index (IRI) values measured over time and between different projects, pavement design features, and/or site condition features. The confirmation process follows the procedure presented in the AASHTO MEPDG Local Calibration Guide (AASHTO, 2010). This report documents use of the LTPP sites in Georgia to determine the bias and accuracy of the MEPDG transfer functions in predicting the distress and performance of those LTPP test sections.

1.3 Study Hypothesis

As stated above, it is impossible to account for all factors in developing a national or global distress/performance simulation model. All models have errors because of simplifying assumptions, so it is good practice to evaluate the applicability of any conceptual and/or statistical model on a limited basis prior to full-scale use. Thus, the LTPP test sections were selected to determine if there are significant differences between the measured and predicted distresses using the global calibration factors of the MEPDG conceptual model. The global calibration factors for each transfer function are included in Section 5 of the MEPDG Manual of Practice (AASHTO, 2008).

The following experimental hypothesis was used to evaluate the accuracy and applicability of the MEPDG transfer functions in predicting pavement distresses and smoothness for the materials, climate, and operational policies used in Georgia. The null hypothesis is:

> <u>Null Hypothesis – Confirmation of Global Calibration Factors:</u> There is no significant error and no bias (i.e., reasonable correlation and accuracy and no overall over or under prediction) between the predicted and measured values for each performance indicator for flexible and rigid pavements and overlays for roadways within GDOT's jurisdiction.

1.4 Definition of Terms

The following provides a definition for some of the terms that are used within this report and study.

- **Accuracy** – The exactness of a prediction to the observed or "actual" value. The concept of accuracy encompasses both precision and bias.

- **Bias** – An effect that deprives predictions of simulating "real world" observations by systematically distorting it, as distinct from a random error that may distort on any one occasion but balances out on the average. A prediction model that is "biased" is significantly over or under predicting observed distress or roughness (as measured by the IRI).

- **Precision** – The ability of a model to give repeated estimates that correlate strongly with the observed values. They may be consistently higher or lower but they correlate strongly with observed values.

- **Residual Error** – The difference between the observed or measured and predicted distress and IRI values (e.g., measured minus predicted values). The residuals explain how well the model predicts the observed distress and IRI.

- **Standard Error of the Estimate (s_e)** – The standard deviation of the residual errors for the pavement sections included in the validation and/or calibration data set for each prediction model. The standard error is usually obtained by taking the square root of the variance divided by the number of observations of the statistic.

- **Verification** – Verification of a model examines whether the operational model correctly represents the conceptual or statistical model that has been formulated. Verification can be done using both measured and predicted data, and if biased, then calibration was performed to remove bias. Verification can also be accomplished by entering typical materials, structural, environmental, and traffic data into the distress and performance models, and then determining through parameter studies whether the program operates rationally and provides outputs that meet the criterion of engineering reasonableness. If this criterion is not met, the computer code maybe erroneous or the conceptual model may be unsatisfactory. In either case, these problems must be remedied before the model enhancement process or use continues. No field data are needed in either of the verification approaches described. Verification is primarily intended to confirm the internal consistency or reasonableness of the model. The issue of how well the model predicts reality is addressed during calibration and validation.

- **Calibration –** A systematic process to eliminate any bias and minimize the residual error between observed or measured results from the real world (e.g., the measured mean rut depth in a pavement section) and predicted results from the model (e.g., predicted mean rut depth from a permanent deformation model). This is accomplished by modifying empirical calibration parameters or transfer functions in the model to minimize the differences between the predicted and observed results. These calibration parameters are necessary to compensate for model simplification and limitations in simulating actual pavement and material behavior.

- **Validation** – A systematic process that reexamines the recalibrated model to determine if the desired accuracy exists between the calibrated model and an independent set of observed data. The calibrated model requires inputs such as the pavement structure, traffic loading, and environmental data. The simulation model must predict results (e.g., rutting, fatigue cracking) that are reasonably close to those observed or measured in the field. Separate and independent data sets should be used for calibration and validation (typically 10 percent of observations). Assuming that the calibrated models are successfully validated, the models can be recalibrated using the combined data sets (calibration and validation) without the need for additional validation to provide a better estimate of the residual error.

The terms validation and verification get used interchangeably in various documents. The title of Task 2 uses verification, but the process is to validate or confirm the applicability of the global calibration factors to GDOT roadways and management practices.

1.5 Scope of Work

The scope of work for the Task 2 validation or confirmation of the global calibration factors consisted of the following activities:

1. Identify the LTPP test sections located in Georgia and compare the site condition features between each of the sties to determine the representative parameters of each site to those encountered in Georgia and determine if the site and design features are representative of the materials and conditions across Georgia. The LTPP test sections were selected because they contain high quality input data.

2. Extract the distress and performance data from the LTPP database. The median and range of the distress values were determined for comparison to typical design criteria. For validation and calibration purposes, it is important the measured distresses equal and/or slightly exceed the design criteria.

3. Extract the material properties and other information from the LTPP database to establish the inputs to the MEPDG software for each site. Most of the MEPDG inputs were available in the LTPP database, and extracted for use in the determining the inputs. MEPDG global defaults and/or Georgia local default values were used for the inputs for which data were unavailable. Sources of data used in model confirmation are presented in Table 1. Some of the inputs were backcasted for the cases when the input value at the time of construction was unavailable in the LTPP database (for example; initial IRI, air void at construction, initial truck traffic volume, etc.).

4. Compare the material properties and other inputs to the values and information from other studies conducted in Georgia to facilitate use of the MEPDG software. This data and information is used to estimate the inputs to the procedure.

5. Execute the MEPDG software to predict the distress and performance of each LTPP test section.

6. Compare the predicted and measured distresses to determine the bias and standard error of the transfer functions for GDOT conditions, materials, and operational policies.

7. Determine if the transfer functions need to be recalibrated to GDOT conditions and materials.

8. Based on the results from activity #6, identify key site condition and design features that exhibit significant differences between the predicted and measured distress values. These differences will establish the extent of the sampling matrix for finding sections that are needed to include the range of typical materials, design strategies, and site features found and practiced in Georgia.

Table 1—Predominant Source of Data Used for Transfer Function Verification in Georgia

Input Group		Input Parameter	Validation Input Level Used	Data Source
Truck Traffic		Initial Average Annual Daily Truck Traffic	Level 1	LTPP Database (backcast value)
		Axle load distributions (single, tandem, tridem)	Level 1	LTPP Database
		Truck volume distribution	Level 1	LTPP Database
		Lane & directional truck distributions	Level 1	LTPP Database
		Tire pressure	Level 3	MEPDG defaults
		Axle configuration, tire spacing	Level 3	MEPDG defaults
		Truck wander	Level 3	MEPDG defaults
Climate		Temperature, wind speed, cloud cover, precipitation, relative humidity	Level 1	Weather Stations in MEPDG
Material Properties	Unbound Layers & Subgrade	Resilient modulus – subgrade	Level 1	LTPP; Lab & Backcalculated Values
		Resilient modulus – unbound aggregate base/subbase	Level 1	LTPP; Lab & Backcalculated Values
		Classification & volumetric properties	Level 1	LTPP Database
		Moisture-density relationships	Level 1	LTPP Database
		Soil-water characteristic relationships	Level 3	MEPDG defaults
		Saturated hydraulic conductivity	Level 3	MEPDG defaults
	HMA	HMA dynamic modulus	Level 3	MEPDG E* Equation
		HMA creep compliance & indirect Tensile strength	Levels 3	MEPDG defaults
		Volumetric properties	Level 1	LTPP Database
		HMA coefficient of thermal expansion	Level 3	MEPDG defaults
	PCC	PCC elastic modulus	Level 1 & 2	LTPP Database
		PCC flexural strength	Level 1 & 2	LTPP Database
		PCC coefficient of thermal expansion	Level 1 &2	LTPP Database
All Materials		Unit weight	Level 1	LTPP Database
		Poisson's ratio	Level 3	MEPDG defaults
		Other thermal properties; conductivity, heat capacity, surface absorptivity	Level 3	MEPDG defaults
Surface Condition (Distress Measurements)		Initial IRI	Level 1	LTPP Database (backcast value)
		Average rut depth and fatigue cracking	Level 1	LTPP Database

II. GEORGIA LTPP TEST SECTIONS

Calibration is required in any M-E based design procedure to establish the relationship between computed structural responses, accumulated damage, and pavement distress measured in the field. The distress mechanisms are far more complex than can be practically modeled. Therefore, the use of an empirical relationship between damage and field observed distress (defined as transfer functions) is necessary to obtain reliable performance predictions.

The distress and IRI models were calibrated using a wide range of pavement sections located across North America. Global models, however, require confirmation at the local level to ensure their accuracy and biasedness. A verification or confirmation study was planned by GDOT to determine if significant differences exist between the global calibration factors and those applicable to Georgia conditions and materials for HMA and PCC pavements and overlays. The confirmation study was based on the LTPP test sections located in Georgia. If significant differences are found between the predicted and measured performance indicators, then it will be necessary to determine what factors are causing these differences so adjustments can be made to the global calibration factors. In addition, even if the Georgia LTPP sites show no bias and reasonable accuracy, the sections may not include some key material types and design features (e.g. Superpave mixes, PG binders, dowel bars) that GDOT would like to use in current and future designs. This may then make it desirable to include other Georgia non LTPP sections that do include these materials and design features.

2.1 LTPP Sites Located in Georgia

There are 10 flexible (conventional and full-depth sections) pavement, 4 semi-rigid pavement, 6 jointed plain concrete pavement (JPCP), and 2 continuously reinforced concrete pavement (CRCP) LTPP sites in Georgia. The number of the LTPP sections with different structures used in the confirmation process is presented in Tables 2 and 3 for the flexible-semi-rigid and rigid pavements, respectively. Figure 1 shows the geographic distribution of these sites in Georgia, while Table 4 provides the GPS coordinates and other location information for these sites.

Appendix A includes a listing of the material type and layer thickness for the LTPP test sections located in Georgia. These test sections are categorized by the general pavement groups identified in Tables 2 and 3, as defined by the MEPDG Manual of Practice. These pavement categories and the number of test sections within each category become important in setting up the sampling matrix for validating the distress transfer functions. The number of individual projects for each pavement type is considered below the minimum required for confirming the accuracy of the transfer functions in accordance with the MEPDG Local Calibration Guide (AASHTO, 2010).

2.2 Climate and Weather Stations

The MEPDG requires the location of a project described in terms of longitude, latitude, and elevation in order to develop project specific climate data. The GPS coordinates are included in Table 4. The climate specific data for each project was generated using the closest weather station. The closest weather station to each LTPP project site is included in Table 5. Typically, each weather station had 96 to 116 months of climate data.

Two other site condition features are required by the MEPDG: (1) the water table depth, and (2) the depth to a rigid layer. The 20-foot boring drilled in the shoulder area at each LTPP site was reviewed to estimate the depth to a rigid layer, a saturated layer, or free water. Wet soil strata or water was observed during the drilling process and recorded on the boring log for some of the sites. Similarly, refusal or presence of weathered rock was recorded on the boring log for some of the sites. The depth to water table and/or a hard or rigid layer are included in Table 5. If water or wet soils or refusal was not recorded on the boring log, the following assumptions were made in setting up the pavement structure in the MEPDG.

- If free water or wet soils were not recorded on the boring log, the depth to the water table was assumed to be 20-feet.
- If a hard pan layer was not encountered or refusal was not recorded on the boring log, the thickness of the subgrade soil was assumed to be infinite.

Table 2—Number of Test Sections: Flexible or Semi-Rigid Pavements, New Construction and Rehabilitation

<table>
<tr><th colspan="3" rowspan="3">Pavement Type</th><th colspan="4">Number of Test Sections</th></tr>
<tr><th colspan="2">With Full Time Series Data</th><th colspan="2">With Only One or Two Observations</th></tr>
<tr><th>Site ID</th><th>Number</th><th>Site ID</th><th>Number</th></tr>
<tr><td rowspan="3">New Construction</td><td rowspan="2">Flexible Pavement</td><td>Conventional</td><td>1001, 1004, 1005, 4111</td><td>4</td><td></td><td>0</td></tr>
<tr><td>Full Depth or Deep Strength</td><td>1031, 4112, 4113, 4119</td><td>4</td><td>SPS-5 Sections</td><td>15</td></tr>
<tr><td colspan="2">Semi-Rigid Pavement</td><td>4092, 4093, 4096, 4420</td><td>4</td><td></td><td>0</td></tr>
<tr><td rowspan="3">Rehabilitation</td><td colspan="2" rowspan="2">HMA Overlay of Flexible Pavement</td><td>SPS-5 Sections</td><td>15</td><td></td><td>0</td></tr>
<tr><td>1031, 4112; 4113</td><td>3</td><td></td><td>0</td></tr>
<tr><td colspan="2">HMA Overlay of Semi-Rigid Pavement</td><td>4096, 4420</td><td>2</td><td></td><td>0</td></tr>
<tr><td colspan="3">TOTAL</td><td colspan="2">32</td><td colspan="2">15</td></tr>
</table>

Table 3—Number of Test Sections: Rigid Pavements, New Construction and Rehabilitation

Pavement Type			Number of Test Sections With Time Series Data				
			Site ID	Number	Dowel Diameter (in.)	Joint Spacing (feet)	PCC-Base Contact Friction (months)
New Construction	Jointed Plain Concrete Pavement	Granular	3007	2	1.125	20	Full, entire design life
			3019		1.125	20	Full, entire design life
		ATB	3011	3	No dowels	Random, 18.5 ft to 22.5 ft	Full, entire design life
			3015		1.25	20	Full, entire design life
			3016		1.25	20	Full, entire design life
		CTB	3017	3	No dowels	Random, 18.5 ft to 22.5 ft	Partial, 120 months
			3018		No dowels	21	Partial, 120 months
			3020		1.125	20	Partial, 120 months
	Continuously Reinforced Concrete Pavement		5023	1	None	None	None
Rehabilitation	CRCP	HMA Overlay	None	0	None	None	None
	JPCP	HMA Overlay	7028	1	1.25	15	Full, entire design life
		CRCP Overlay	4118	1	None	None	None
TOTAL			11				

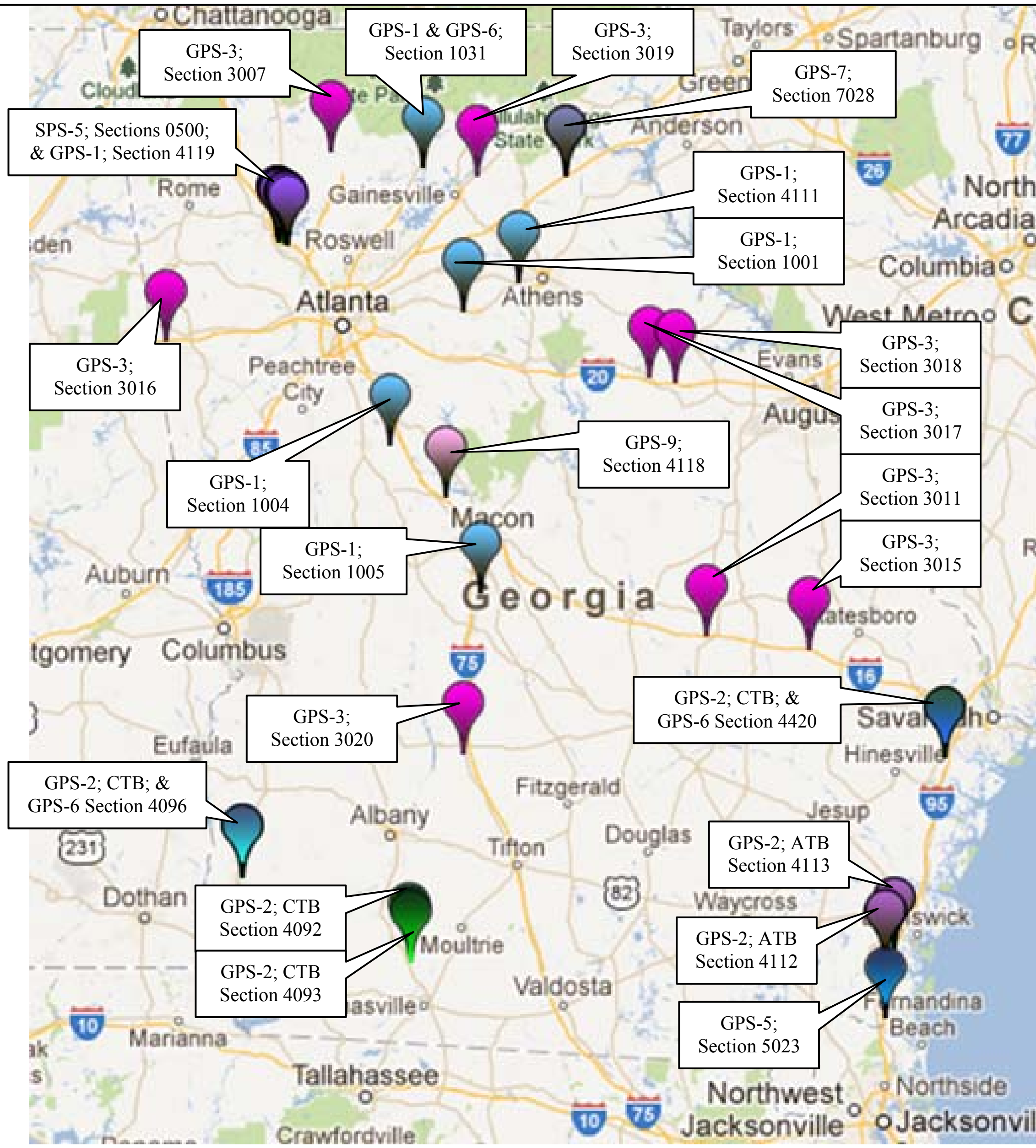

Legend:

- GPS-1; flexible pavement, AC over aggregate base
- GPS-2; flexible pavement; AC over ATB or full-depth
- GPS-2; flexible pavement; AC over CTB or soil cement, semi-rigid

Legend:

- GPS-6; AC overlay of flexible pavement
- SPS-5; AC overlay of flexible pavement
- GPS-3; rigid pavement, JPCP
- GPS-5; rigid pavement, CRCP
- GPS-7; AC overlay of rigid pavement
- GPS-9; PCC overlay of rigid pavement

Figure 1—Location of LTPP Sites in Georgia

Table 4—LTPP Sections Used for Confirming the MEPDG Transfer Functions in Georgia

LTPP ID No.	Pavement Type	County	Route	Elevation, ft	Longitude, deg	Latitude, deg	Constr. Year
0502 to 0566	HMA Overlay; Deep Strength	Bartow	I-401	815	-84.7265	34.1005	June 1993
1001	Flexible	Walton	SR 10	905	-83.7900	33.8075	Sept 1986
1004	Flexible	Spalding	SR 16	760	-84.1688	33.2381	June 1983
1005	Flexible	Houston	SR 247	452	-83.6999	32.6154	June 1986
1031	Flexible	Dawson	SR 247C	120	-84.005	34.4036	June 1981
1031	HMA Overlay; Flexible	Dawson	SR 247C	120	-84.005	34.4036	June 1997
3007	JPCP	Pickens	SR 5	1422	-84.4634	34.4733	Dec 1981
3011	JPCP	Treutlen	I-16	248	-82.567	32.4285	Dec 1975
3015	JPCP	Candler	I-16	178	-82.0424	32.3734	Sept 1978
3016	JPCP	Haralson	I-20	1218	-85.2932	33.6814	Dec 1977
3017	JPCP	Taliaferro	I-20	583	-82.8635	33.5185	Dec 1973
3017	JPCP	Taliaferro	I-20	583	-82.8635	33.5185	May 2001
3018	JPCP	Warren	I-20	550	-82.7273	33.5034	July 1973
3019	JPCP	Hall	US-23	1042	-83.7264	34.3731	Dec 1981
3020	JPCP	Crisp	SR 300	307	-83.7887	31.9234	Sept 1985
3020	JPCP	Crisp	SR 300	307	-83.7887	31.9234	June 2006
4092	Semi-Rigid	Thomas	SR 300	278	-84.0583	31.0225	June 1986
4093	Semi-Rigid	Thomas	SR 300	350	-84.071	31.0529	June 1986
4096	Semi-Rigid	Early	SR 62C	270	-84.9171	31.3944	June 1985
4096	HMA Overlay; Semi-Rigid	Early	SR 62C	270	-84.9171	31.3944	Apr 2001
4111	Flexible	Oconee	US-78	735	-83.5134	33.9224	Nov 1980
4112	Full Depth	Camden	I-95	13	-81.6565	31.0261	June 1987
4112	HMA Overlay; Full Depth	Camden	I-95	13	-81.6565	31.0261	Sept 1998
4113	Full Depth	Camden	I-95	13	-81.6143	31.0818	June 1987
4113	HMA Overlay; Full Depth	Camden	I-95	13	-81.6143	31.0818	Sept 1998
4118	CRCP Overlay of JPCP	Monroe	I-401	750	-83.8845	33.0149	June 1963
4119	HMA with ATB	Bartow	I-401	815	-84.706	34.0886	June 1978
4420	Semi-Rigid	Bryan	US-17	17	-81.3633	31.9042	Apr 1984
4420	HMA Overlay; Semi-Rigid	Bryan	US-17	17	-81.3633	31.9042	Oct 1992
5023	CRCP	Camden	I-95	25	-81.6561	30.7787	June 1974
7028	HMA Overlay; JPCP	Franklin	I-85	850	-83.2783	34.3684	Nov 1986
7028	2nd HMA Overlay; JPCP	Franklin	I-85	850	-83.2783	34.3684	July 1998

Table 5—Weather Station and other Climate Data for the Georgia LTPP Sites

LTPP ID No.	Weather Station	Water Table		Hard Layer	
		Depth, ft.	Description	Depth, ft.	Description
0500	Cartersville, GA	---	None except as noted	---	None except as noted
0502		---		8.5	Weathered Rock
0504, 0505, 0506, 0507		---		5.5	
0563		---		3	
0565		---		5	
0503		8.5	Seasonal	19.5	Refusal; Hard Layer
4119	Cartersville, GA	15	High Moisture; Seasonal	4	Weathered Rock Pieces
1001	Athens, GA	12	Seasonal; Gravel Seam	---	
1004	Atlanta, GA	12	Water Table	---	
1005	Macon, GA	16	Seasonal	---	
1031	Gainesville, GA	---		---	
3007	Cartersville, GA	12	Moist; Seasonal	---	
3011	Alma, GA	9	Water Table	---	
3015	Savannah, GA	10	Water Table	---	
3016	Anniston, AL	---		5	Weathered Rock
3017	Athens, GA	---		12	Weak Rock
3018	Athens, GA	---		---	
3019	Gainesville, GA	---		---	
3020	Albany, GA	12	Wet Soil; Seasonal	---	
4092	Albany, GA	15	Very Wet Soil; Seasonal	---	
4093	Albany, GA	---		13	Refusal
4096	Dothan, AL	---		---	
4111	Athens, GA	---		---	
4112	Brunswick, GA	5	Water Table	---	
4113	Brunswick, GA	10	Water Table	---	
4118	Macon, GA	---		---	
4420	Savannah, GA	10	Water Table	---	
5023	Jacksonville, FL	4	Water Table	---	
7028	Athens, GA	15	Wet Soil; Seasonal	---	

2.3 Truck Traffic Inputs

Many of the truck traffic inputs for the Georgia LTPP sections are at level 1 (see Table 1) since volume and portable WIM data were available for all LTPP sites in Georgia. The Georgia WIM study, however, recommended the portable WIM data not be used because of potential errors in the data, except for a couple of sites. The truck axle weight data were processed under the WIM study, and a detailed description of all traffic data for the LTPP WIM sites in Georgia is presented within the WIM study documents. Table 6 summarizes the functional classes and MEPDG truck traffic classification (TTC) groups for each site. The subsections that follow discuss the different truck traffic inputs and the values used for validating or confirming the MEPDG global calibration coefficients (see Table 1).

Table 6—Basic Truck Traffic Information for the Georgia LTPP Sites

LTPP ID No.	County	Route	Functional Class	MEPDG TTC Group	Initial AADTT (LTPP Lane)	Growth Function	Growth Rate
0502 to 0566	Bartow	I-401	Rural Interstate	8	5330	None	---
1001	Walton	SR 10	Rural Principal Arterial	12	690	None	---
1004	Spalding	SR 16	Rural Minor Arterial	8	140	Linear	14.8
1005	Houston	SR 247	Rural Major Collector	14	400	Linear	3.6
1031 New	Dawson	SR 247C	Rural Principal Arterial	12	125	Compound	6.0
1031 Rehab	Dawson	SR 247C	Rural Principal Arterial	12	275	Compound	6.0
3007	Pickens	SR 5	Rural Principal Arterial	12	190	Linear	8.0
3011	Treutlen	I-16	Rural Interstate	7	590	Linear	4.7
3015	Candler	I-16	Rural Interstate	11	500	Linear	7.0
3016	Haralson	I-20	Rural Interstate	1	1230	Compound	4.2
3017	Taliaferro	I-20	Rural Interstate	6	610	Compound	5.4
3017	Taliaferro	I-20	Rural Interstate	6	2730	Compound	5.4
3018	Warren	I-20	Rural Interstate	9	950	Compound	4.3
3019	Hall	US-23	Rural Principal Arterial	14	270	Compound	6.5
3020 New	Crisp	SR 300	Rural Principal Arterial	4	200	Linear	7.5
3020 Rehab	Crisp	SR 300	Rural Principal Arterial	4	600	Linear	7.5
4092	Thomas	SR 300	Rural Principal Arterial	14	300	Compound	5.5
4093	Thomas	SR 300	Rural Principal Arterial	14	300	Compound	5.5
4096	Early	SR 62C	Rural Minor Collector	8	50	Compound	7.0
4096	Early	SR 62C	Rural Minor Collector	8	180	Compound	7.0
4111	Oconee	US-78	Rural Minor Collector	17	500	None	---
4112	Camden	I-95	Rural Interstate	8	2400	Linear	2.1
4112	Camden	I-95	Rural Interstate	8	3600	Linear	2.1
4113	Camden	I-95	Rural Interstate	11	1300	Compound	5.0
4113	Camden	I-95	Rural Interstate	11	4100	Compound	5.0
4118	Monroe	I-401	Rural Interstate	5	4500	Linear	0.7
4119	Bartow	I-401	Rural Interstate	8	5330	None	---

Table 6—Basic Truck Traffic Information for the Georgia LTPP Sites (Continued)

LTPP ID No.	County	Route	Functional Class	MEPDG TTC Group	Initial AADTT (LTPP Lane)	Growth Function	Growth Rate
4420	Bryan	US-17	Rural Principal Arterial	11	140	Compound	4.0
4420	Bryan	US-17	Rural Principal Arterial	11	200	Compound	4.0
5023	Camden	I-95	Rural Interstate	12	1100	Compound	5.7
7028	Franklin	I-85	Rural Interstate	8	1900	Linear	7.2
7028	Franklin	I-85	Rural Interstate	8	3536	Linear	7.2

2.3.1 Initial AADTT and Truck Growth Factors

The two-way average annual daily truck traffic (AADTT) is an important input parameter to the MEPDG, as well as the truck traffic growth over time. Truck traffic volume data are available for all of the sites, but for some of the sites, AADTT is only available many years after construction. For the cases where AADTT was unavailable at construction, the starting value was backcasted to the year of construction. The AADTT values included in the LTPP database were also used to estimate the growth rate and function of truck traffic for each site.

Figures 2 and 3 include examples of the backcasting method to determine the initial AADTT and growth throughout the monitoring period for four of the Georgia sites. These four sites were selected to illustrate the process used for varying discrepancies between the historical and monitoring data included in the LTPP database. Appendix B includes graphical presentations of the historical and monitored data sets for each of the LTPP test sections. The following summarizes the assumptions applied to the historical and monitoring data related to each of these sites, while Table 6 lists the initial AADTT, growth rate, and function for each LTPP site in Georgia.

- LTPP Site 13-1001 (Figure 2) – There is a significant discrepancy between the historical and monitored data sets for this site. For the LTPP sites that exhibit this type of discrepancy between the historical and monitored data sets, the monitored data was used to estimate the initial AADTT, and to determine the growth rate and function.
- LTPP Site 13-1004 (Figure 2) – The historical and monitored data sets show similar increases in truck traffic or AADTT over time. For this case, the historical data set exhibits slightly lower AADTT values than the monitored data set. For the LTPP sites that exhibit this type of trend between the historical and monitored data sets, both sets of data were used to estimate the growth rate and function, but only the monitored data set was used to backcast the initial AADTT.
- LTPP Site 13-3018 (Figure 3) – The historical and monitored data set have a lot of dispersion in the AADTT value reported over time, but exhibit similar trends and growth in the AADTT. For other sites that exhibit this type of trend between the historical and monitored data sets, both sets of data were used to estimate the growth rate and function and backcast the initial AADTT.

- LTPP Site 13-4118 (Figure 3) – The historical data set has a value much higher than the monitored data set. For cases where the historical data sets were slightly higher or lower than the monitored data set and only contained a few data points, the monitored data was used to estimate the growth rate and function and backcast the initial AADTT.

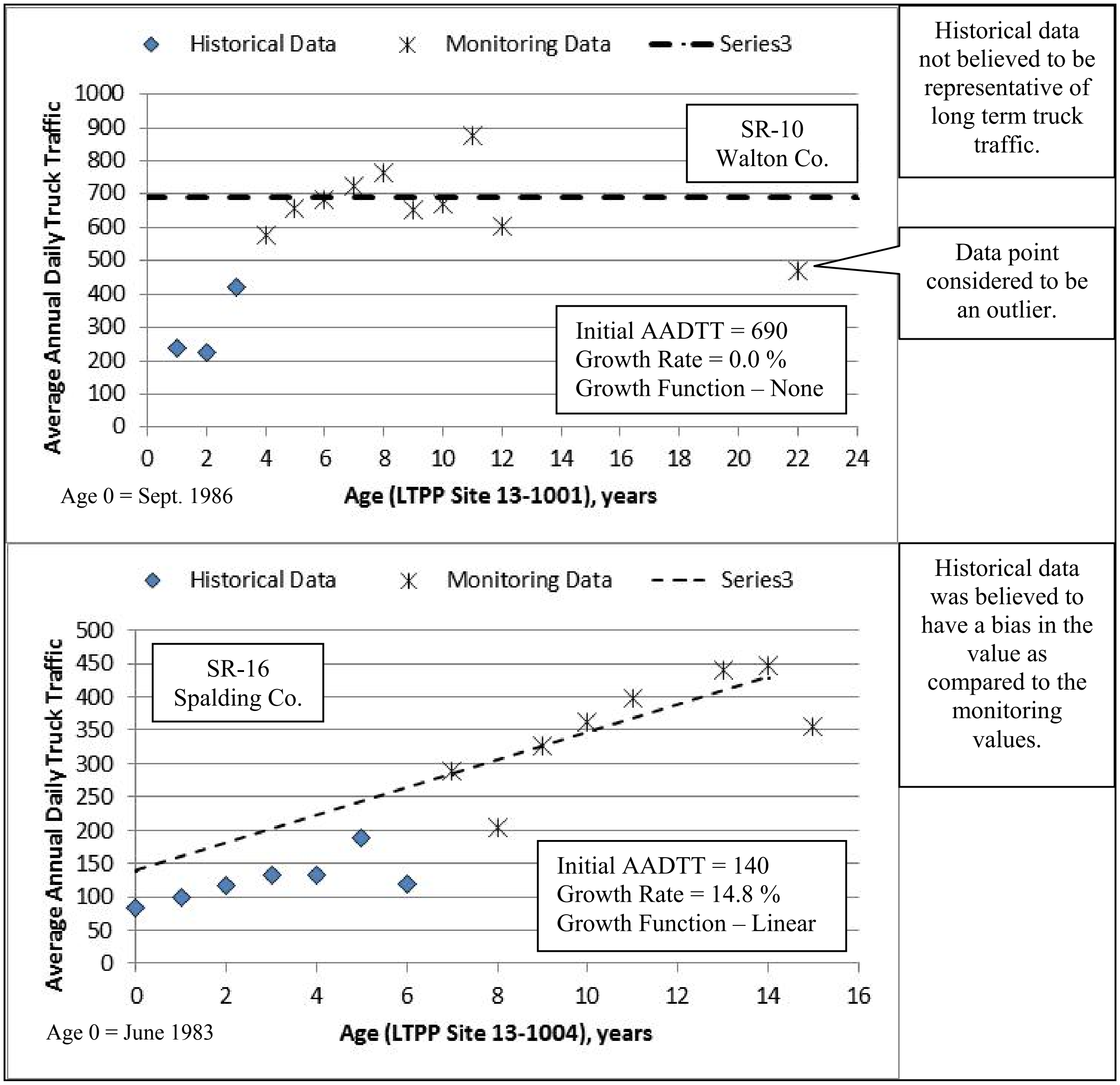

Figure 2—Illustration of the Process used to Backcast the Initial AADTT for LTPP Test Sections; Flexible Pavements

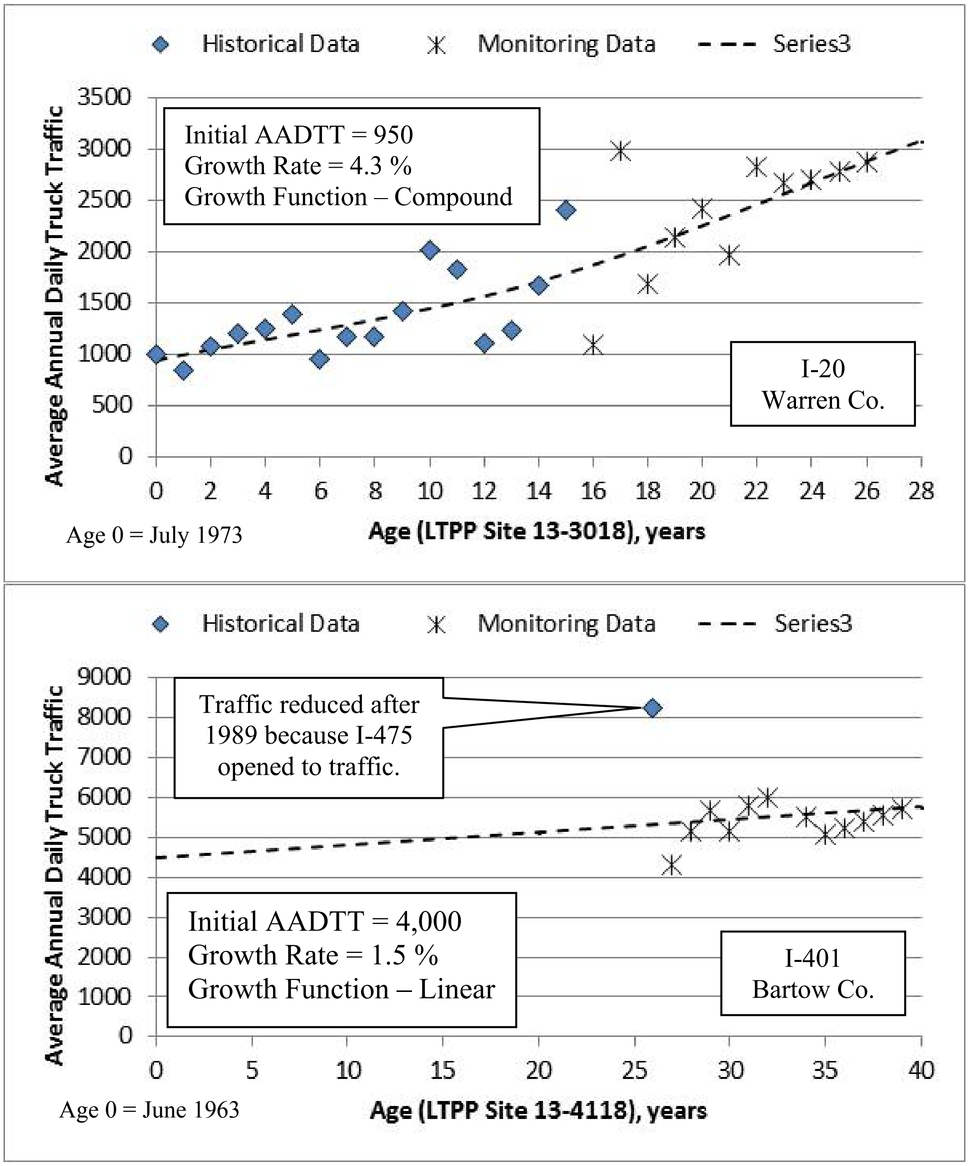

Figure 3—Illustration of the Process used to Backcast the Initial AADTT for LTPP Test Sections; Rigid Pavements

2.3.2 Normalized Vehicle Class Volume Distribution

The normalized vehicle class volume distribution was computed using AVC and WIM data available in LTPP for all the sections used in the analysis. A summary of the data is presented in Table 7. These values represent the average normalized volume distribution for each site. For a few sites, significant deviations in the normalized truck class distribution were observed in the data. Any anomalies or outliers were removed from the data set used to determine the average values listed in Table 7.

2.3.3 Monthly Volume Adjustment Factors

Sufficient data to determine the monthly adjustment factor (MAF) information was unavailable for many of the LTPP sites in Georgia. The MAF for the sites with sufficient data are included in Appendix C. Two MAF data sets were determined for use in the validation study using the LTPP sites. These MAF values are provided in Tables 8 and 9. Table 8 includes the MAF values for sites that exhibit seasonally dependent truck traffic, while Table 9 includes the MAF values for seasonally independent truck traffic. Table 10 defines the Georgia LTPP sites for which the heavy truck traffic is seasonally dependent or independent.

2.3.4 Hourly Distribution Factors

The MEPDG default hourly truck distribution was used for all LTPP sections analyzed. The hourly distribution factors are only used for predicting the performance of the rigid pavements.

Table 7—Average Normalized Truck Class Volume Distribution

LTPP	Truck or Vehicle Class									
ID	4	5	6	7	8	9	10	11	12	13
0500	9.653	14.318	5.935	1.669	13.936	46.607	1.009	3.709	0.714	2.451
1001	8.467	41.581	5.191	0.199	12.041	29.920	0.791	0.908	0.314	0.588
1004	5.753	14.107	9.287	0.442	17.557	42.357	2.099	0.247	0.021	8.130
1005	7.344	55.807	4.697	0.085	11.870	20.068	0.085	0.043	0.000	0.000
1031	5.510	46.803	12.636	0.728	11.351	20.029	1.119	0.266	0.182	1.377
3007	7.243	34.269	5.626	0.465	16.945	31.585	1.163	0.280	0.261	2.164
3011	4.167	23.788	4.706	0.150	23.799	40.375	0.842	1.499	0.362	0.312
3015	10.070	18.658	5.849	0.951	25.365	32.998	1.417	1.526	0.386	2.780
3016	3.095	5.802	0.900	0.004	12.769	70.227	0.549	4.514	2.141	0.000
3017	1.067	37.318	1.902	0.612	5.751	49.139	1.818	1.530	0.706	0.158
3018	0.829	36.680	3.085	5.166	6.864	40.554	4.784	1.208	0.649	0.180
3019	2.866	72.163	3.701	0.277	4.470	15.907	0.263	0.091	0.027	0.236
3020	2.866	72.163	3.701	0.277	4.470	15.907	0.263	0.091	0.027	0.236
4092	1.788	70.756	6.339	0.339	6.352	12.406	0.461	0.309	0.122	1.128
4093	1.902	66.707	7.640	0.490	7.184	13.865	0.545	0.254	0.117	1.297
4096	2.933	10.126	5.013	21.416	13.730	39.959	2.914	0.120	0.452	3.337
4111	16.866	26.414	12.313	7.301	16.764	13.618	2.075	0.709	0.565	3.376
4112	5.889	16.970	3.941	0.300	20.630	46.954	0.710	3.031	0.740	0.834
4113	9.845	22.147	4.833	1.123	19.512	35.168	1.146	2.776	0.563	2.888
4118	7.279	10.651	8.899	2.212	20.458	44.150	1.644	3.041	1.114	0.552
4119	9.653	14.318	5.935	1.669	13.936	46.607	1.009	3.709	0.714	2.451
4420	5.756	19.062	19.796	3.235	10.335	24.775	5.811	0.316	0.117	10.797
5023	12.90	43.58	2.68	0.39	11.50	25.62	0.61	1.66	0.40	0.65
7028	8.222	17.023	3.425	0.263	13.366	49.079	1.332	4.042	1.011	2.237

Table 8—Monthly Adjustment Factors for the LTPP Sites; Heavy Trucks are Seasonally Dependent

Month	Truck Classification									
	4	5	6	7	8	9	10	11	12	13
January	0.17	0.11	0.79	1.6	0.22	0.22	1.94	0.16	0.51	1.12
February	0.23	0.06	0.74	1.53	0.28	0.39	2.06	0.39	0.67	0.65
March	0.74	0.56	0.91	0.89	0.91	0.84	1.42	0.74	0.86	0.74
April	1.41	1.26	1.08	0.6	1.29	1.34	0.65	1.28	1.07	0.81
May	1.71	1.65	1.08	0.12	1.51	1.45	0.36	1.61	1.26	0.57
June	1.54	1.97	1.08	0.12	1.53	1.5	0.24	1.72	1.32	0.57
July	1.49	2.14	1.02	0.12	1.4	1.4	0.19	1.46	1.07	0.65
August	1.41	1.95	1.19	0.12	1.52	1.63	0.25	1.63	1.3	0.96
September	1.46	1.2	1.03	0.56	1.54	1.55	0.42	1.61	1.56	1.11
October	1.29	0.78	1.15	1.19	1.18	1.17	1	1.01	1.13	2.18
November	0.33	0.16	1.08	2.87	0.39	0.34	1.93	0.28	0.79	1.28
December	0.22	0.16	0.85	2.28	0.23	0.17	1.54	0.11	0.46	1.36

Table 9—Monthly Adjustment Factors for the LTPP Sites; Heavy Trucks are Seasonally Independent

Month	Truck Classification									
	4	5	6	7	8	9	10	11	12	13
January	0.6	0.84	1.56	0.96	0.96	1.06	1.32	0.96	1.08	1.32
February	0.72	0.96	1.2	0.96	1.08	1.06	1.2	0.96	1.14	0.96
March	0.96	1.08	0.96	0.6	1.08	1.06	0.96	0.96	1.14	0.96
April	1.44	1.2	0.96	0.48	1.08	0.96	0.96	0.96	1.08	0.84
May	1.08	0.96	0.84	0.48	1.08	0.96	0.96	0.96	0.84	0.48
June	1.08	1.08	0.72	0.6	1.08	0.96	0.96	1.08	0.96	0.6
July	0.72	0.84	1.08	1.08	0.96	0.84	0.84	0.96	0.84	0.6
August	0.84	0.72	0.96	1.32	1.08	0.96	0.84	1.08	0.96	0.84
September	0.84	0.84	0.84	1.32	0.84	0.96	0.96	1.08	0.96	0.84
October	1.44	1.32	0.96	1.44	0.96	1.06	0.96	1.08	1.08	1.32
November	1.32	1.2	0.96	1.44	0.96	1.06	0.96	0.96	1.08	1.44
December	0.96	0.96	0.96	1.32	0.84	1.06	1.08	0.96	0.84	1.8

Table 10—Summary of Predominant Truck Traffic Seasonal Distribution and Normalized Axle Load Distribution Used in Validation Effort

LTPP ID No.	County	Route	Functional Class	MAF Seasonal	NALS Designation
0502 to 0566	Bartow	I-401	Rural Interstate	Independent	H1
1001	Walton	SR 10	Rural Principal Arterial	Dependent	H1
1004	Spalding	SR 16	Rural Minor Arterial	Dependent	GA-U&R-MA
1005	Houston	SR 247	Rural Major Collector	Dependent	H1
1031	Dawson	SR 247C	Rural Principal Arterial	Independent	H1
3007	Pickens	SR 5	Rural Interstate	Independent	GA-RI-MA
3011	Treutlen	I-16	Rural Interstate	Independent	175-0247-3-1
3015	Candler	I-16	Rural Interstate	Independent	175-0247-3-1
3016	Haralson	I-20	Rural Interstate	Dependent	175-0196-3-1
3017	Taliaferro	I-20	Rural Interstate	Dependent	M
3018	Warren	I-20	Rural Interstate	Dependent	M
3019	Hall	US-23	Rural Principal Arterial	Independent	H2
3020	Crisp	SR 300	Rural Principal Arterial	Dependent	M
4092	Thomas	SR 300	Rural Principal Arterial	Dependent	081-0347-7-1
4093	Thomas	SR 300	Rural Principal Arterial	Dependent	081-0347-7-1
4096	Early	SR 62C	Rural Minor Collector	Dependent	081-0347-7-1
4111	Oconee	US-78	Rural Minor Collector	Independent	M
4112	Camden	I-95	Rural Interstate	Independent	GA-RI-MA
4113	Camden	I-95	Rural Interstate	Independent	GA-RI-MA
4118	Monroe	I-401	Rural Interstate	Independent	H1
4119	Bartow	I-401	Rural Interstate	Independent	H1
4420	Bryan	US-17	Rural Principal Arterial	Independent	H1
5023	Camden	I-95	Rural Interstate	Dependent	H1
7028	Franklin	I-85	Rural Interstate	Independent	GA-RI-MA

2.3.5 Axle Load Distribution Factors

The MEPDG requires single, tandem, tridem, and quad normalized axle load spectra (NALS) factors for analysis. The Georgia WIM project analyzed the axle weight data collected at all LTPP sites and other non-LTPP sites (almost 90 portable WIM sites were analyzed under the WIM project). For all sections analyzed, the single and tandem NALS factors were developed using WIM data obtained from the LTPP sites. Most of the data collected over a short time period with the use of portable devices were considered not reliable. For these cases, default NALS were recommended for use for the LTPP sites from the Georgia WIM study. Table 10 lists the default or local NALS that were used in predicting pavement distress for each of the LTPP sites. The following procedure was used in determining whether the site specific WIM data was used, or if the WIM data was considered inappropriate, for which default NALS developed from the Georgia WIM study were used.

1. Use portable WIM data to construct single and tandem load spectrum for class 9 vehicles. Class 9 is considered to be the dominant heavy truck observed on GDOT State roads.
2. Conduct initial quantitative assessment of axle load distributions:

a. For single axles:
    i. Bell-shaped distribution is expected with peak percentage of loads around 10,000-11,000 lb.
    ii. Very few loads exceeding 18,000 lb is expected (less than 3percent).
b. For tandem axles:
    i. "Camel-back" distribution is expected with two peaks. It is possible but uncommon to see only one peak (either loaded or unloaded) at the location of either the first or second peak described below.
    ii. First peak around 12,000-14,000 lbs (this is an optional check)
    iii. Second peak around 30,000 – 36,000 lbs.
    iv. Less than 30 percent of loads exceeding legal limit of 34,000 lb is expected. (Majority of sites have less than 10 percent.)
    v. Very few loads exceeding 40,000 lb is expected (less than 3 percent).

3. If initial assessment does not indicate anomalies in axle load distribution (i.e. expected Class 9 tandem shape is observed, as outlined in step 2 above), assume that WIM equipment collects data without bias and proceed with evaluation of loading conditions based on Relative Pavement Performance Impact Factor (RPPIF) or percent of heavy axle analysis. The table below was used to assign the NALS loading condition.
    a. Assign GDOT MEPDG default or site-related MEPDG-quality load spectra from a nearby site on the same road (i.e. site-related Level 2 input) based on similarities in observed loading conditions. The loading condition or NALS were developed from the Georgia WIM study.

Loading Condition	RPPIF	Percent Heavy Loads
M (Medium)	<0.3	<30%
H1(Heavy 1)	0.3-0.4	30-40%
H2(Heavy 2)	0.4-0.5	40-50%
VH1(Very Heavy 1)	0.5-1.0	50-75%
VH2(Very Heavy 2)	>1.0	>75%

4. If initial assessment indicates that axle load distribution does not have expected attributes, two outcomes are possible:
    a. Site location represents unusual loading conditions due to local trucking activities. In this case, obtain information from the freight office about the nature of truck movements at the site and document this information; proceed with evaluation of loading conditions based on RPPIF analysis.
    b. WIM equipment set-up, sampling duration, and/or site conditions resulted in axle load spectrum of limited quality. In this case, assess if tandem axle load spectrum at least has an expected "camel-back" shape.
        i. If distribution has expected shape, proceed with evaluation of loading conditions based on analysis of the ratio between unloaded and loaded peak of tandem axle distribution.

Loading Condition	Unloaded/Loaded Peak Ratio
M	1.3-2.8
H1	0.6-1.3
H2	0.3-0.6
VH1	0.3-0.1
VH2	<0.1

1. Use assigned loading condition to identify if MEPDG-quality load spectra from a nearby WIM site located on the same road (i.e.) is available. If site-related spectrum found, use it as site-related Level 2 MEPDG input.
2. If no nearby WIM site with similar loading condition is found, select LTPP or GDOT MEPDG default for roads with similar loading condition.
3. If no default with similar loading condition is found, GDOT MEPDG default load spectra default based on rules developed for different road functional classes in GDOT (see the following step).

ii. If shape of distribution is unexpected, stop further analysis and label this WIM data set unusable for pavement applications.

1. Assign GDOT MEPDG load spectra default based on rules developed for different road functional classes in GDOT:
    a. For GDOT <u>Rural</u> Interstates and Major Arterial Roads, default NALS are based on LTPP "Heavy 2" default loading condition (40-50 percent heavily loaded class 9 trucks) for class 9 and "typical" default loading condition (most frequently observed in the national study) for all other vehicle classes. (Default Name: GA_RI&MA)

    b. For GDOT <u>Urban</u> Interstates and Major Arterial Roads, use LTPP "Heavy 1 (typical)" default loading condition (30-40% heavily loaded class 9 trucks) for class 9 and "typical" default loading condition (most frequently observed in the national study) for all other vehicle classes. (Default Name: GA_UI&MA)

    c. For GDOT Urban and Rural <u>Minor Arterial</u> Roads and other lower functional class roads, use LTPP "Heavy 1 (typical)" default (30-40% heavily loaded class 9 trucks) and "typical" default loading condition (most frequently observed in the national study) for all other vehicle classes. (Default Name: GA_U&R_MiA)

2.3.6 General Traffic Inputs

MEPDG general truck traffic input requirements are as follows:

- **Tire pressure**: The MEPDG default value of 120 psi was assumed and used for all validation sections.
- **Axle configuration**: MEPDG defaults were adopted for this input for all validation sections.
- **Wheelbase**: National defaults were adopted for this input for all the validation sections. The values are 17%, 22%, and 61%.
- **Lateral traffic wander**: The MEPDG default value was used for this input for all the validation sections.
- **Number of axles per truck**: The number of axles per truck was estimated using LTPP AVC and WIM data. Based on the reasonableness of computed number of axles per truck, a combination of LTPP computed estimates and MEPDG defaults were used as inputs. Table 11 includes the default monthly truck volume distribution factors to be used where insufficient data is available. Appendix D includes the number of axles per truck class for the LTPP sites with sufficient WIM data.

Table 11—Default Values for the Number of Axles per Truck Class

Truck Class	Number of Axles per Truck Class			
	Single Axles	Tandem Axles	Tridem Axles	Quad Axles
4	1.3	0.7	0	0
5	2.0	0	0	0
6	1.0	1.0	0	0
7	1.0	0.26	0.83	0
8	2.4	0.6	0	0
9	1.2	1.6	0	0
10	1.3	1.3	0.5	0.02
11	4.7	0.1	0.01	0
12	3.9	1.0	0.01	0
13	2.0	2.0	0.20	0.06

2.4 Layer/Material Properties

For all layers or material groups, detailed information was obtained from the LTPP database to determine the layer properties including: thickness, unit weight, gradation, volumetric properties of HMA and unbound materials, resilient modulus of unbound materials and soils, classification information, PCC flexural strength, PCC coefficient of thermal expansion (CTE), and PCC modulus of elasticity. Most of the key material properties in the LTPP database were obtained through laboratory testing of mix samples or extracted cores. For other material properties such as PCC zero stress temperature, thermal conductivity, dynamic modulus of HMA, and so on, MEPDG or Georgia-specific defaults were assumed. The sources of key material properties to estimate the MEPDG inputs are described in the following subsections for each material.

2.4.1 HMA Layers/Mixtures

The inputs for all HMA, asphalt stabilized base, and other bituminous layers are listed in Table 12. The HMA layer properties were obtained through laboratory testing of bulk mixtures or cores. The test results from asphalt content, aggregate gradation and maximum specific gravity at the time of sampling were assumed to be unchanged or the same as the time at construction. Thus, the average of test results stored in the LTPP database were used as inputs for each layer or mixture tested within the LTPP program.

- Aggregate specific gravity was assumed for all mixtures and based on typical values for the different types of aggregate used in Georgia.

- The maximum specific gravity of the HMA mixtures was measured as part of the LTPP test program and is available in the LTPP database.

- The air voids and density at construction (bulk specific gravity) change over time and the values at construction are unavailable for most of the flexible pavement sites. Air voids or bulk specific gravities are only available at the time of sampling for the GPS sites. For these cases, the air void at construction was backcast using the average air voids measured at the pavement's age of sampling and a densification function shown below. Figures 4 and 5 illustrate use of the densification function for backcasting the initial HMA air voids for four of the LTPP sites. Appendix E includes a listing of the backcasted initial air voids.

$$V_a(t) = (D + V_d)10^{-a\left(\frac{t}{5}\right)^b} \tag{1}$$

Where:

$V_a(t)$ = Air voids at time or age t.
V_d = Design air voids for selecting the asphalt content, %
t = Time or age of HMA mixture after construction, years.
D = Regression constant; expected maximum change or decrease in air voids and defined at the age or time of sampling.
a, b = Regression constants fitting the decrease in air voids over time (a=0.1 and b=0.25). These regression coefficients for typical dense graded mixtures (estimated from previous projects).

- Effective asphalt content by volume was calculated using the assumed aggregate specific gravity and other volumetric properties (bulk specific gravity of compacted mix, asphalt specific gravity, and total asphalt content by weight). Appendix E includes a listing of the effective asphalt content by volume along with the air voids estimated at the time of construction for all LTPP test sections. Figure 6 shows a comparison of the asphalt content and air voids at construction. As shown, there is extensive dispersion between the asphalt content and air voids; no definite relationship was found. However, this information can be used to judge the cracking and rutting resistance of different mixtures. Mixtures that exhibit lower air voids at construction in comparison to sites with higher air voids for similar design asphalt contents should have greater resistance to rutting and cracking.

- Dynamic modulus and creep compliance for the HMA mixtures and asphalt binder properties are unavailable for the time of construction for all sites, even for the SPS-5 project. Thus, input level 3 was used for all mixtures. The dynamic modulus is calculated by the MEPDG software using the gradation and binder grade. The gradation was measured on the aggregates extracted from the cores recovered during sampling, while the binder grade is included in the LTPP database.

Table 12—Asphalt Materials and the Test Protocols for Measuring the Material Property Inputs for New and Existing HMA Layers

Design Type	**Measured Property**	**Source of Data**		**Recommended Test Protocol and/or Data Source**
		Test	**Estimate**	
New HMA (new pavement and overlay mixtures), as built properties prior to opening to truck traffic	Dynamic modulus	X		AASHTO T 79; use input level 3.
	Tensile strength	X		AASHTO T 322 ; use input level 3.
	Creep Compliance	X		AASHTO T 322; use input level 3.
	Poisson's ratio		X	National test protocol unavailable. Select MEPDG default relationship
	Surface shortwave absorptivity		X	National test protocol unavailable. Use MEPDG global default value.
	Thermal conductivity	X		ASTM E 1952; Use global default value.
	Heat capacity	X		ASTM D 2766; Use global default value.
	Coefficient of thermal contraction		X	National test protocol unavailable. Use MEPDG default values.
	Effective asphalt content by volume	X		AASHTO T 308; calculated from other volumetric properties.
	Air voids	X		AASHTO T 166
	Aggregate specific gravity	X		AASHTO T 84 and T 85
	Gradation	X		AASHTO T 27
	Unit Weight	X		AASHTO T 166
	Voids filled with asphalt (VFA)	X		AASHTO T 209
Existing HMA mixtures, in-place properties at time of pavement evaluation	FWD backcalculated layer modulus	X		AASHTO T 256 and ASTM D 5858
	Poisson's ratio		X	National test protocol unavailable. Use MEPDG default values.
	Unit Weight	X		AASHTO T 166 (cores)
	Asphalt content	X		AASHTO T 164 (cores)
	Gradation	X		AASHTO T 27 (cores or blocks)
	Air voids	X		AASHTO T 209 (cores)
	Asphalt recovery	X		AASHTO T 164/T 170/T 319 (cores)
Asphalt Binder (new, overlay, and existing mixtures)	Asphalt Performance Grade (PG); OR Asphalt binder complex shear modulus (G*) and phase angle (δ); OR Penetration; OR Ring and Ball Softening Point Absolute Viscosity	X X X X		AASHTO T 315 AASHTO T 49 AASHTO T 53 AASHTO T 202 AASHTO T 201 AASHTO T 228

Design Type	Measured Property	Source of Data		Recommended Test Protocol and/or Data Source
		Test	Estimate	
	Kinematic Viscosity Specific Gravity; OR Brookfield Viscosity	X		AASHTO T 316

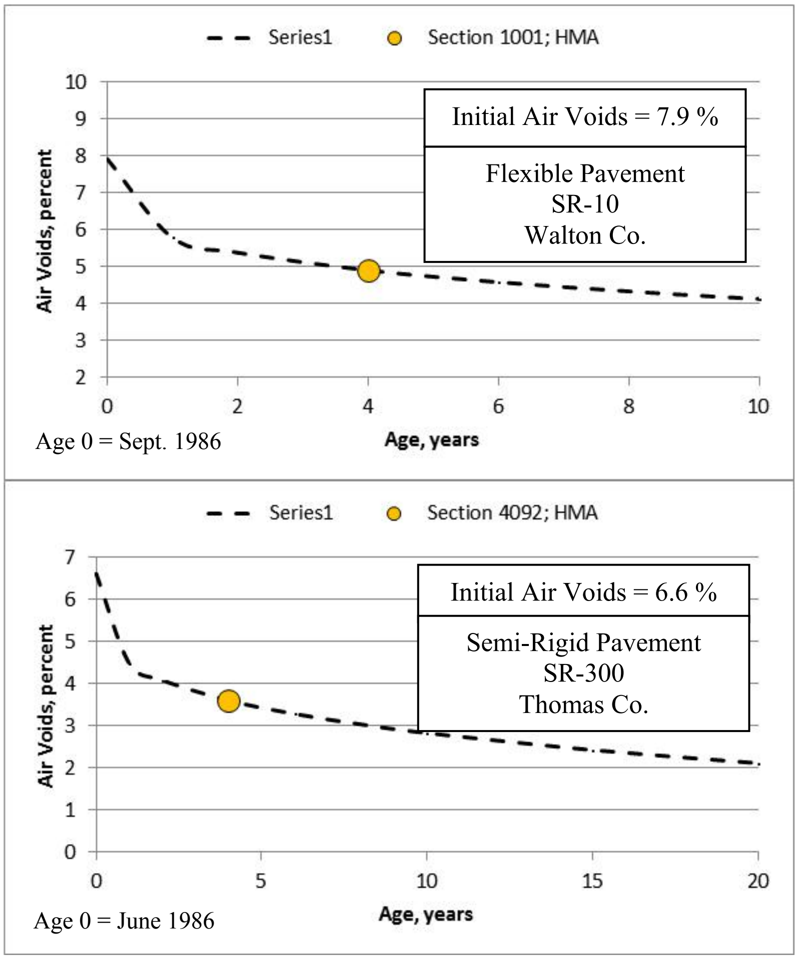

Figure 4—Illustration of the Process used to Backcast the Initial Air Voids of HMA Layers with Adequate Compaction

2.4.2 PCC Layers/Mixtures

Several input categories for PCC layers are required by the MEPDG, which are defined in the MEPDG Manual of Practice, and listed in Table 13. Most of the inputs were extracted from the LTPP database or from other GDOT sponsored projects and/or construction records, so input levels 1 and 2 were used for the validation of the rigid transfer functions. The sources of data are presented in Table 14. Key inventory, design, materials, and construction data was assembled for each selected project for review, identification/elimination of outliers and anomalies, and eventual inclusion in the GDOT MEPDG verification database. In populating the GDOT MEPDG verification database the following was considered:

- Only data deemed reasonable as based on engineering experience was included in the database.
- Questionable data was removed and replaced with typical values or with project specific information from other sources.

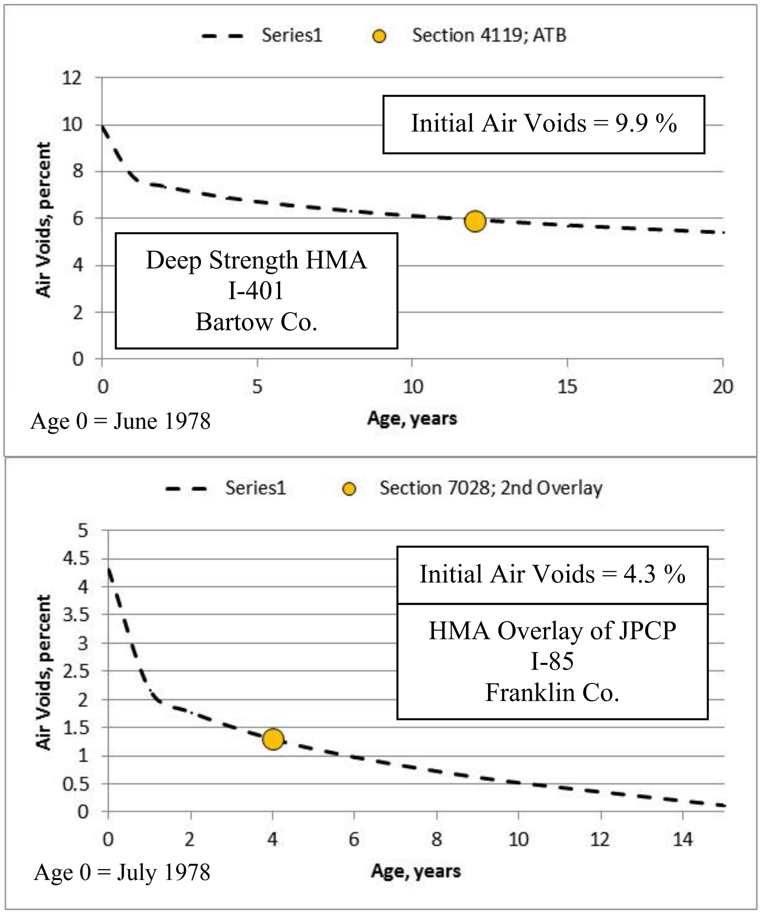

Figure 5—Illustration of the Process used to Backcast the Initial Air Voids of HMA Layers with under and Over-Compaction

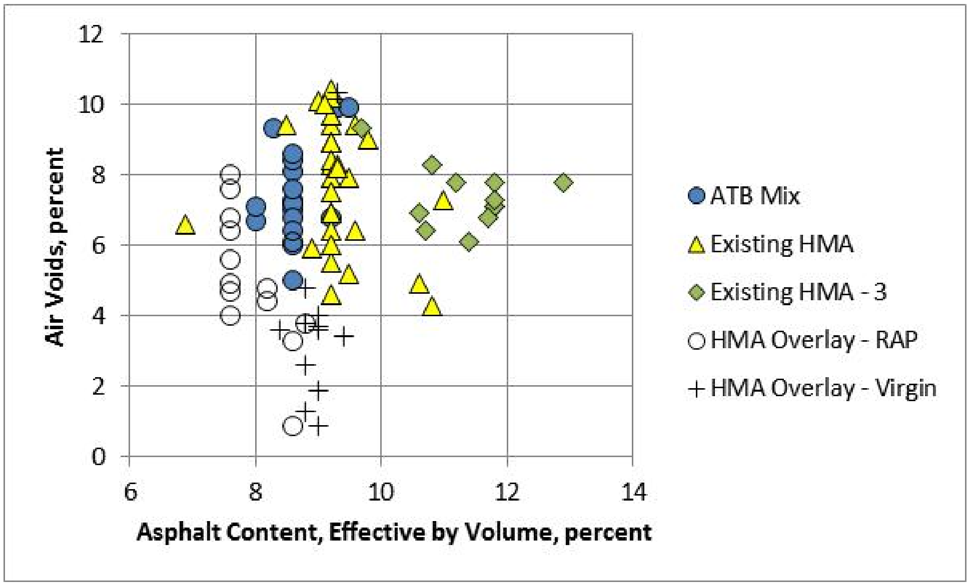

Figure 6—Initial Air Voids Compared to the Effective Asphalt Content by Volume for the HMA Mixtures

The PCC input level 1 material properties were identified in Tables 13 and14. For the other properties, input levels 2 or 3 were used. The level 3 input requirements are as follows:

- Thermal
  - Unit weight
  - Poisson's ratio
  - Coefficient of thermal expansion
  - Surface shortwave absorptivity; select MEPDG default value of 0.85.
  - Thermal conductivity; select MEPDG default value of 1.25 BTU/hr-ft-°F.
  - Heat capacity; select MEPDG default value of 0.28 BTU/lb-°F.
- Mix
  - Cement type; select based on PCC mix type.
  - Cementitious material content; selected based on PCC mix type.
  - Water to cement ratio; select based on PCC mix type.
  - Aggregate type; selected based on actual or expected aggregate source.
  - PCC zero stress temperature; estimated from cement content and mean monthly temperatures at project location.
  - Ultimate shrinkage (at 40 percent RH); estimated from compressive strength, cement type, curing type, cement content, and water-to-cementitious materials (w/c) ration.
  - Reversible shrinkage (50 percent of ultimate shrinkage); select MEPDG default value of 50 percent.
  - Time to develop 50 percent of ultimate shrinkage; select MEPDG default value of 35 days.
  - Curing method; select based on GDOT construction practices.
- Strength

- 7-, 14-, 28-, and 90- day compressive strength (Level 2) OR
- 28-day compressive strength and/or 28-day elastic modulus (Level 3) OR
- 28-day flexural strength and/or 28-day elastic modulus (Level 3)

For the GPS sections, only the long-term (mostly 5 years or more) compressive and tensile strength and elastic modulus was tested. The initial flexural or compressive strength and elastic modulus were backcasted for the time at construction using the laboratory test values at the age of the pavement when the samples were recovered for testing. The strength-modulus gain or growth model included in the MEPDG was used to backcast the strength and modulus of the Georgia LTPP PCC mixtures.

Histograms of the more important PCC material property inputs are presented in Figures 7 through 9. The CTE values were from the NCHRP 20-07 corrected values for these GA sections along with the proper calibration factors range from 4 to 6 in./in./deg °F (see Figure 7), the 28-day flexural strengths range from 600 to 800 psi (see Figure 8), and the 28-day elastic modulus values range from 3,000,000 to 5,000,000 psi (Figure 9). An important observation from the 28-day elastic modulus data is that no modulus values were found with the mid-range (4,000,000 psi).

Table 13—PCC Material Inputs and Test Protocols for New and Existing PCC Layers

Design Type	Measured Property	Source of Data		Recommended Test Protocol and/or Data Source
		Test	Estimate	
New PCC and PCC overlays and existing PCC when subject to a bonded PCC overlay	Elastic modulus	X		ASTM C469; input level 1.
	Poisson's ratio	X		ASTM C469; input level 1.
	Flexural strength	X		AASHTO T97; input level 1
	Indirect tensile strength (CRCP only)	X		AASHTO T198; input level 1.
	Unit weight	X		AASHTO T121; input level 1.
	Air Content	X		AASHTO T 152 or T 196
	Coefficient of thermal expansion	X		AASHTO T336; input level 1.
	Surface shortwave absorptivity		X	National test protocol unavailable; use MEPDG default value
	Thermal conductivity	X		ASTM E 1952; use global default value
	Heat capacity	X		ASTM D 2766; use global default value
	PCC zero-stress temperature		X	National test protocol not available. Estimate using agency historical data or select MEPDG defaults
	Cement type		X	Select based on actual or expected cement source
	Cementitious material content		X	Select based on actual or expected concrete mix design
	Water to cement ratio		X	Select based on actual or expected concrete mix design
	Aggregate type		X	Select based on actual or expected aggregate source
	Curing method		X	Select based on agency recommendations and practices
	Ultimate shrinkage		X	Testing not practical. Estimate using prediction equation in MEPDG
	Reversible shrinkage		X	Estimate using agency historical data or select MEPDG defaults
	Time to develop 50 percent of ultimate shrinkage[1]		X	Estimate using agency historical data or select MEPDG defaults
Existing intact and fractured PCC	Elastic modulus	X		ASTM C469 (extracted cores) AASHTO T 256 (non-destructive deflection testing)
	Poisson's ratio	X		ASTM C469 (extracted cores)
	Flexural strength	X		AASHTO T97 (extracted cores)
	Unit weight	X		AASHTO T121 (extracted cores)
	Surface shortwave absorptivity		X	National test protocol not available. Use MEPDG defaults
	Thermal conductivity	X		ASTM E 1952 (extracted cores)
	Heat capacity	X		ASTM D 2766 (extracted cores)

Table 14—Sources of MEPDG Input Data for PCC Mixtures and Rigid Pavement Design Features

Data Category	LTPP Data Table	Material Properties or Index Properties
PCC Materials	TST_PC01	Compressive strength of cores and cylinders, test date
	TST_PC02	Tensile strength, test date
	TST_PC03	CTE, aggregate type, test date
	TST_PC04	Elastic modulus, Poisson's ratio, unit weight, test date
	TST_PC09	Modulus of rupture, test date
	INV_PCC_MIXTURE	Mix design, cement type and content, entrained air content, curing method for GPS
	INV_AGE	Construction date for GPS
Stabilized Materials	TST_TB02	Compressive strength
Design Features	INV_GENERAL	PCC slab width
	INV_PCC_JOINT	Joint spacing, dowel bar size & spacing, shoulder type/tied shoulder
	INV_PCC_STEEL	CRCP steel content (% steel), depth of steel reinforcement

While concrete modulus of rupture was the main material input for the AASHTO 1993 rigid pavement design procedure (along with the modulus of elasticity), the MEPDG allows correlations through level 2 inputs with compressive strength and requires other volumetric properties such as shrinkage, coefficient of thermal expansion (CTE), specific heat, and thermal conductivity for analysis. In addition, strength parameters that are used in the analysis include compressive strength, modulus of elasticity, and tensile strength for CRCP. The modulus of elasticity has a much greater effect on performance with the MEPDG than with the AASHTO 1993 procedure. In other words, the MEPDG offers a framework to optimize mix designs to balance a whole range of strength, modulus, CTE, shrinkage and other engineering properties for improved performance.

2.4.2.1. Slab / Base Friction Factors

The months of full friction between the slab and base used in the analyses are as follows for each base type:

- Aggregate base: Full friction for entire design life
- Asphalt treated base: Full friction for entire design life
- Cement treated base: Full friction for 10 years

2.4.2.2 Permanent Curl/Warp Effective Temperature

PCC permanent curl/warp effective temperature difference used in the analyses is -10^{0}F. It defines the temperature difference between top and bottom of the PCC slab at the time of construction.

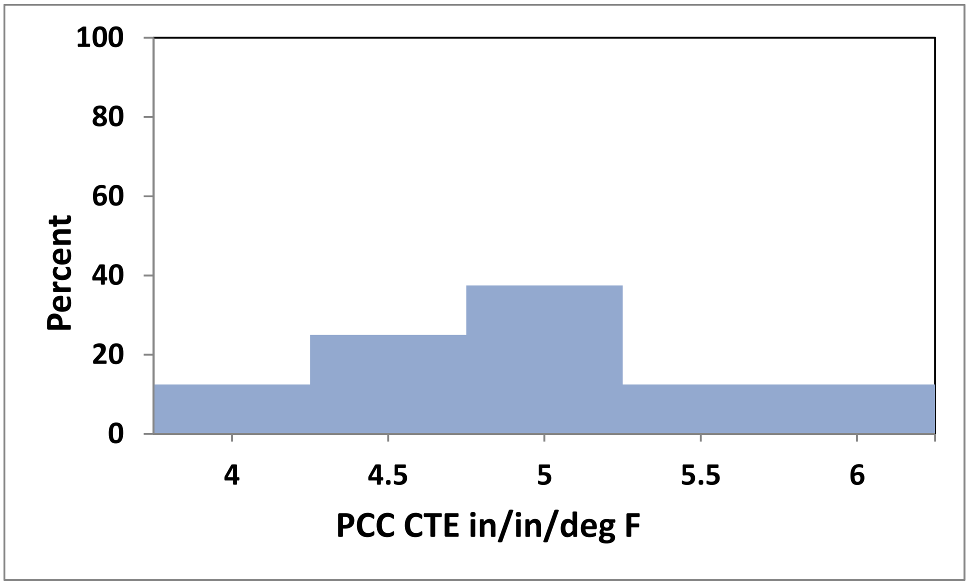

Figure 7—Normalized Distribution or Histogram of PCC CTE from Georgia LTPP Projects (NCHRP 20-07 corrected CTEs)

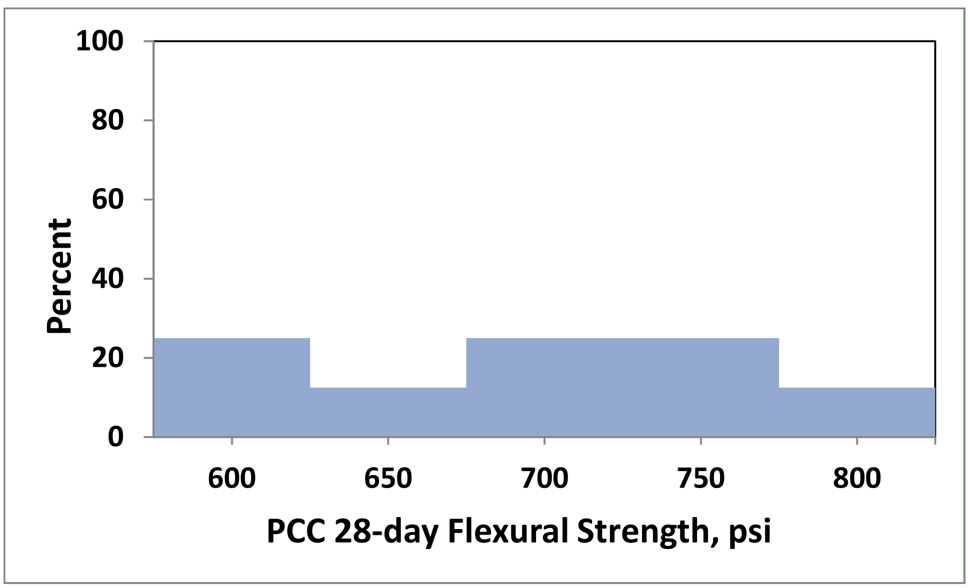

Figure 8—Normalized Distribution or Histogram of PCC 28-day Flexural Strength from Georgia LTPP Projects

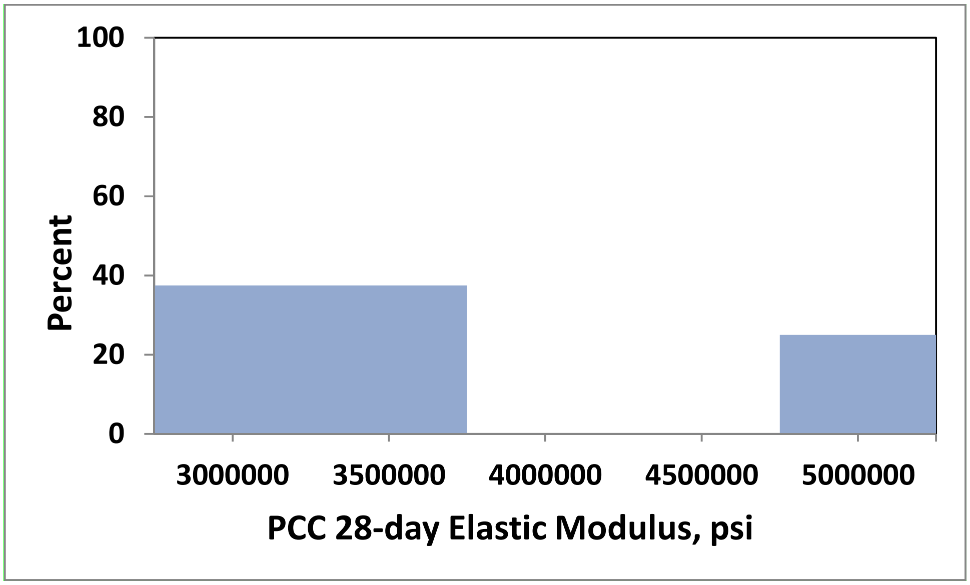

Figure 9—Normalized Distribution or Histogram of PCC 28-day Elastic Modulus from Georgia LTPP Projects

2.4.3 Unbound Aggregate Base and Soil Layers/Materials

The inputs for all unbound aggregate base layers, embankments, and subgrades are listed in Table 15. The gradation, Atterberg limits, optimum water content, and maximum dry density test results are included in the LTPP database. The average values from the LTPP database were the input values used for each site and layer. The maximum dry density and optimum water content are also included in the LTPP database. Figure 10 provides a comparison between the optimum water content and maximum dry unit weight for all unbound layers because these values are an important input to the MEPDG. The resilient modulus, however, was not always measured on specimens prepared at optimum conditions. Thus, the water content and dry density reported for the resilient modulus tests for all unbound layers were entered as input level 1.

Two approaches were used to determine the resilient modulus at the time of construction: (1) laboratory repeated load resilient modulus tests, and (2) backcalculation of elastic modulus from deflection basins. The backcalculated modulus values adjusted to laboratory conditions is the much preferred and recommended technique for rehabilitation design because the resulting layer modulus value is an equivalent value of the materials that vary horizontally and vertically. The laboratory resilient modulus test represents a discrete specimen in the horizontal and vertical direction. More importantly, unbound layers and foundations that contain large boulders or aggregates are difficult or impossible to test in the laboratory.

Multiple backcalculation programs provide the elastic layer modulus typically used for pavement evaluation and rehabilitation design. ASTM D 5858, *Standard Guide for Calculating In Situ Equivalent Elastic Moduli of Pavement Materials Using Layered Elastic Theory* is a procedure for analyzing deflection basin test results to determine layer elastic moduli (i.e., Young’s modulus).

Table 15—Unbound Aggregate Base, Subbase, Embankment, and Subgrade Soil Material Requirements and Test Protocols for New and Existing Materials

Design Type	Measured Property	Source of Data		Recommended Test Protocol and/or Data Source
		Test	Estimate	
New (lab samples) and existing (extracted materials)	Resilient Modulus Two Options: Regression coefficients k_1, k_2, k_3 for the generalized constitutive model that defines resilient modulus as a function of stress state and regressed from laboratory resilient modulus tests. Determine the average design resilient modulus for the expected in-place stress state from laboratory resilient modulus tests.	X		AASHTO T 307 The generalized model used in MEPDG design procedure is: $M_r = k_1 p_a \left(\frac{\theta}{P_a}\right)^{k_2} \left(\frac{\tau_{oct}}{P_a}+1\right)^{k_3}$ Where: M_r = resilient modulus, psi θ = bulk stress = $\sigma_1 + \sigma_2 + \sigma_3$ σ_1 = major principal stress. σ_2 = intermediate principal stress σ_3 = minor principal stress confining pressure τ_{oct} = octahedral shear stress $\frac{1}{3}\sqrt{(\sigma_1-\sigma_2)^2+(\sigma_1-\sigma_3)^2+(\sigma_2-\sigma_3)^2}$ P_a = normalizing stress K_1, k_2, k_3 = regression constants
	Poisson's ratio		X	No national test standard, use default values included in the MEPDG.
	Maximum dry density	X		AASHTO T 180
	Optimum moisture content	X		AASHTO T 180
	Gradation	X		AASHTO T 88
	Plasticity Index	X		AASHTO T 90
	Liquid Limit	X		AASHTO T 89
	Specific gravity	X		AASHTO T 100
	Saturated hydraulic conductivity	X		AASHTO T 215, however, use default values in MEPDG.
	Soil water characteristic curve parameters	X		Use default values included in the MEDG.
Existing material to be left in place	FWD backcalculated modulus	X		AASHTO T 256 and ASTM D 5858
	Poisson's ratio		X	No national test standard, use default values included in the MEPDG.
	Dry density & water content	X		In place values during FWD testing or AASHTO T 180 if default resilient modulus is entered.
	Gradation, Atterberg Limits, Specific Gravity, Saturated hydraulic conductivity & Soil-water Characteristics	X		Same as for New Materials

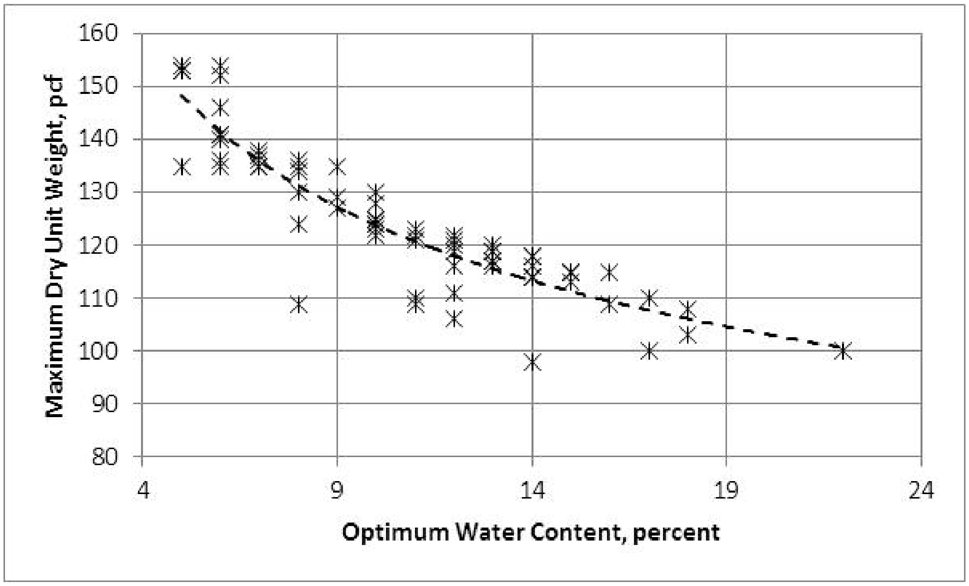

Figure 10—Relationship between Optimum Water Content and Maximum Dry Unit Weight for all Unbound Materials and Soils for the Georgia LTPP Sites

The absolute error or Root Mean Squared (RMS) error is the value that is used to judge the reasonableness of the backcalculated modulus values. The absolute error term is the absolute difference between the measured and computed deflection basins expressed as a percent error or difference per sensor; the RMS error term represents the goodness-of-fit between the measured and computed deflection basins. The RMS and absolute error terms needs to be as small as possible. An RMSE value in excess of 3 percent generally implies that the layer modulus values calculated from the deflection basins are inaccurate or questionable. RMSE values less than 3 percent should be used in selecting the layer modulus values for determining the minimum overlay thickness.

Repeated load resilient modulus lab test results are included in the LTPP database for most unbound layers. Appendix F includes a graphical representation of the resilient modulus tests on the soils and coarse-grained base materials. The laboratory resilient modulus at optimum moisture content is the specified input when the ICM is used to determine the seasonal effects over time. For rigid pavements, the laboratory resilient modulus of the subgrade soil is used to backcalculate a k-value for each month which is used in to calculate the stresses and deflections used to compute damage (for JPCP). However, LTPP does not provide the required subgrade lab resilient modulus at optimum moisture content. Thus, for both HMA and JPCP pavements, FWD data from the LTPP database were used to backcalculate the in place subgrade resilient modulus and k-value as appropriate.

The point in time chosen for the backcalculation was selected to represent the time at which the soils and materials were sampled. This time was selected so the laboratory measured resilient modulus at an equivalent stress state below the pavement surface was determined under the same conditions during which the deflection basins were measured with the FWD. Estimating both of these values at the same time or subsurface conditions, permits the

AASHTO C-factor to be determined and compared to the values recommended for use in the MEPDG Manual of Practice. The procedure summarized by Von Quintus and Killingsworth was used to estimate the in place resilient modulus for each site.

Tables 16 and 17 lists the laboratory measured resilient modulus at equivalent in place stress states, backcalculated resilient modulus, dry density and water content for the unbound layers of each site in comparison to the default values. Table 16 includes the material condition for subgrade soils or embankment layers, while Table 17 includes the same information except for the unbound aggregate base layers. Figures 11 and 12 include a graphical comparison of the laboratory derived resilient modulus and backcalculated derived elastic modulus values. As shown, there is a lot of variability between the laboratory and in place modulus values. Table 18 summarizes the average C-factors for the different types of structures, in comparison to the values recommended in the MEPDG Manual of Practice. Some observations from the LTPP test sections:

- The resilient modulus of the unbound aggregate base and subbase layers is low (see Table 17). One reason for the low resilient modulus values could be related to the water content or the amount of fines or percent passing the Number 200 sieve.
- The average AASHTO c-factors determined from the GDOT-LTPP sites are only similar to those in the Manual of Practice for the subgrade soils below an unbound aggregate base (c-factor = 0.35 in the MEPDG Manual of Practice; see Table 18). The average c-factors for the Georgia LTPP sites are reasonably consistent and vary from 0.30 to 0.40, with the exception for the rigid pavement sections with an average value of about 0.2. This average value was derived from a relatively few number of test sections and should not be used without additional sections being used to confirm the low value.
- The aggregate base layers are weak for most of the LTPP test sections in Georgia. It is unknown whether the percentage of fines, water content, and/or dry density is the cause of the low values, in comparison to the values recommended for use in the MEPDG Manual of Practice. The resilient modulus global default values included in the MEPDG for coarse-grained aggregate base layers vary from 20,000 to 30,000 psi.

Figure 13 includes a comparison between the water contents measured on bulk or undisturbed samples of the subgrade soil and aggregate base material and the optimum water content. As shown, the water content for many of the aggregate base layers and subgrade soil is slightly greater than the optimum water content. The poorly graded sand and other coarse-grained materials (considered to have high permeability) are the predominant material where the in place water content is lower than the optimum water content.

Table 16—Laboratory Equivalent Resilient Modulus and Backcalculated Elastic Layer Modulus for the Subgrade Soil or Embankment

Structure ID	Test Section ID	Material Type	Lab Resilient Modulus, psi	Backcalc. Elastic Modulus, psi	AASHTO c-Factor	Water Content, %	Dry Density, pcf
SPS-5; Flexible with Aggr. Base	0502	Silty Sand with Gravel; A-2-6	8,600	19,000	0.453	13.6	128
	0503		9,200	58000	0.159	13.6	128
	0504		8,700	32000	0.272	13.6	128
	0505		8,400	22000	0.382	13.6	128
	0506		8,400	45000	0.187	13.6	128
	0507		8,800	28000	0.314	13.6	128
	0508		8,400	66000	0.127	13.6	128
	0509		8,200	10000	0.820	13.6	128
	0560		9,200	29000	0.317	13.6	128
	0561		9,300	40000	0.233	13.6	128
	0562		9,300	44000	0.211	13.6	128
	0563		8,200	15000	0.547	13.6	128
	0564		8,700	23000	0.378	13.6	128
	0565		9,400	41000	0.229	13.6	128
	0566		9,300	28000	0.332	13.6	128
Flexible with Aggr. Base	1001	Fine Sandy Silt/A-7-6	9,300	16000	0.58	20.2	109
	1004	Sandy Lean Clay/A-6	11,400	26000	0.44	17.6	115
	1005	Clayey Sand/A-4	11,200	26000	0.43	10.6	122.5
	1031	Silty Sand/A-4	5,700	16000	0.35	11.3	117.5
	4111	Sandy Clay/A-6	10,000	22000	0.45		
	4119	Sandy Silt/A-4	7,900	37000	0.21		
Rigid with Aggr. Base	3007	Sandy Silt/A-2-4	5,500	15000	0.37	20.7	109
	3016	Silty Sand/A-4	6,800	11000	0.62	12.6	123
	3019	Sandy Lean Clay/A-6	8,600	8000	1.1	15.0	116.5
	7028	Clayey Sand/A-4	9,500	43000	0.22	17.8	114
Full-Depth HMA	4112	Poorly Graded Sand/A-3	10,000	25000	0.400	7.0	107.5
	4113	Poorly Graded Sand w/Silt/A-3	10,000	46000	0.217	12.1	99
Soil Below PCC	4118	Clayey Sand/A-4	10,000	21000	0.476	15.1	117.5
Soil below Stabilized Base	3011	Silty Sand/A-4	11,300	48000	0.235	8.8	126
	3015	Poorly Graded Sand/A-4	10,100	21000	0.481	10.0	123
	3017	Silty Sand/A-5	7,400	15000	0.493	10.2	123.5
	3018	Clayey Sand/A-4	11,000	20000	0.550	13.5	120
	3020	Clayey Sand/A-6	10,800	45000	0.240	13.1	118.5
	4092	Clayey Sand/A-4	10,000	47000	0.213	11.6	122.5
	4093	Clayey Sand/A-4	8,000	50000	0.160	11.0	120
	4096	Clayey Sand/A-4	10,500	41000	0.256	10.9	120.5
	4420	Silty Sand/A-2-4	4,800	33000	0.145	13.6	113.5
	5023	Clayey Sand/A-2-4	8,600	32000	0.269	9.3	109.5

Table 17—Laboratory Equivalent Resilient Modulus and Backcalculated Elastic Layer Modulus for the Unbound Aggregate Base Layers

Structure ID	Test Section ID	Material Type	Lab Resilient Modulus, psi	Backcalc. Elastic Modulus, psi	AASHTO c-Factor	Water Content, %	Dry Density, pcf
SPS-5; Below HMA Layer	0502	Soil-Aggr. Mix; A-1-b	12,300	36000	0.342	5.0	152
	0503		12,300	38000	0.324	5.0	152
	0504		12,500	25000	0.500	5.0	152
	0505		12,500	52000	0.240	5.0	152
	0506		12,500	45000	0.278	5.0	152
	0507		12,400	39000	0.318	5.0	152
	0508		12,500	71000	0.176	5.0	152
	0509		12,300	25000	0.492	5.0	152
	0560		12,600	54000	0.233	5.0	152
	0561		12,600	73000	0.173	5.0	152
	0562		12,600	35000	0.360	5.0	152
	0563		12,500	33000	0.379	5.0	152
	0564		12,500	54000	0.231	5.0	152
	0565		12,800	56000	0.229	5.0	152
	0566		12,600	41000	0.307	5.0	152
Non-SPS-5; Below HMA Layer	1001	Crushed Gravel/A-1-a	10,000	26000	0.385	6.9	135
	1004	Soil Aggr. Mix/A-1-a	14,500	23000	0.630	6.1	135.5
	1005	Soil Aggr Mix/A-1-a	15,500	30000	0.517	7.4	136.5
	1031	Fine-Grained Soil/A-1-b	12,000	57000	0.211	6.0	138.5
	4111	Soil Aggr Mix/A-1-a	17,000	29000	0.586	6.5	134.5
	4119	Soil Aggr Mix/A-1-a	15,000	47000	0.319	6.4	154
Below Stab. Layer	3016	Soil Aggr Mix/A-1-a	8,000	55000	0.145	6.9	136.5
	7028	Other/A-1-b	12,000	26000	0.462	8.4	143.5
Below PCC Layer	3007	Soil Aggr Mix/A-1-b	10,000	38000	0.263	5.6	143.5
	3019	Soil Aggr Mix/A-1-a	6,500	59000	0.110	6.7	137.5

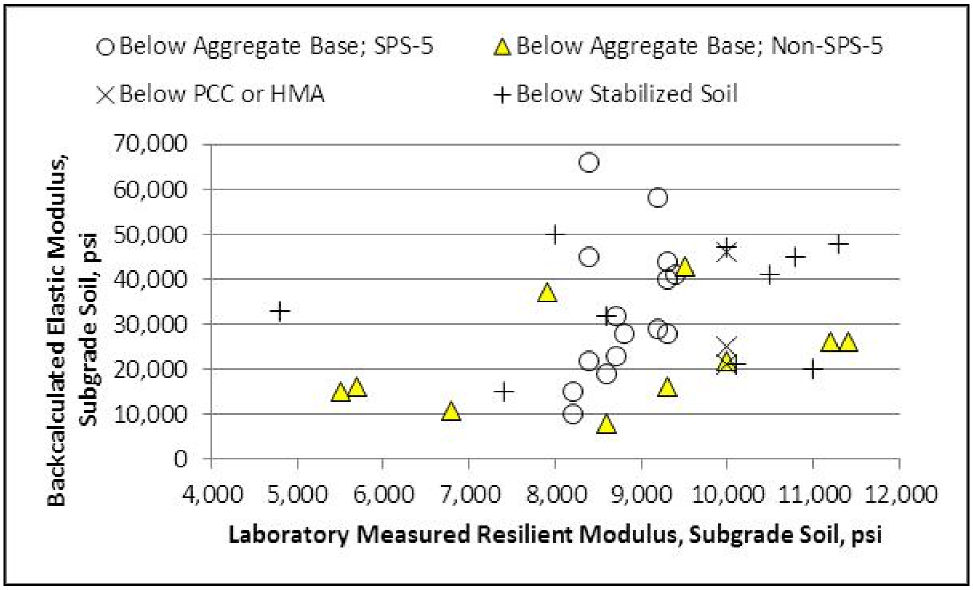

Figure 11—Laboratory-Derived Resilient Modulus Values Compared to the Field-Derived Backcalculated Elastic Modulus Values for the Subgrade Soils – Georgia LTPP Test Sections

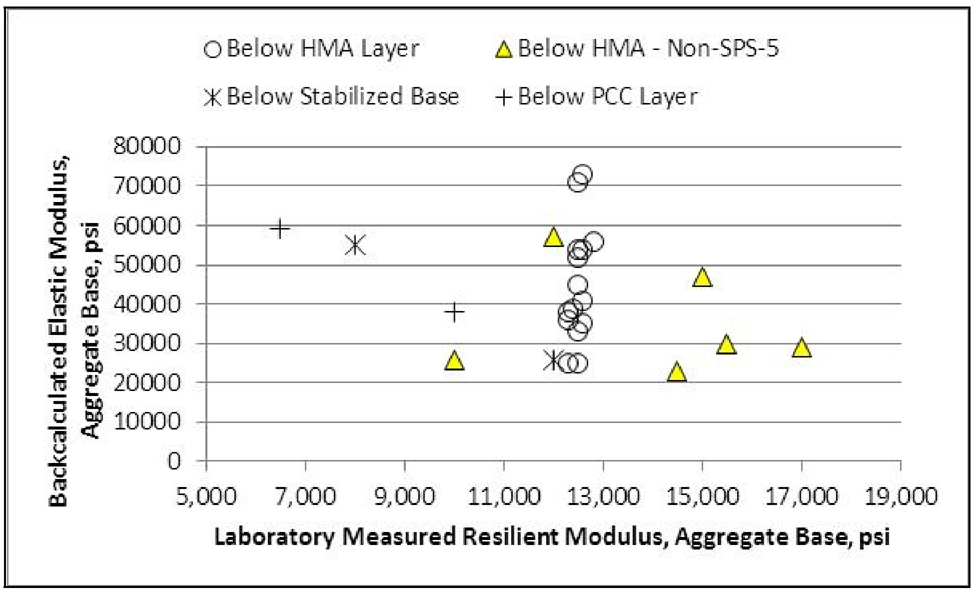

Figure 12—Laboratory-Derived Resilient Modulus Values Compared to the Field-Derived Backcalculated Elastic Modulus Values for the Aggregate Bases – Georgia LTPP Test Sections

Table 18—Average AASHTO c-Factors for the Georgia LTPP Test Sections

Layer Type	Location	C-Value or M_r/E_{FWD} Ratio	
		MEPDG MOP	Georgia LTPP Sites
Aggregate Base/Subbase	Between a Stabilized & HMA Layer	1.43	0.303
	Below a PCC Layer	1.32	0.187
	Below an HMA Layer	0.62	0.373
Subgrade-Embankment	Below a Stabilized Subgrade/Embankment	0.75	0.304
	Below an HMA or PCC Layer	0.52	0.365
	Below an Unbound Aggregate Base	0.35	0.404

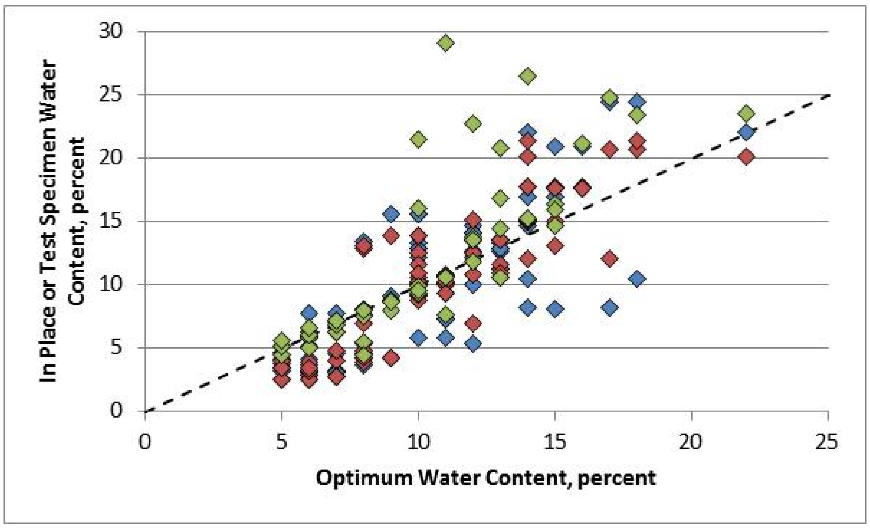

Figure 13—In Place Water Content Compared to the Optimum Water Content for the Georgia LTPP Test Sections

2.5 Initial Smoothness

The initial IRI is a required input to the MEPDG, but was only available for a few of the Georgia LTPP test sections. Thus, the initial value was backcast from the monitored IRI data, similar to the backcasting procedure used for the initial AADTT, with one major exception. Unlike for AADTT, IRI does not change significantly until distresses begin to occur, as illustrated in Figure 14 for a couple of SPS-5 test sections (sections 0503 and 0506). The IRI-time relationship for some time after construction is relatively flat, and only starts to increase after the occurrence of surface distress. The following equation was used to backcast the initial IRI values, which has been used in other studies.

$$IRI_t = IRI_i (e)^{g_1 \left(\frac{t}{20}\right)^{g2}} \qquad (2)$$

Where:

IRI_t = IRI measured at time t.
IRI_i = Initial IRI measured or estimated at time of construction.
t = Time or age of pavement, years.
g_1, g_2 = Regression constants determined from the monitored IRI-time values.

Figures 15 and 16 include examples of using the empirical IRI-time relationship to estimate the initial IRI for the older LTPP test sections. A summary of initial IRI values for all the LTPP sections is presented in Table 19.

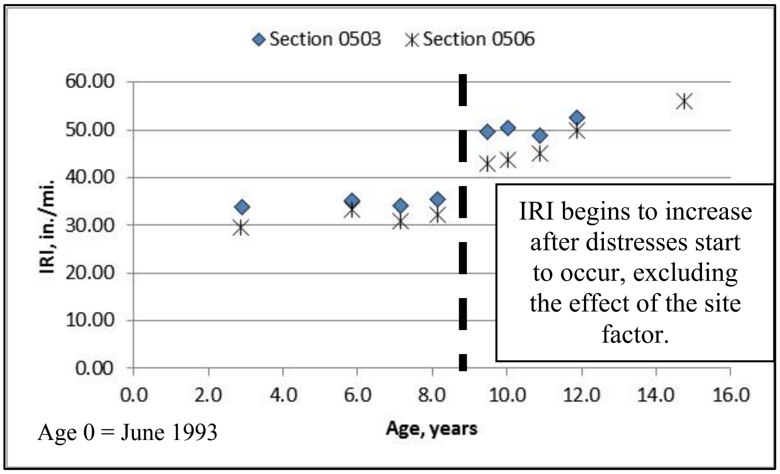

I-401
Bartow Co.
HMA Overlay:

- 0503-Dense graded mix with RAP.
- 0506-Dense graded mix without RAP.

Figure 14—IRI Measured over Time for Two of the Georgia SPS-5 Flexible Pavement Test Sections

2.6 Distress/Performance Data

Distress and IRI data were obtained from the LTPP database. Since MEPDG performance indicators measuring units was obtained from LTPP database, by default all the LTPP projects had distress/IRI measured and reported in units that are equivalent to the MEPDG distress predictions.

A diverse range of distress values are needed for verification and validation of the distress transfer functions. For instance, if the measured HMA alligator cracking and JPCP transverse cracking are significantly lower than GDOT’s design criteria, the accuracy and bias of the transfer function may not be well defined at the values that trigger major rehabilitation. This section of the interim report discusses the measured distresses and smoothness relative to established design criteria recommended in the MEPDG Manual of Practice.

2.6.1 Flexible Pavement and HMA Overlays

Table 20 includes a comparison of the MEPDG recommended design criteria and the magnitudes of the time-series distress and IRI data for the Georgia LTPP projects. The following paragraphs provide a brief discussion on the appropriateness of this data for use in validating the flexible pavement transfer functions.

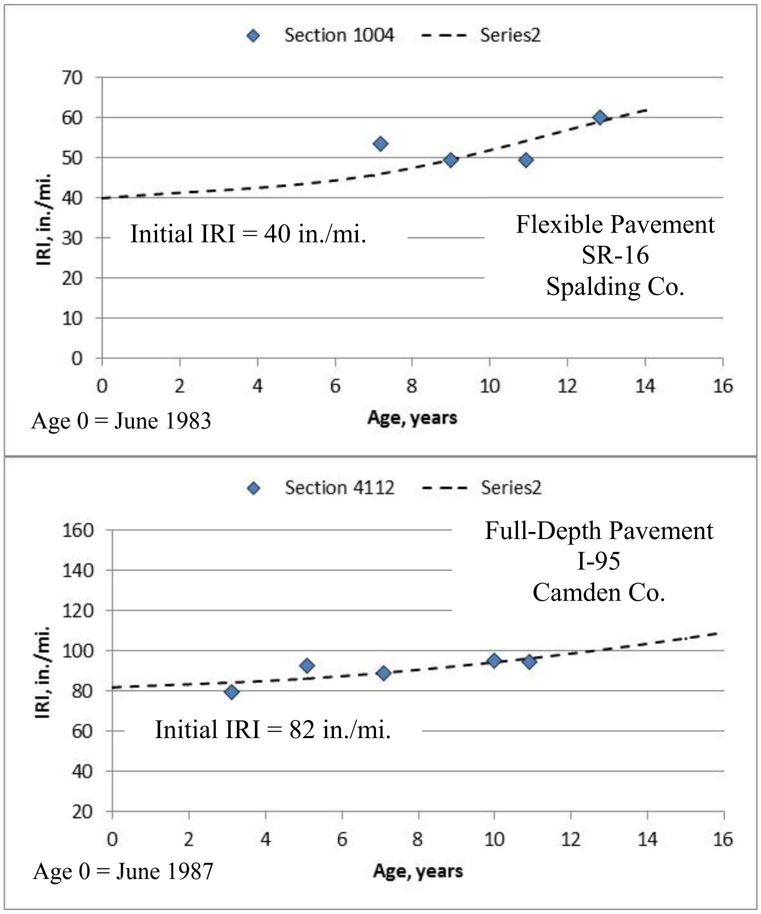

Figure 15—Illustration of the Process used to Backcast the Initial IRI for LTPP Test Sections, Flexible Pavements

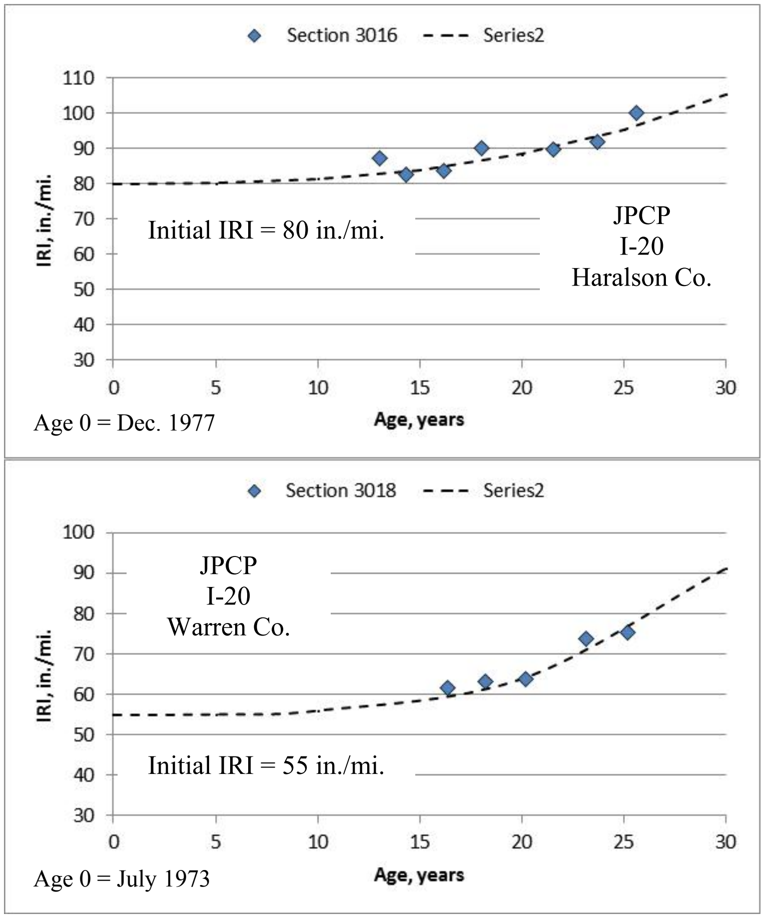

Figure 16—Illustration of the Process used to Backcast the Initial IRI for LTPP Test Sections, Rigid Pavements

Rut Depths

Figure 17 shows a histogram of the measured rut depths for all 14 LTPP flexible and semi-rigid pavement sites (see Table 2). Few of the LTPP rut depth measurements are above a rut depth of 0.4 inches. The measured rut depths generally cover a reasonable range of values, but the magnitude of the rutting is weighted towards the SPS-5 project because it contains 15 different test sections. The SPS-5 test sections with and without an overlay exhibit the greater amount of rut depth.

More importantly, the SPS-5 test sections have a high rate of rut depth increasing over time in comparison to the GPS test sections (see Figures 18 an 19). Figure18 illustrates the increase in rut depth for some of the SPS-5 test sections. As shown, some of the test sections exhibit rutting increasing at an increasing rate (for example; 0507 and 0509). Most of the GPS test sections exhibit consistently lower rut depths and the values remain relatively constant over time – even for the sections that exhibit the higher rut depths (for example; section 1031 for new construction in Figure 19). The SPS-5 consistently has a greater slope or incremental increase in measured rut depths over time. The first point plotted for the SPS-

5 sections is the measured rut depth on the existing pavement without any overlay. Only one of the other LTPP test sections exhibited a comparable magnitude of rutting – section 1031.

Table 19—Initial IRI Estimated for all LTPP Sections in Georgia

LTPP Section ID		Initial IRI, in/mi	LTPP Section ID	Initial IRI, in/mi
SPS-5 Test Sections; HMA Overlay	0502	33	3016- JPCP	80
	0503	34	3017- JPCP	78
	0504	30	3017- CPR	38
	0505	34	3018 – JPCP	55
	0506	30	3019 – JPCP	88
	0507	30	3020 – JPCP	84
	0508	42	3020 – HMA Overlay	85
	0509	33	4092 – Semi-Rigid	43
	0560	28	4093 – Semi-Rigid	44
	0561	30	4096 – Semi-Rigid	57
	0562	34	4096 – HMA Overlay	53
	0563	39	4111 – Flexible	45
	0564	30	4112 – Full-Depth	82
	0565	31	4113 – Full-Depth	62
	0566	41	4113 – HMA Overlay	40
1001-Flexible		50	4118 – CRC Overlay	35
1004-Flexible		40	4119 – Flexible	60
1005-Flexible		59	4420 – Semi-Rigid	58
1031-Flexible		42	4420 – HMA Overlay	49
1031-HMA Overlay		34	5023 – CRCP	80
3007-JPCP		110	7028 – HMA Overlay	63
3011-JPCP		65	7028 – HMA Overlay	38
3015 – JPCP		65		

The HMA mixtures or overlays placed along the SPS-5 project with and without RAP are believe to be exhibiting stripping or moisture damage which will result in much higher increases in rutting measured over time. All of the SPS-5 sections also have more alligator cracking than the other LTPP sections. The MEPDG assumes that HMA mixtures will not exhibit stripping or moisture damage. As such, the SPS-5 test sections should not be used to make revisions to the calibration coefficients, if moisture damage has occurred.

The other important observation from reviewing the rut depth time-series data is the total rutting measured on the conventional flexible pavements and semi-rigid pavements are about the same. The conventional flexible pavement structures do not exhibit significantly higher rut depths than the semi-rigid pavement structures. The MEPDG also assumes that little to no rutting will occur in the unbound layers below the cement treated base or soil cement layers. That being the case, it can be assumed that the majority of rutting is confined to the HMA layers of the LTPP test sections.

Table 20—Comparison of the Flexible Pavement Distress and IRI Magnitudes to the Design Criteria or Threshold Values included in the MEPDG Manual of Practice

Distress or Performance Indicator	Design Criteria in MEPDG Manual of Practice*	Median Distress Value	Range	
			Minimum	Maximum
Rut Depth. Inches	0.4 to 0.5	0.2	0.04	0.55
Area Fatigue Cracking, %	10 to 20	0	0	28
Transverse Cracking, ft./mi.	500 to 700	0	0	3,700
IRI or Smoothness, in./mi.	160 to 200	50	27.6	112.7
*The design criteria listed above are for an interstate or primary arterial roadway.				

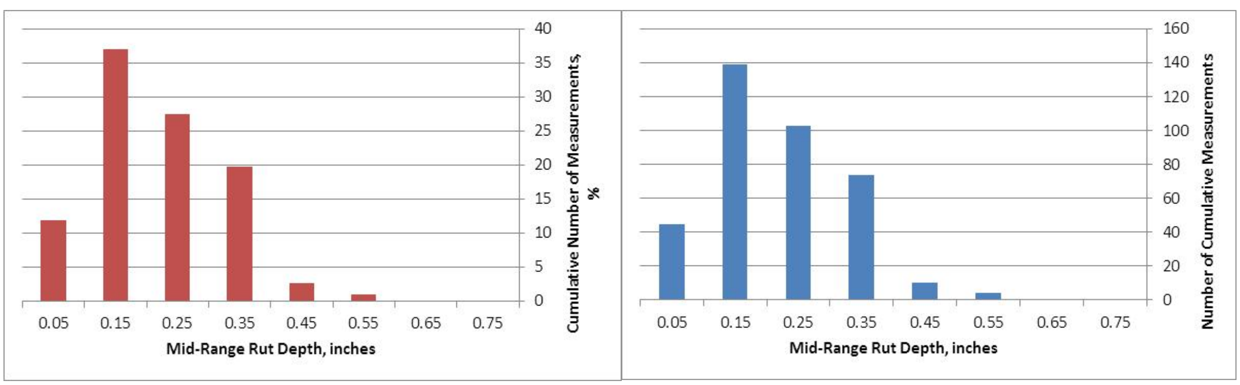

(a) (b)

Figure 17—(a) Histogram and (b) Normalized Frequency Distribution of Rut Depths for the LTPP Test Sections.

Area Fatigue Cracking (In Wheel Path Area)

Figure 20 shows a histogram of the measured area fatigue cracking in the wheel paths for all 14 LTPP flexible and semi-rigid pavement sites. Few of the LTPP fatigue cracking measurements are greater than a total lane area of 5 percent; most of the area cracking is less than 2 percent (see Table 20).

More importantly, area fatigue cracking has only occurred on the LTPP SPS-5 project. The SPS-5 sections have the highest truck traffic by far than any other section in GA. None of the other test sections exhibit wheel path alligator cracking. As noted above, moisture damage is believed to have occurred on the SPS-5 test sections which could explain the cracking confined to these test sections. That being the case, the SPS-5 test sections need to be treated as an anomaly judging the accuracy of the transfer functions.

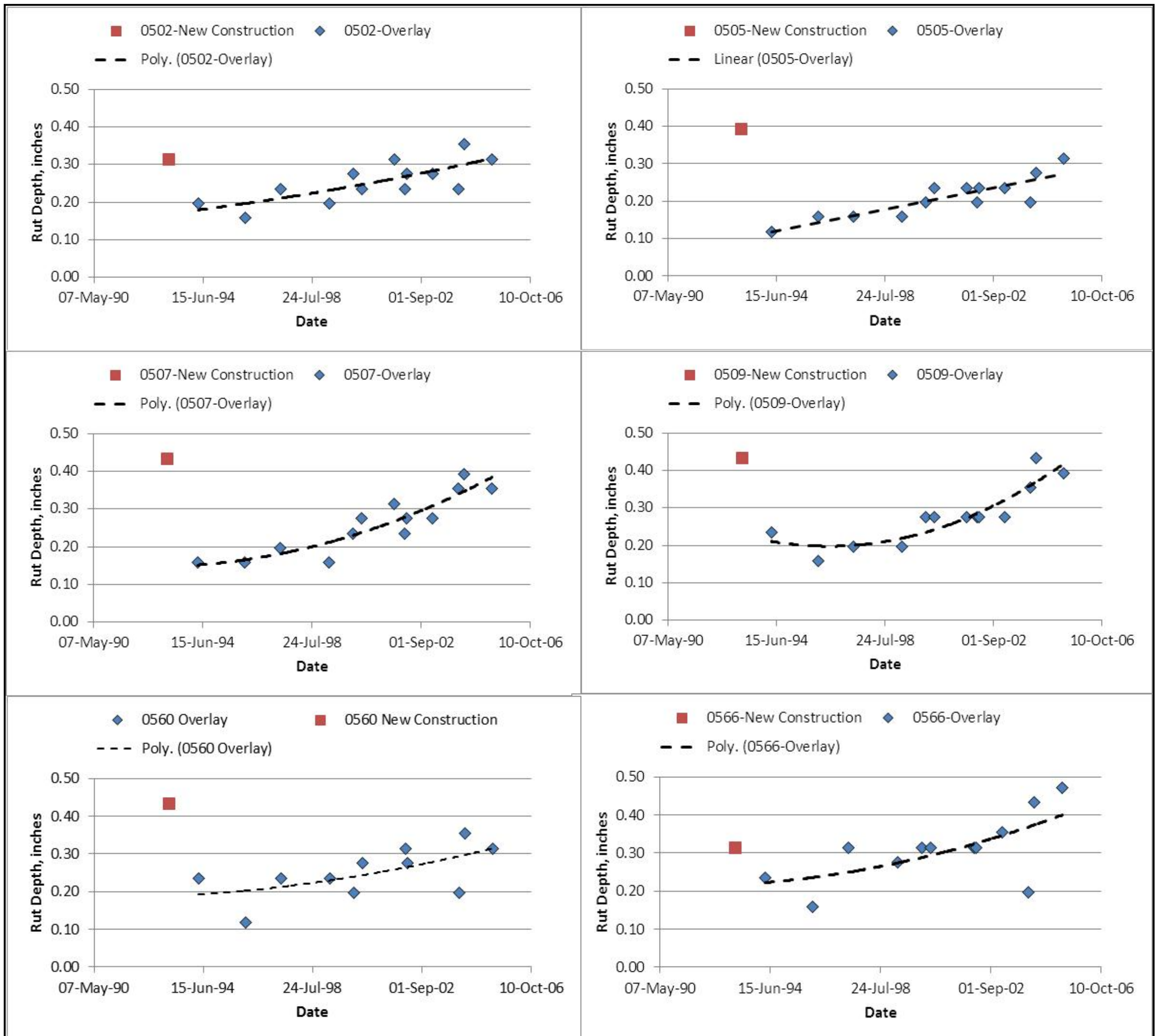

I-401
Bartow County
Original Construction: All sections are deep-strength HMA pavements.
Overlays include mixtures with and without RAP.

Figure 18—Rut Depth Time-Series Data for the Georgia SPS-5 Test Sections

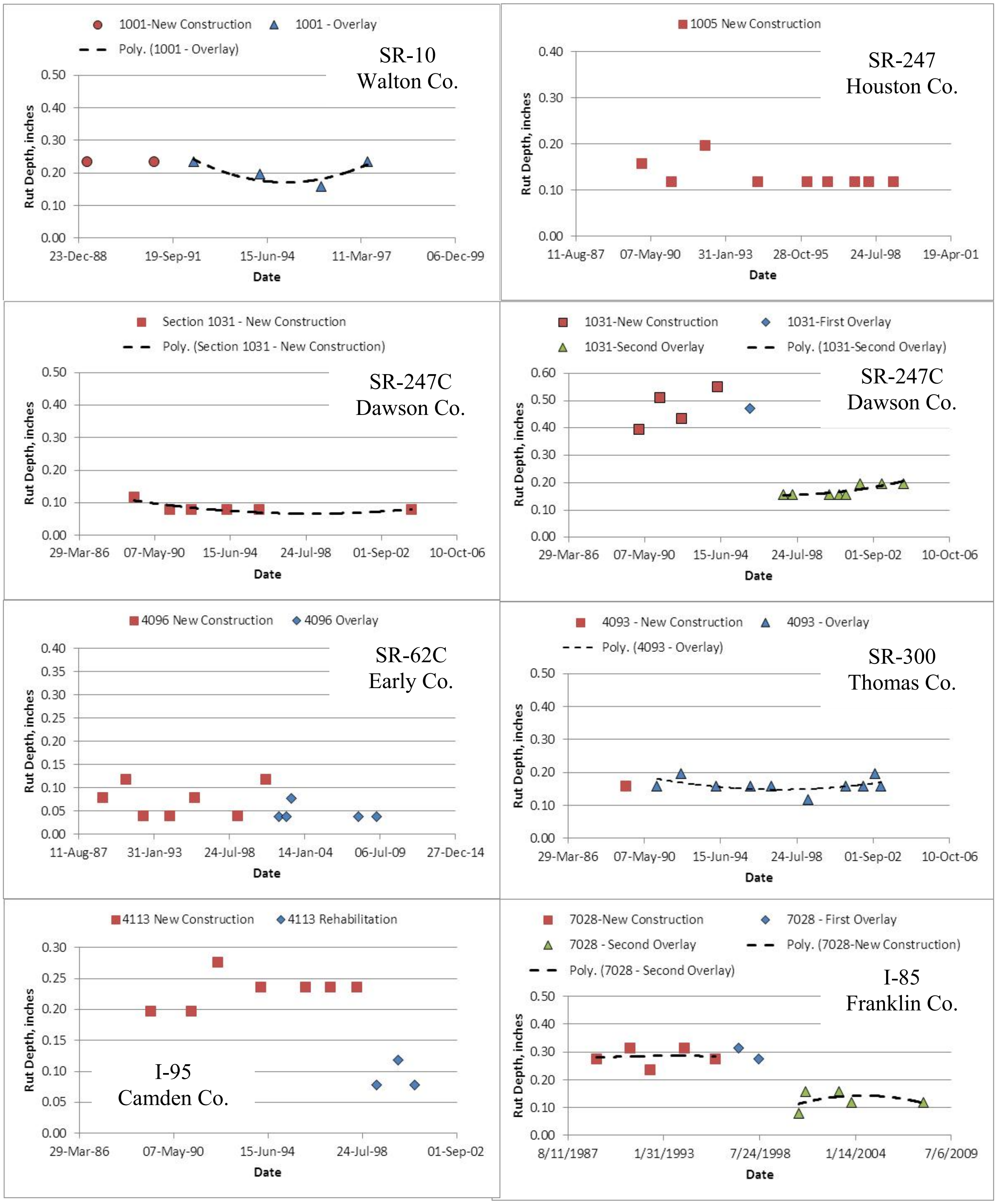

Figure 19—Rut Depth Time-Series Data for the Georgia Non-SPS-5 Test Sections

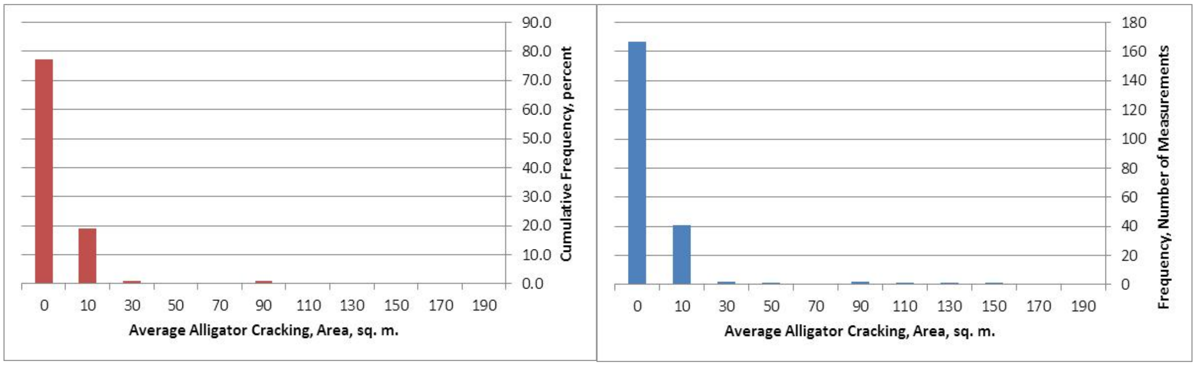

(a) (b)

Figure 20—(a) Histogram and (b) Normalized Frequency Distribution of the Area of Fatigue Cracking for the LTPP Test Sections

Transverse Cracking

Figure 21 provides a histogram of the length of transverse cracking measurements on the Georgia LTPP test sections. Very few of the LTPP test sections exhibit any transverse cracking, with most measurements being less than 20 meters in length. Transverse cracking is not an issue for the LTPP test sections.

IRI or Smoothness

Figure 22 provides a histogram of thee IRI or smoothness measurements on the Georgia LTPP test sections. All of the IRI values are less than 120 in./mi. which is still considered smooth. Based on LTPP, it appears the threshold values used by Georgia in maintaining their roadway system are lower than those included in Table 18.

Summary

Excluding the SPS-5 test sections, few of the other LTPP sections are exhibiting any distresses that approach the design criteria listed in Table 18. As such, it will be difficult to conclusively accept or reject the experimental hypothesis and in revising the global calibration coefficients.

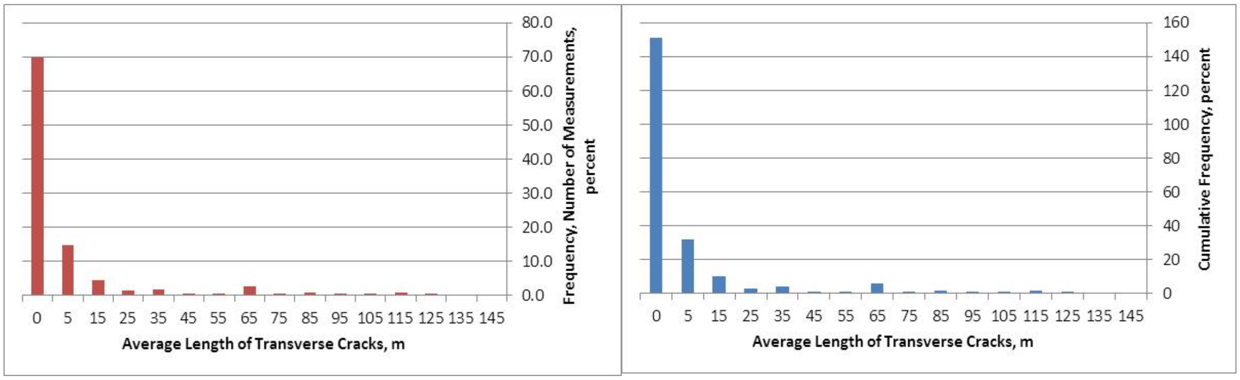

(a) (b)

Figure 21—(a) Histogram and (b) Normalized Frequency Distribution of the Length of Transverse Cracks for the LTPP Test Sections

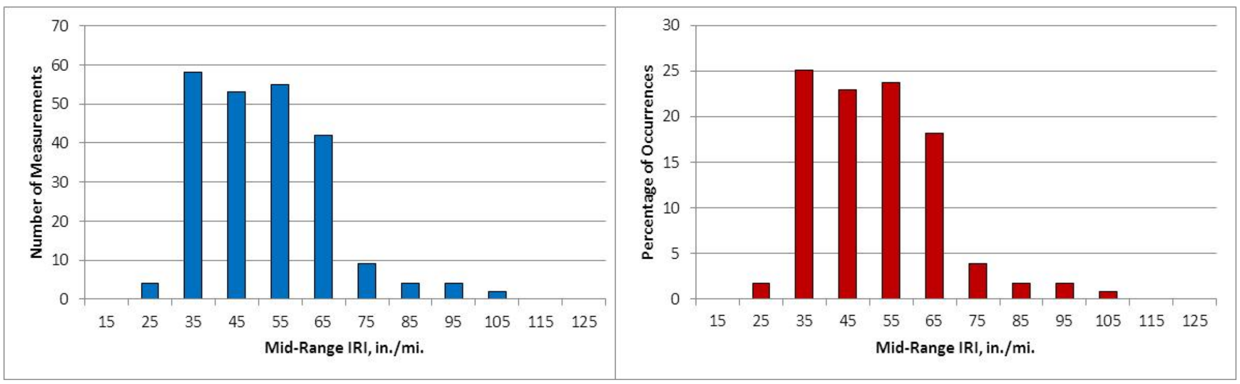

(a) (b)

Figure 22—(a) Histogram and (b) Normalized Frequency Distribution of IRI Values for the LTPP Test Sections

2.6.2 Rigid Pavement and PCC Overlays

A summary of the magnitudes of time-series distress/IRI from the identified LTPP projects with mean and range of values for each distress type and IRI is presented in Table 21. Figures 23 through 31 summarize the results of the comparison between sites. As shown, the only distress with levels of distress that approach the design criteria is the transverse cracking on the HMA overlay of JPCP and it is expected that most of these cracks are really joint reflection cracks. The following briefly summarizes the magnitude of rigid pavement distresses.

- Almost none of the LTPP test sections exhibit any transverse cracking of the JPCP slabs. Thus, making any revisions to the calibration coefficients will be difficult.
- Mean joint faulting is also considered low for most of the JPCP test sections.
- The IRI values are significantly lower than the design criteria or threshold values.

- One of the CRCP projects exhibit a higher amount of punchouts, but only two projects are available for use under the LTPP program.

Table 21—Comparison of Range of Distress/IRI Values with Design Criteria or Threshold Values

Pavement Type	Distress or Performance Indicator	Typical Distress Threshold in Local Calibration Guide	Median Value	Range	
				Minimum	Maximum
JPCP	Transverse cracking, percent slabs cracked	10	0	0	28
	Transverse joint faulting, in	0.15	0.0374	0	0.1417
	IRI, in/mi	160	93	34	124
New CRCP /Unbonded CRCP over JPCP	CRCP Punchouts, number per mile	6	0	0	21.1
	IRI, in/mile	160	43	36	91
AC overlaid JPCP	Alligator cracking, percent lane area	10	0	0	0
	Transverse “thermal” cracking, ft/mi	1000	1271	0	2411
	Rutting, in	0.5	0.2	0.08	0.28
	IRI, in/mi	160	57	30	71
	Transverse cracking, percent slabs cracked	10	0	0	0

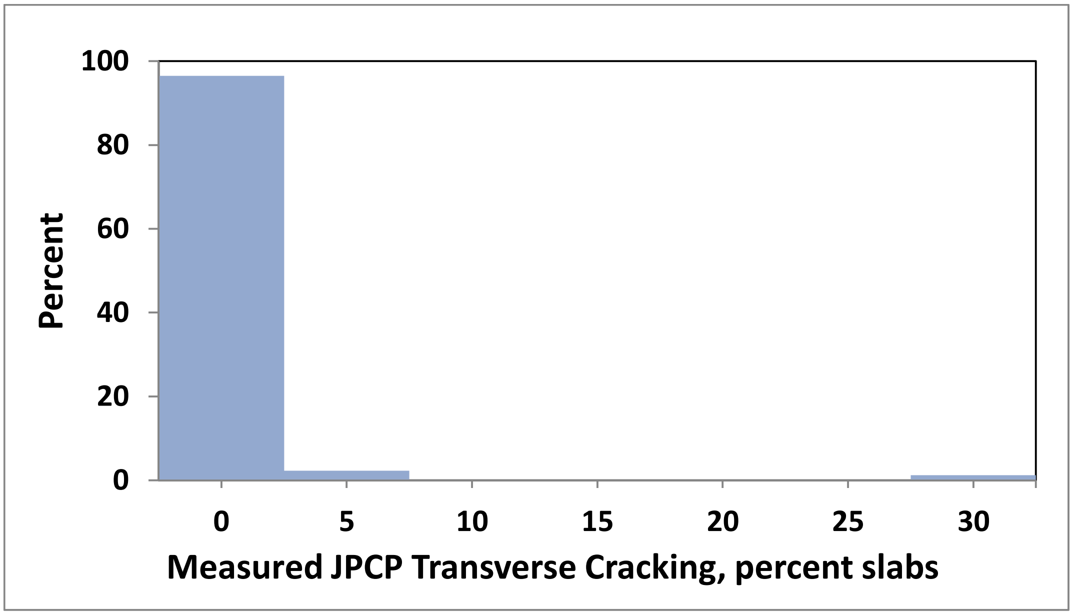

Figure 23—Histogram of Measured Transverse Cracking for LTPP New JPCP Projects in Georgia

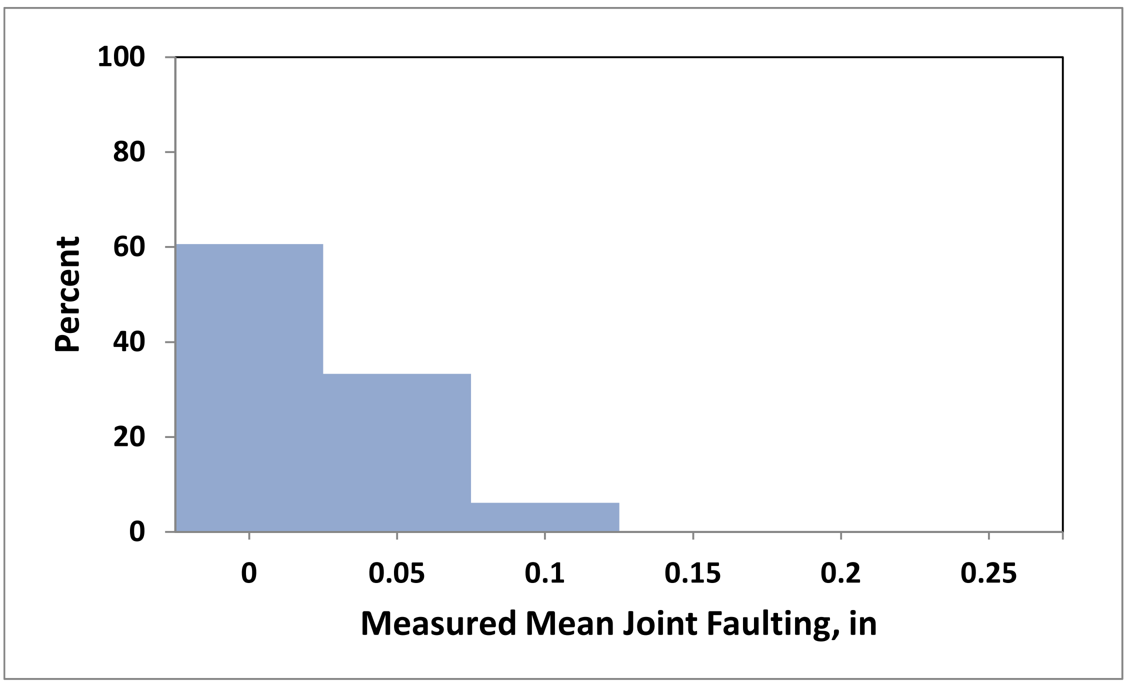

Figure 24—Histogram of Measured Mean Joint Faulting for LTPP New JPCP Projects in Georgia

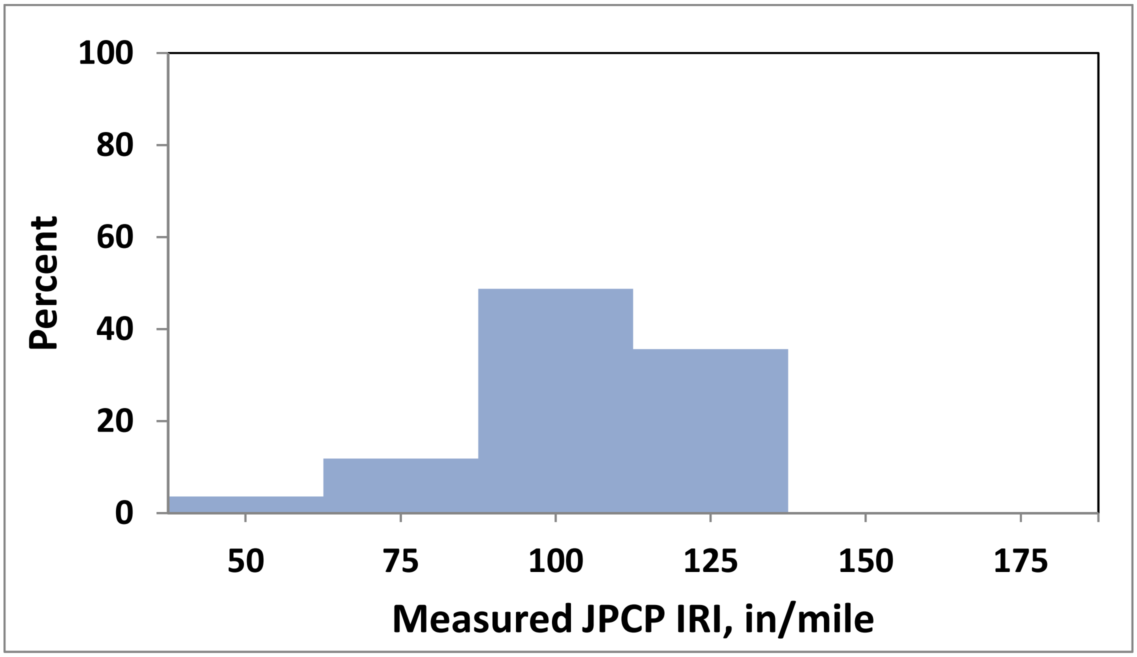

Figure 25—Histogram of Measured IRI for LTPP New JPCP Projects in Georgia

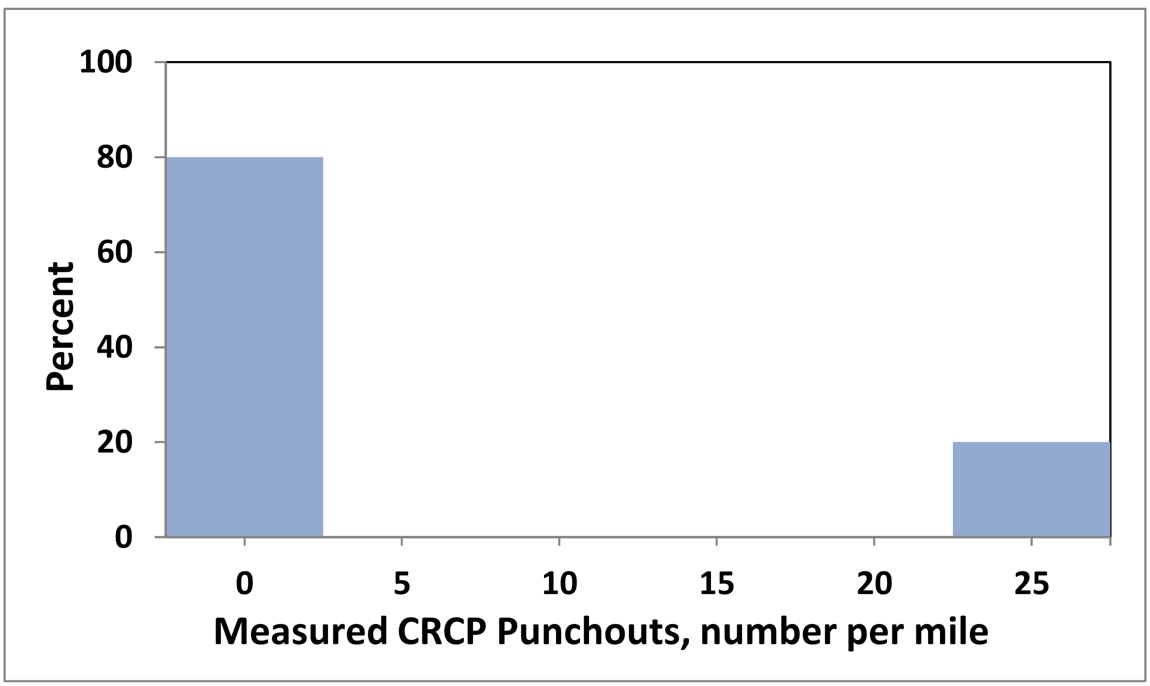

Figure 26—Histogram of Measured Punchouts for LTPP CRCP Projects in Georgia

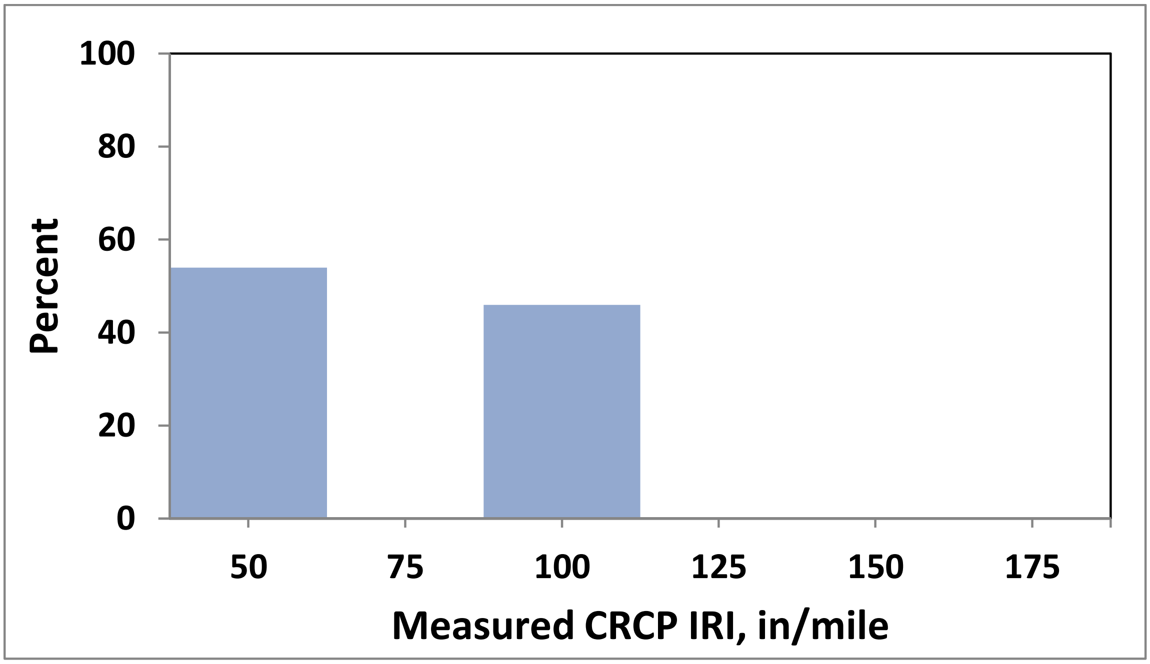

Figure 27—Histogram of Measured IRI for LTPP CRCP Projects in Georgia

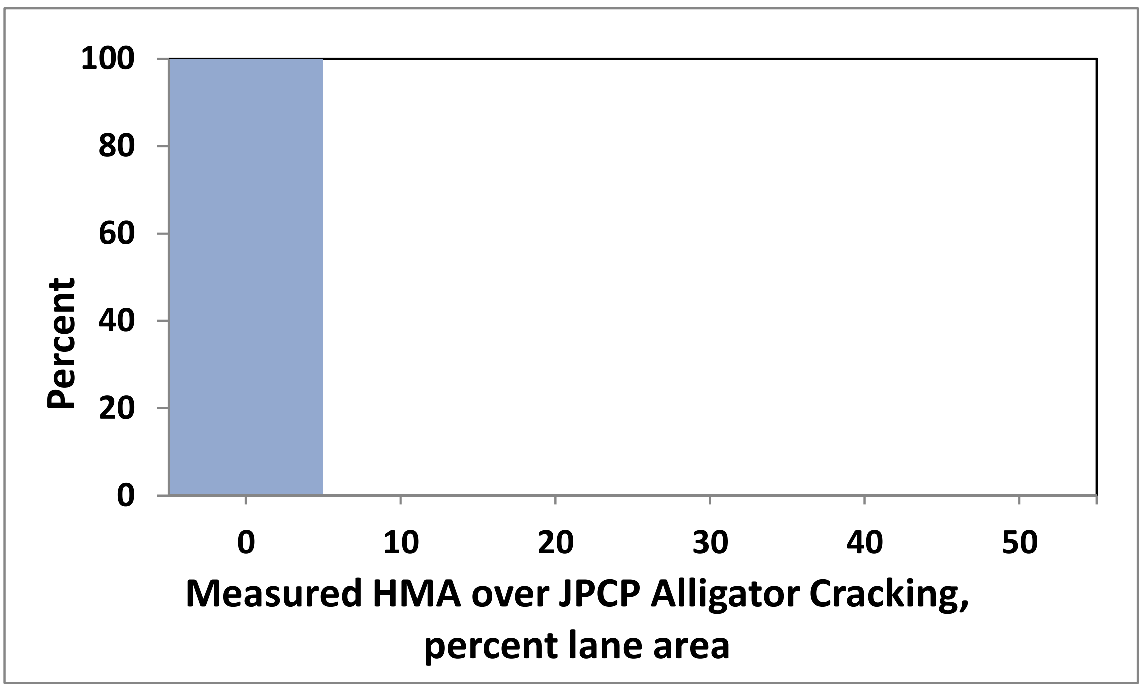

Figure 28—Histogram of Measured Alligator Cracking for LTPP HMA over JPCP Projects in Georgia

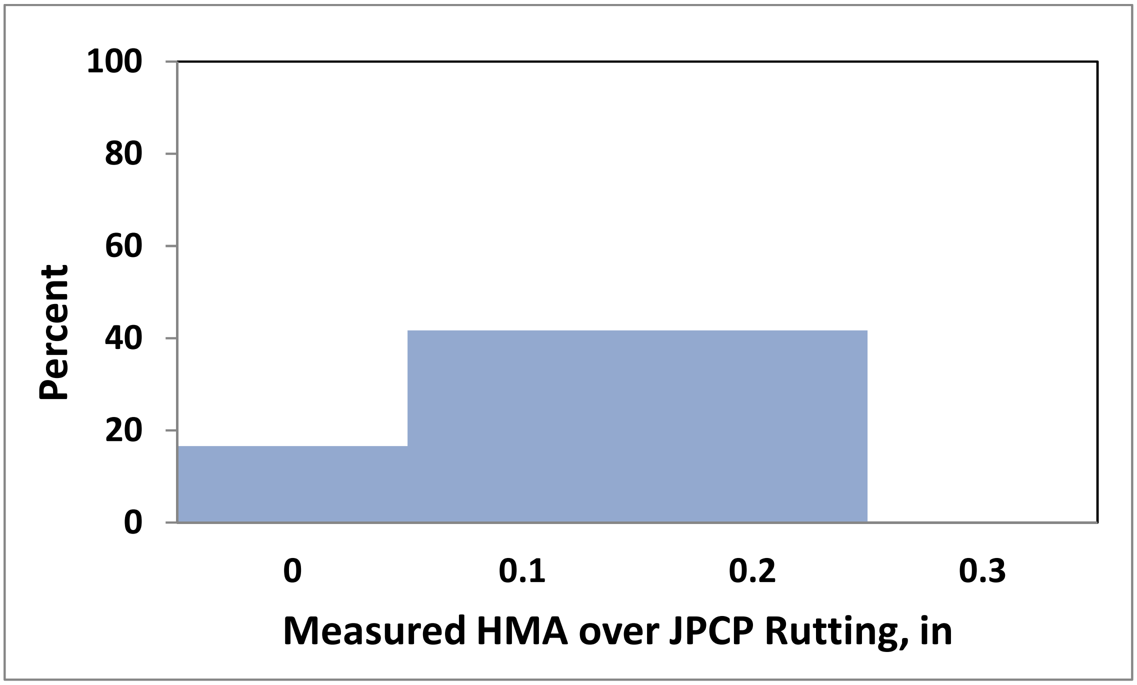

Figure 29—Histogram of Measured Rutting for LTPP HMA over JPCP Projects in Georgia

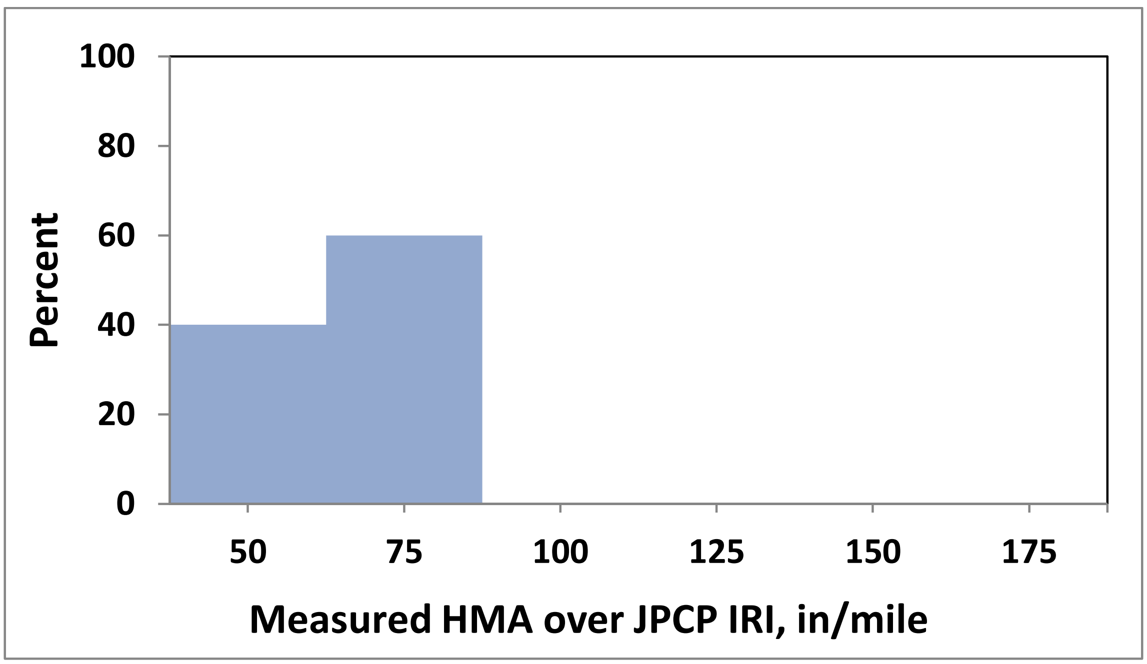

Figure 30—Histogram of Measured IRI for LTPP HMA over JPCP Projects in Georgia

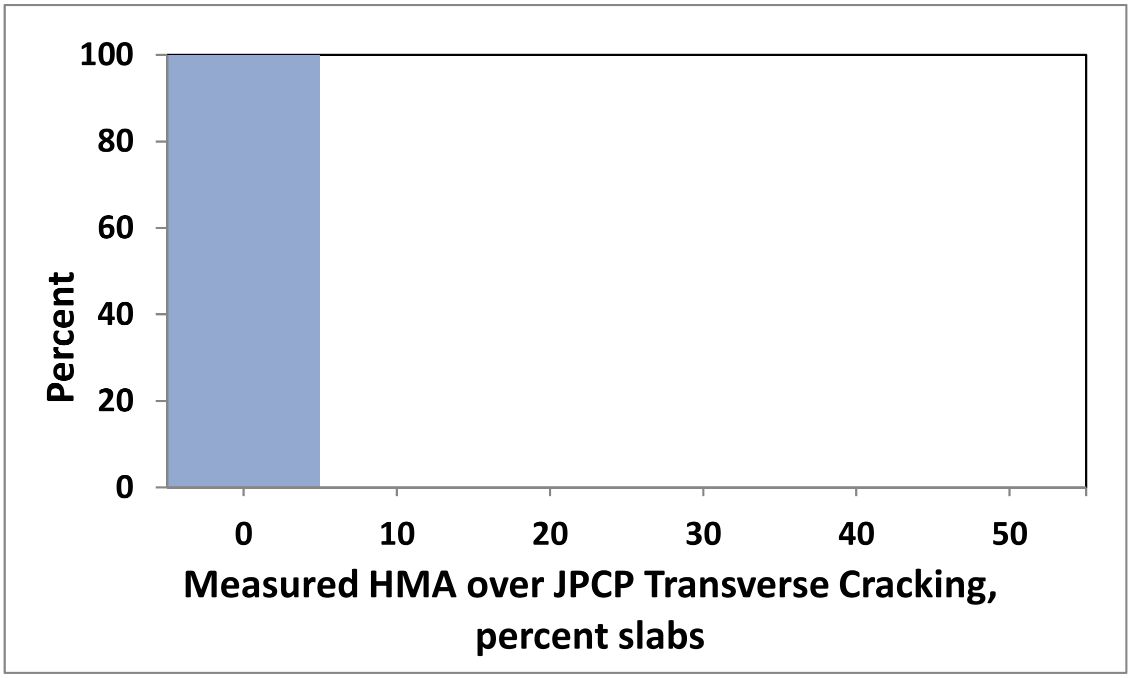

Figure 31—Histogram of Measured JPCP Transverse Cracking for LTPP HMA over JPCP Projects in Georgia

III. PREDICTED DISTRESSES – FLEXIBLE PAVEMENTS AND HMA OVERLAYS

Validation of the MEPDG "global" calibration coefficients of the flexible pavement transfer functions for Georgia conditions consisted of the running M-E Pavement for the Georgia LTPP projects and evaluating goodness-of-fit and bias for 32 LTPP test sections. The input values used in predicting pavement distress of each test section were discussed and identified under section 2.

The predicted values are compared to the observed or measured values over time to determine if the transfer function exhibits significant bias and determine the standard error. These results are used to confirm or reject the experimental hypothesis provided in section 1. The AASHTO MEPDG Local Calibration Guide (AASHTO, 2010) recommends both the intercept and slope of the relationship between the predicted and measured values be used to evaluate the null hypothesis (slope = 1 and intercept = 0). If the hypothesis is rejected for either test (the intercept or slope), the results from the confirmation runs are used with additional calibration sites to revise the coefficients of the distress transfer functions (this is part of Task 3, see Section 1).

3.1 Rut Depth Transfer Function

Two transfer functions are used to predict the total rut depth of flexible pavements and HMA overlays: one for the HMA layers and the other one for all unbound aggregate base layers and subgrades.

The HMA calibrated transfer function was based on laboratory repeated load plastic deformation tests and is shown below.

$$\Delta_{p(HMA)} = \varepsilon_{p(HMA)} h_{HMA} = \beta_{1r} k_z \varepsilon_{r(HMA)} 10^{k_{1r}} n^{k_{2r}\beta_{2r}} T^{k_{3r}\beta_{3r}} \tag{3}$$

Where:

$\Delta_{p(HMA)}$ = Accumulated permanent or plastic vertical deformation in the HMA layer/sublayer, in.

$\varepsilon_{p(HMA)}$ = Accumulated permanent or plastic axial strain in the HMA layer/sublayer, in/in.

$\varepsilon_{r(HMA)}$ = Resilient or elastic strain calculated by the structural response model at the mid-depth of each HMA sublayer, in/in.

$h_{(HMA)}$ = Thickness of the HMA layer/sublayer, in.

n = Number of axle load repetitions.

T = Mix or pavement temperature, °F.

k_z = Depth confinement factor.

$k_{1r,2r,3r}$ = Global field calibration parameters (from the NCHRP 1-40D recalibration; k_{1r} = -3.35412, k_{2r} = 0.4791, k_{3r} = 1.5606).

$\beta_{\square r}$, β_{2r}, β_{3r}, = Local or mixture field calibration constants; for the global calibration, these constants were all set to 1.0.

$$k_z = (C_1 + C_2 D)0.328196^D \tag{4}$$

$$C_1 = -0.1039(H_{HMA})^2 + 2.4868 H_{HMA} - 17.342 \tag{5}$$

$$C_2 = 0.0172(H_{HMA})^2 - 1.7331 H_{HMA} + 27.428 \tag{6}$$

D = Depth below the surface, in.

H_{HMA} = Total HMA thickness, in.

Equation 7 shows the field-calibrated transfer function for the unbound layers and subgrade.

$$\Delta_{p(soil)} = \beta_{s1} k_{s1} \varepsilon_v h_{soil} \left(\frac{\varepsilon_o}{\varepsilon_r} \right) e^{-\left(\frac{\rho}{n}\right)^{\beta}} \tag{7}$$

Where:

$\Delta_{p(Soil)}$ = Permanent or plastic deformation for the layer/sublayer, in.

n = Number of axle load applications.

ε_o = Intercept determined from laboratory repeated load permanent deformation tests, in/in.

ε_r = Resilient strain imposed in laboratory test to obtain material properties ε_o, β, and ρ, in/in.

ε_v = Average vertical resilient or elastic strain in the layer/sublayer and calculated by the structural response model, in/in.

h_{Soil} = Thickness of the unbound layer/sublayer, in.

k_{s1} = Global calibration coefficients; k_{s1}=1.673 for granular materials and 1.35 for fine-grained materials.

β_{s1} = Local calibration constant for the rutting in the unbound layers; the local calibration constant was set to 1.0 for the global calibration effort.

$$Log\beta = -0.61119 - 0.017638(W_c) \tag{8}$$

$$\rho = 10^9 \left(\frac{C_o}{\left(1 - (10^9)^\beta\right)} \right)^{\frac{1}{\beta}} \tag{9}$$

$$C_o = Ln\left(\frac{a_1 M_r^{b_1}}{a_9 M_r^{b_9}} \right) = 0.0075 \tag{10}$$

W_c = Water content, percent.
M_r = Resilient modulus of the unbound layer or sublayer, psi.
$a_{1,9}$ = Regression constants; a_1=0.15 and a_9=20.0.
$b_{1,9}$ = Regression constants; b_1=0.0 and b_9=0.0.

The rut depths for all HMA surfaced pavements (see Table 2 and Appendix A) were calculated with *M-E Pavement* using the input values discussed and identified in section 2. Two different materials characterization procedures were used for predicting rutting: (1) laboratory measured resilient modulus values at equivalent stress states; and (2) in place volumetric conditions and backcalculated elastic modulus values.

Table 22 compares the bias and standard error for the predicted rut depth of the two sets of data or inputs for characterizing the unbound layers. As shown, there is a significant difference between the two characterization procedures. There is a significant positive bias for the predict rut depths when using the laboratory equivalent resilient modulus values at the in place stress state and volumetric conditions of water content and dry density, and a much lower bias when using the backcalculated elastic modulus values.

Table 22—Comparison of Results from Using Laboratory Measured Resilient Modulus and Backcalculated Elastic Modulus Values for Predicting Rut Depths

Pavement Type	Bias Value, in.		Standard Error, in.	
	Lab Measured Modulus Value	**Backcalculated Modulus Value**	**Lab Measured Modulus Value**	**Backcalculated Modulus Value**
Full Depth Structures	0.412	0.0883	0.0776	0.0523
Pavement with Aggregate Base	0.206	0.0703	0.111	0.130
HMA Overlay of Flexible Pavements	0.0718	-0.0158	0.121	0.0739
SPS-5; HMA Overlay with RAP	0.363	0.0235	0.0731	0.0518
SPS-5; HMA Overlay without RAP	0.366	0.0260	0.0729	0.0526

Figure 32 includes a comparison of the predicted versus measured rut depth using the global calibration coefficients (see equations 3 and 7), and a comparison of the predicted rut depth and residual error. As shown in Table 22 and Figure 32, there is a significant bias in the predicted rut depths and the goodness-of-fit is poor. In addition, the residual error is dependent on or related to the predicted rut depths. The bias is significantly lower for the predicted rut depths when using the backcalculated elastic modulus values. Figure 33 includes the same information as graphically presented in Figure 32, except the predicted rut depths are based on using the backcalculated elastic layer modulus values.

As stated in section 2, the LTPP SPS-5 test sections consistently exhibit higher rut depth rates and magnitudes. The GPS overlay test sections exhibit a significantly lower standard error as compared to the SPS-5 test sections and those sections classified as full-depth and conventional pavement structures. This observation or finding is similar to other local calibration studies. It is expected that the MEPDG is over predicting the rut depth in the unbound layers of new pavement construction and moisture damage is believed to have occurred in the HMA mixtures of the SPS-5 sections. Figure 34 includes some examples comparing the predicted and measured rut depths for four of the LTPP test sections for the flexible pavements and HMA overlays.

Removing the SPS-5 test sections from the statistical comparison, however, still results in a significant bias in terms of the intercept. The following lists some of the findings from the comparison of the predicted and measured rut depths.

- The slope of the GPS overlay test sections is significantly different from 1.0.
- The intercept for the full-depth structures are also significantly different from 1.0. The reason for this observation is related to the HMA thickness and resilient modulus of the subgrade soils.
- The conventional flexible pavement structures (HMA over an aggregate base) are highly variable. The reason for this observation is related to the HMA thickness and moisture content of the unbound aggregate base and subgrade.

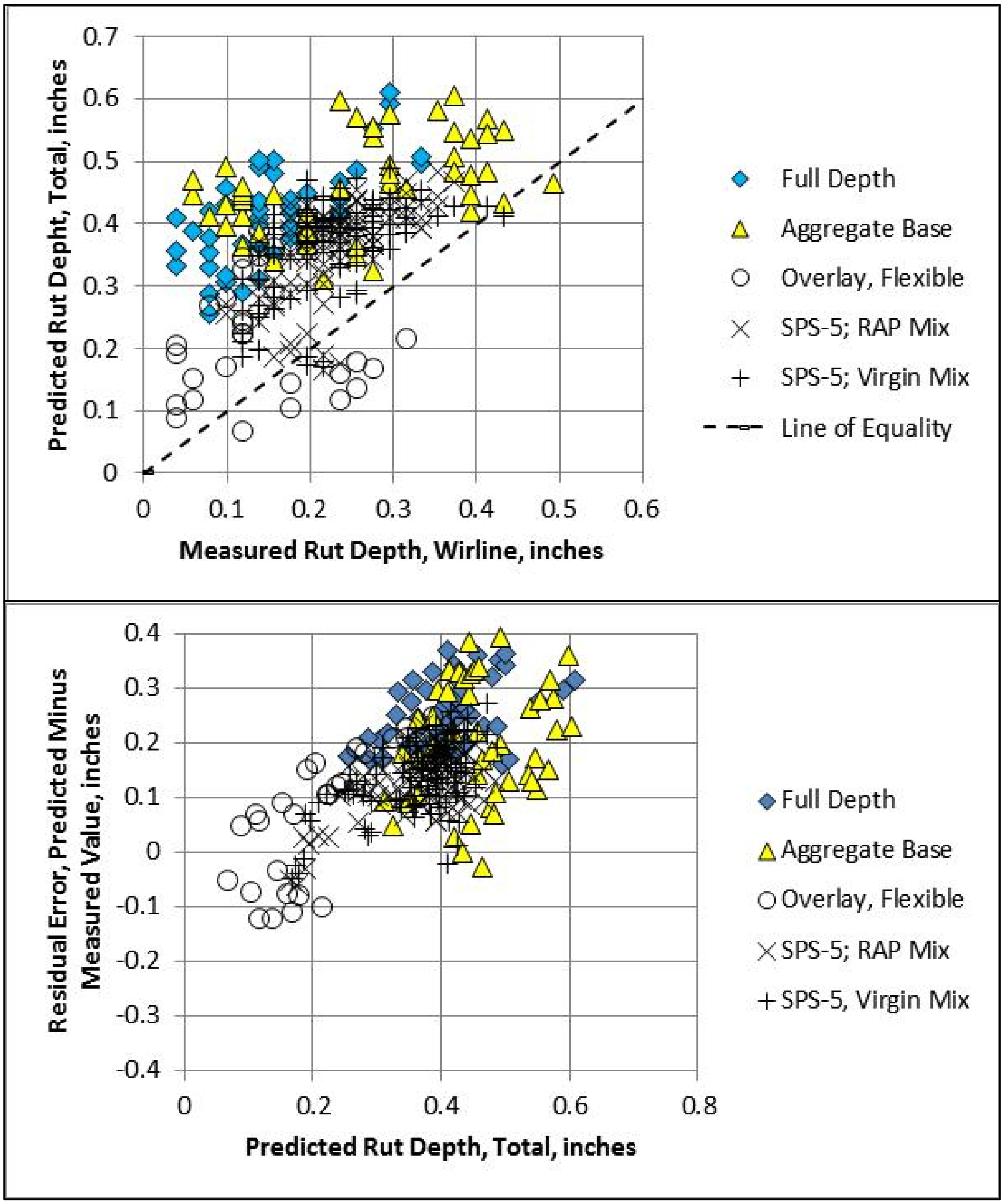

Figure 32—Predicted versus Measured Rut Depth for different Pavement Types based on Using Laboratory Measured Resilient Modulus Values for the Unbound Layers

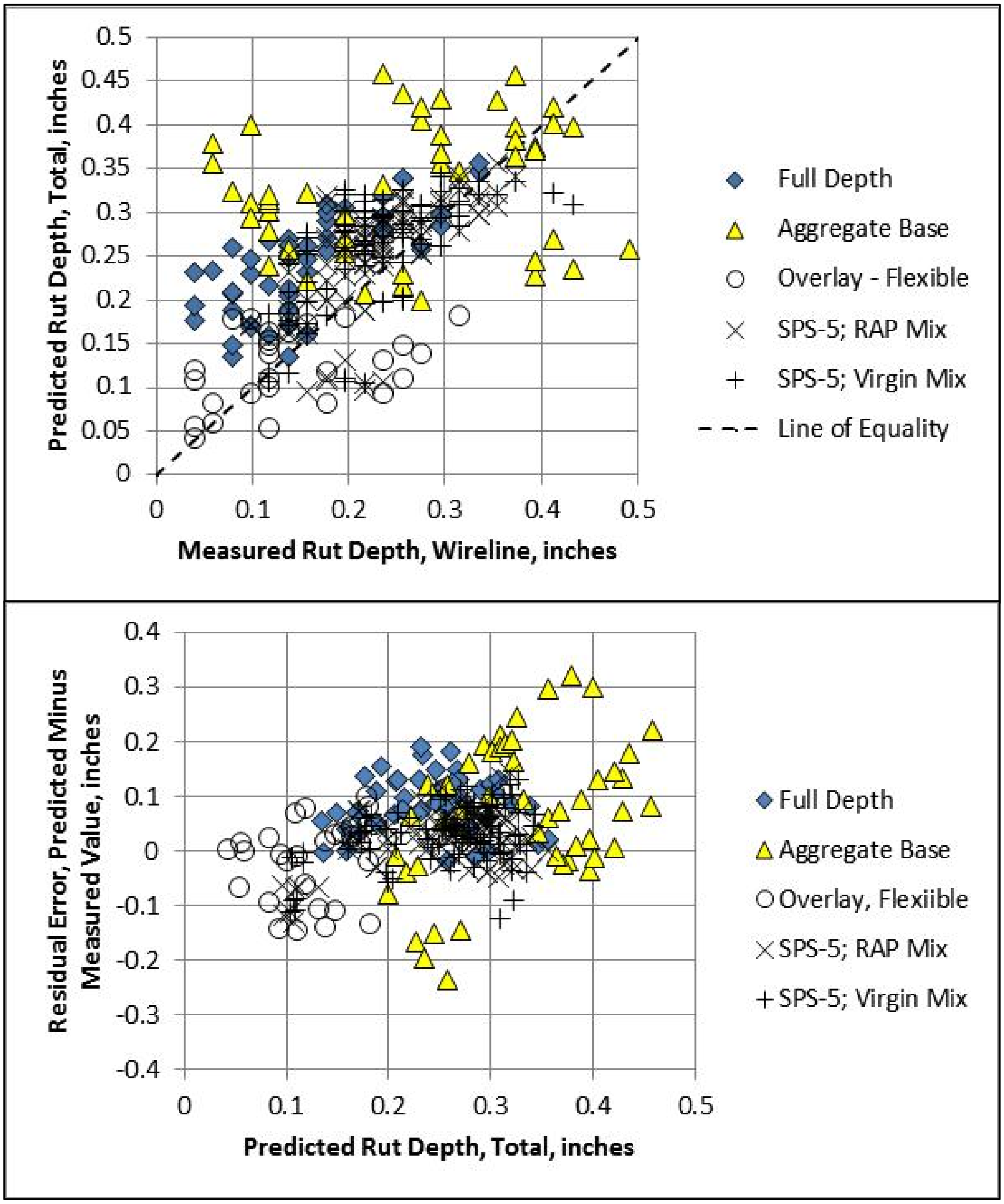

Figure 33—Predicted versus Measured Rut Depth for different Pavement Types based on Using Backcalculated Elastic Modulus Values for the Unbound Layers

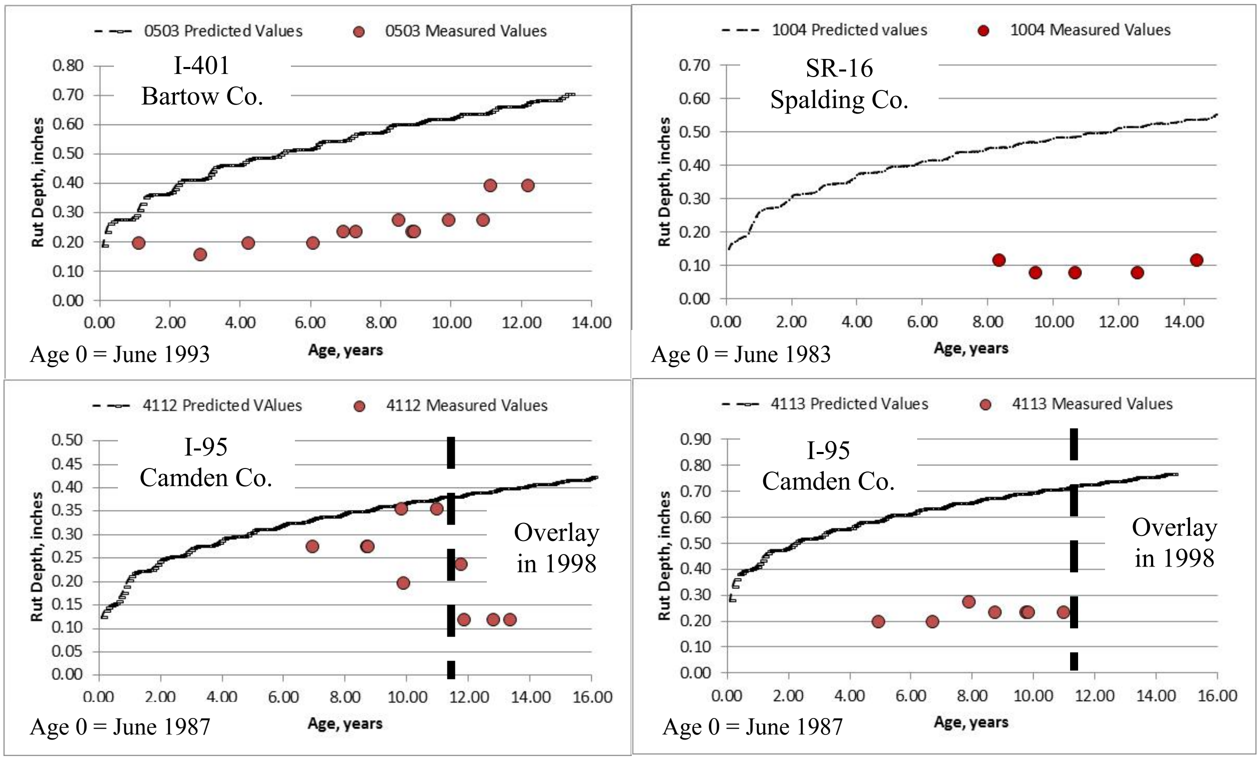

Figure 34—Predicted versus Measured Rut Depth for Selected LTPP Flexible Pavement and HMA Overlay Test Sections

3.2 Bottom-Up Area Fatigue Cracking Transfer Function

Two types of load-related cracks are predicted by the MEPDG, alligator cracking and longitudinal cracking. The MEPDG assumes alligator or area cracks initiate at the bottom of the HMA layers and propagate to the surface with continued truck traffic, while longitudinal cracks are assumed to initiate at the surface. The MEPDG Manual of Practice recommends that top-down or longitudinal cracking transfer function not be used to make design revisions, because of the debate and controversy on the appropriateness of the mechanism for surface initiated cracks and field investigations were not used to confirm longitudinal cracks initiated at the surface.

The allowable number of axle load applications needed for the incremental damage index approach to predict both types of load related cracks (alligator and longitudinal) is shown below.

$$N_{f-HMA} = k_{f1}(C)(C_H)\beta_{f1}(\varepsilon_t)^{k_{f2}\beta_{f2}}(E_{HMA})^{k_{f3}\beta_{f3}} \quad (11)$$

Where:

- $N_{f\text{-}HMA}$ = Allowable number of axle load applications for a flexible pavement and HMA overlays.
- ε_t = Tensile strain at critical locations and calculated by the structural response model, in/in.
- E_{HMA} = Dynamic modulus of the HMA measured in compression, psi.

k_{f1}, k_{f2}, k_{f3} = Global field calibration parameters (from the NCHRP 1-40D re-calibration; k_{f1} = 0.007566, k_{f2} = -3.9492, and k_{f3} = -1.281).
β_{f1}, β_{f2}, β_{f3} = Local or mixture specific field calibration constants; for the global calibration effort, these constants were set to 1.0.

$$C = 10^M \tag{12}$$

$$M = 4.84\left(\frac{V_{be}}{V_a + V_{be}} - 0.69\right) \tag{13}$$

V_{be} = Effective asphalt content by volume, percent.
V_a = Percent air voids in the HMA mixture.
C_H = Thickness correction term, dependent on type of cracking.

$$C_H = \frac{1}{0.000398 + \dfrac{0.003602}{1 + e^{(11.02 - 3.49 H_{HMA})}}} \tag{14}$$

H_{HMA} = Total HMA thickness, in.

The cumulative damage index (DI) is determined by summing the incremental damage indices over time, as shown below.

$$DI = \sum (\Delta DI)_{j,m,l,p,T} = \sum \left(\frac{n}{N_{f-HMA}}\right)_{j,m,l,p,T} \tag{15}$$

Where:
n = Actual number of axle load applications within a specific time period.
j = Axle load interval.
m = Axle load type (single, tandem, tridem, quad, or special axle configuration.
l = Truck type using the truck classification groups included in the MEPDG.
p = Month.
T = Median temperature for the five temperature intervals or quintiles used to subdivide each month, °F.

The area of alligator cracking and length of longitudinal cracking are calculated from the total damage over time using different transfer functions. The relationship used to predict the amount of alligator cracking on an area basis, FC_{Bottom}, is shown below.

$$FC_{Bottom} = \left(\frac{1}{60}\right)\left(\frac{C_4}{1 + e^{\left(C_1 C_1^* + C_2 C_2^* Log\left(DI_{Bottom} * 100\right)\right)}}\right) \tag{16}$$

Where:
FC_{Bottom} = Area of alligator cracking that initiates at the bottom of the HMA layers, percent of total lane area.
DI_{Bottom} = Cumulative damage index at the bottom of the HMA layers.
$C_{1,2,4}$ = Transfer function regression constants; C_4= 6,000; C_1=1.00; and C_2=1.00

$$C_1^* = -2C_2^* \tag{17}$$

$$C_2^* = -2.40874 - 39.748(1 + H_{HMA})^{-2.856} \tag{18}$$

H_{HMA} = Total HMA thickness, in.

Area fatigue cracks for all HMA surfaced pavements (see Table 2 and Appendix A) were calculated with *M-E Pavement* using the input values discussed and identified in section 2. As explained for the rut depths, two different materials characterization procedures were used for predicting rutting: (1) laboratory measured resilient modulus values at equivalent stress states; and (2) in place volumetric conditions and backcalculated elastic modulus values.

Table 23 compares the bias and standard error for the predicted areas of fatigue cracking of the two sets of data or inputs for characterizing the unbound layers. As shown, there is not much of a difference between the two characterization procedures for fatigue cracking predictions. The other important observation is that the bias and standard error for the HMA overlay group of pavements is very low. The reason for the low bias and standard error is the measured areas of fatigue cracking are also very small – few of these test sections exhibit fatigue cracking (see Figure 20).

Table 23—Comparison of Results from Using Laboratory Measured Resilient Modulus and Backcalculated Elastic Modulus Values for Predicting Fatigue Cracking

Pavement Type	Bias Value, in.		Standard Error, in.	
	Lab Measured Modulus Value	**Backcalculated Modulus Value**	**Lab Measured Modulus Value**	**Backcalculated Modulus Value**
Full Depth Structures	-0.662	-0.901	4.06	4.02
Pavement with Aggregate Base	-2.94	-2.41	5.93	5.55
HMA Overlay of Flexible Pavements	-0.45	-0.595	1.14	1.17
SPS-5; HMA Overlay with RAP	0.052	0.019	0.073	0.023
SPS-5; HMA Overlay without RAP	0.036	0.015	0.038	0.016

Figures 35 and 36 show the predicted versus measured fatigue cracking and predicted fatigue cracking versus the residual error for the two characterization methods for the unbound layers. As shown, the MEPDG under predicts the area of fatigue cracking for most of the LTPP test sections with the exception of some of the SPS-5 sections with higher areas of fatigue cracking in the existing HMA layer. The SPS-5 HMA overlay test sections exhibit little to no fatigue cracking, but do exhibit various lengths of longitudinal cracking in the wheel path. Whether these cracks initiated at the surface or not requires the use of cores. Most of the test sections exhibiting area fatigue cracking are the conventional flexible pavement structures, as shown in Figure 37.

Table 23 and Figure 35 illustrate there is a bias in the predicted fatigue cracking and the goodness-of-fit is poor for the conventional flexible pavements. Figure 36 includes the same information as graphically presented in Figure 35, except the predicted fatigue cracking are based on using the backcalculated elastic layer modulus values. As stated in section 2, the LTPP SPS-5 test sections consistently exhibit greater amounts of fatigue cracks even though the magnitudes of fatigue cracks are small. Figure 37 provides some examples of the comparison between the predicted and measured fatigue cracking due to very heavy truck traffic on the SPS-5 section.

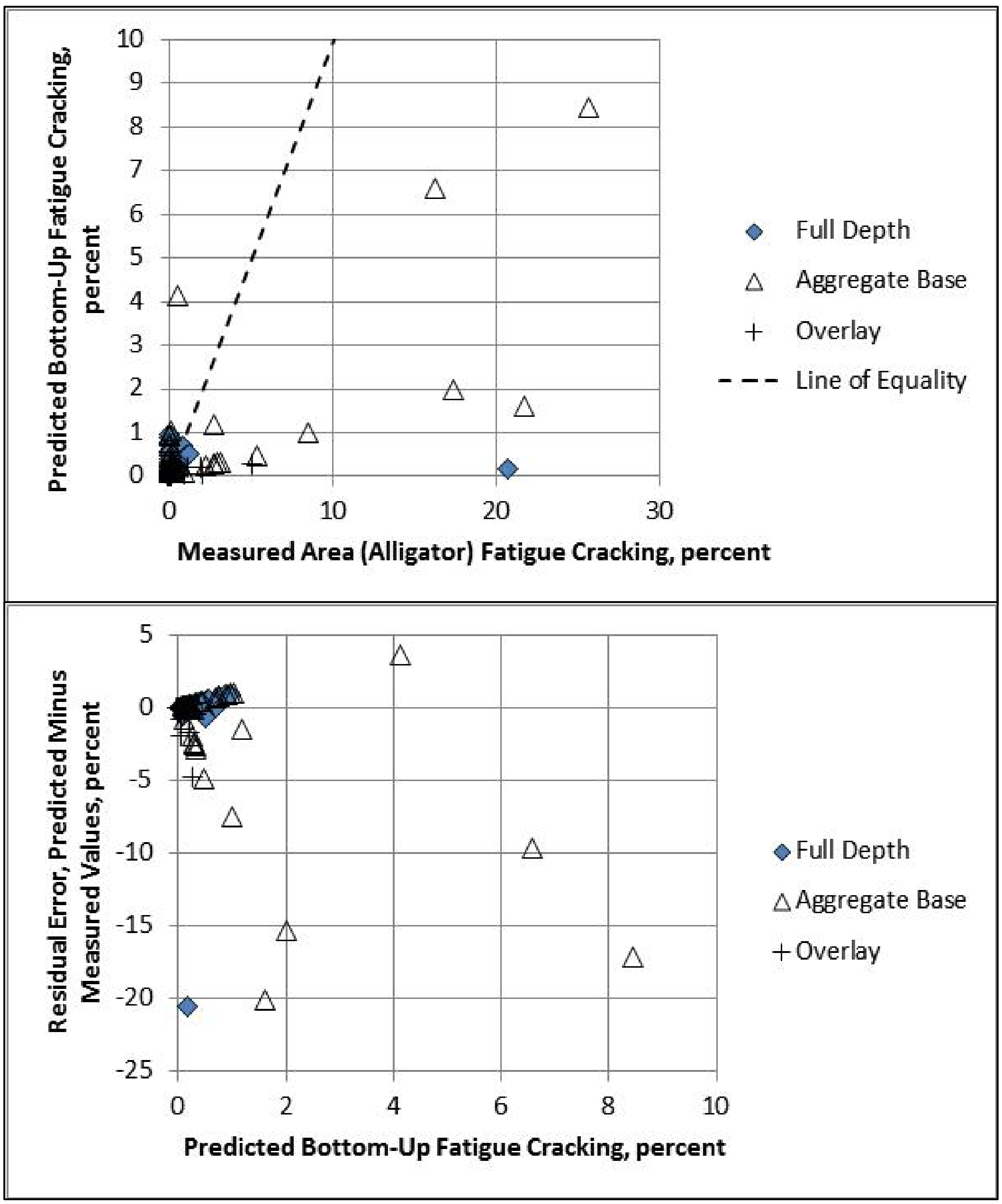

Figure 35—Predicted versus Measured Fatigue Cracking for different Pavement Types based on Using Laboratory Measured Resilient Modulus Values for the Unbound Layers

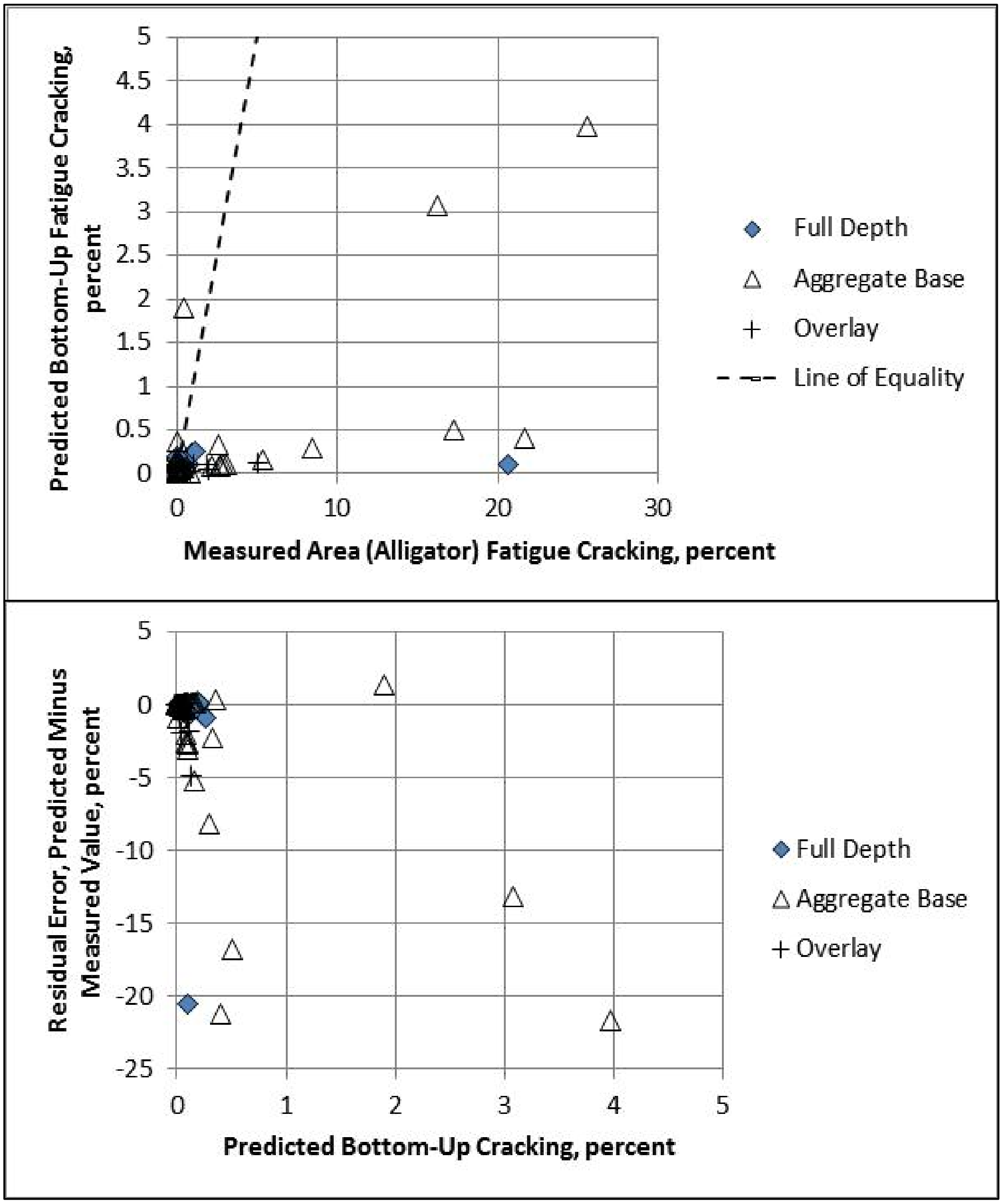

Figure 36—Predicted versus Measured Fatigue Cracking for different Pavement Types based on Using Backcalculated Elastic Modulus Values for the Unbound Layers

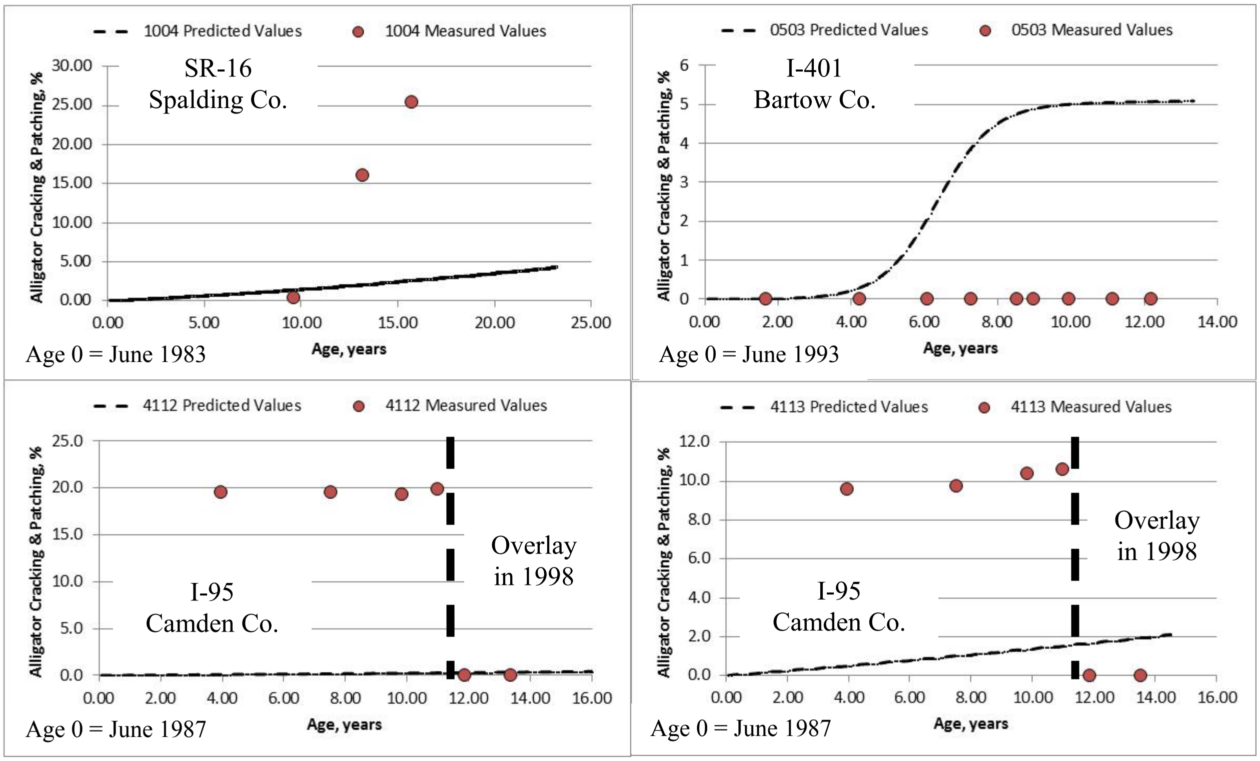

Figure 37—Predicted versus Measured Fatigue Cracking for different Pavement Types for Selected LTPP Test Sections

3.3 Fatigue Cracking Transfer Function of Semi-Rigid Pavements

For fatigue cracks in CTB layers, the allowable number of load applications, $N_{f\text{-}CTB}$, is determined in accordance with equation 19 and the amount or area of fatigue cracking is calculated in accordance with equation 20. These damage and distress transfer functions were never calibrated under any of the NCHRP projects. Montana DOT has completed a local calibration study of fatigue cracking in semi-rigid pavements. The calibration coefficients were found to be highly dependent on the condition or strength of the CTB layer. Thus, the transfer function is provided below, but is not recommended for use until the transfer function has been calibrated to the CTB materials and Georgia's climate.

$$N_{f-CTB} = 10^{\left[\frac{k_{c1}\beta_{c1}\left(\frac{\sigma_t}{M_R}\right)}{k_{c2}\beta_{c2}}\right]} \qquad (19)$$

$$FC_{CTB} = C_1 + \frac{C_2}{1 + e^{(C_3 - C_4 Log(DI_{CTB}))}} \qquad (20)$$

Where:

$N_{f\text{-}CTB}$ = Allowable number of axle load applications for a semi-rigid pavement.
σ_t = Tensile stress at the bottom of the CTB layer, psi.

M_R = 28-day Modulus of rupture for the CTB layer, psi. (NOTE: Although the MEPDG requires that the 28-day modulus of rupture be entered for all cementitious stabilized layers of semi-rigid pavements, the value used in all calculations is 650 psi, irregardless of the value entered into the MEPDG software.

DI_{CTB} = Cumulative damage index of the CTB or cementitious layer.

$k_{c1,c2}$ = Global calibration factors – Undefined because prediction equation was never calibrated; these values are set to 1.0 in the software. From other studies, k_{c1}=0.972 and k_{c2}=0.0825.

$\beta_{c1,c2}$ = Local calibration constants; these values are set to 1.0 in the software.

FC_{CTB} = Area of fatigue cracking, sq ft.

$C_{1,2,3,4}$ = Transfer function regression constants; C_1=1.0, C_2=1.0, C_3=0, and C_4=1,000, however, this transfer function was never calibrated and these values will likely change once the transfer function has been calibrated.

The computational analysis of incremental fatigue cracking for a semi-rigid pavement uses the damaged modulus approach. In summary, the elastic modulus of the CTB layer decreases as the damage index, DI_{CTB}, increases. The following equation is used to calculate the damaged elastic modulus within each season or time period for calculating critical pavement responses in the CTB and other pavement layers.

$$E_{CTB}^{D(t)} = E_{CTB}^{Min} + \left(\frac{E_{CTB}^{Max} - E_{CTB}^{Min}}{1 + e^{\left(-4+14\left(DI_{CTB}\right)\right)}} \right) \tag{21}$$

Where:

$E_{CTB}^{D(t)}$ = Equivalent damaged elastic modulus at time t for the CTB layer, psi.

E_{CTB}^{Min} = Equivalent elastic modulus for total destruction of the CTB layer, psi.

E_{CTB}^{Max} = 28-day elastic modulus of the intact CTB layer, no damage, psi.

LTPP test sections 4092, 4093, 4096, and 4420 are semi-rigid pavements (see Table 2) and have exhibited little to no fatigue cracking, with the exception of section 4022. Section 4022 exhibited a large amount of fatigue cracking, but after the HMA overlay had been placed on this section. Whether this amount of cracking is a result of damage in the existing HMA layer or a loss of bond between the HMA overlay and existing HMA layers can only be determined through the use of cores. Thus, the LTPP will provide little data in calibrating the fatigue cracking of semi-rigid pavements without additional investigation.

3.4 Thermal or Transverse Cracking Transfer Function

The degree of cracking predicted by the MEPDG uses an assumed relationship between the probability distribution of the log of the crack depth to HMA layer thickness ratio and the percent of cracking. The following equation is used to determine the extent of thermal cracking.

$$TC = \beta_{t1} N \left[\frac{1}{\sigma_d} Log\left(\frac{C_d}{H_{HMA}} \right) \right] \tag{22}$$

Where:

TC = Observed amount of thermal cracking, ft/mi.
β_{t1} = Regression coefficient determined through global calibration (400).
$N[z]$ = Standard normal distribution evaluated at [z].
σ_d = Standard deviation of the log of the depth of cracks in the pavement (0.769), in.
C_d = Crack depth, in.
H_{HMA} = Thickness of HMA layers, in.

The crack depth or amount of crack propagation induced by a given thermal cooling cycle is predicted using the Paris law of crack propagation.

$$\Delta C = A\left(\Delta K\right)^n \tag{23}$$

Where:

ΔC = Change in the crack depth due to a cooling cycle.
ΔK = Change in the stress intensity factor due to a cooling cycle.
A, n = Fracture parameters for the HMA mixture, which are obtained from the indirect tensile creep-compliance and strength of the HMA in accordance with the following equations.

$$A = 10^{k_t \beta_t \left(4.389 - 2.52 Log\left(E_{HMA} \sigma_m n\right)\right)} \tag{24}$$

Where:

$$\eta = 0.8\left[1 + \frac{1}{m}\right] \tag{25}$$

k_t = Coefficient determined through global calibration for each input level (Level 1 = 5.0; Level 2 = 1.5; and Level 3 = 3.0).
E_{HMA} = HMA indirect tensile modulus, psi.
σ_m = Mixture tensile strength, psi.
m = The m-value derived from the indirect tensile creep compliance curve measured in the laboratory.
β_t = Local or mixture calibration factor.

The stress intensity factor, K, is defined or estimated by the use of the following simplified equation.

$$K = \sigma_{tip}\left(0.45 + 1.99\left(C_o\right)^{0.56}\right) \tag{26}$$

Where:

σ_{tip} = Far-field stress from pavement response model at depth of crack tip, psi.
C_o = Current crack length, feet.

Transverse cracks were measured on some of the LTPP test sections (see Figure 21), but many exhibit no transverse cracking. The test sections exhibiting the higher length of transverse cracking (greater than 1,000 ft./mi.) include: all of the semi-rigid pavements (4092, 4093, 4096, and 4420) so these measured cracks are probably reflection cracks from the CTB layer; and flexible or rigid pavements with HMA overlays (1031 and 7028) so these measured cracks are also probably reflection cracks. Test section 1001 (conventional flexible pavement was the only conventional flexible pavement to exhibit a higher length of transverse cracking.

The MEPDG, however, did not predict any thermal cracks for any of the test sections. Thus, there is a bias of the transfer function. A detailed analysis of the sites with measured transverse cracks using more test sections will be needed to calibrate the thermal cracking transfer function. This observation is not uncommon for the southern climates.

3.5 Reflection Cracking Regression Equation – HMA Overlays

The MEPDG predicts reflection cracks in HMA overlays or HMA surfaces of semi-rigid pavements using an empirical equation. The empirical equation is used for estimating the amount of fatigue and thermal cracks from a non-surface layer that has reflected to the surface after a certain period of time. This empirical equation predicts the percentage of area of cracks that propagate through the HMA as a function of time using the relationship shown below. This empirical equation, however, was never calibrated under any of the NCHRP Projects.

$$RC = \frac{100}{1 + e^{a(c)+bt(d)}} \tag{27}$$

Where:

- *RC* = Percent of cracks reflected. [NOTE: The percent area of reflection cracking is output with the width of cracks being 1 ft.]
- *t* = Time, years.
- *a, b* = Regression fitting parameters defined through calibration process.
- *c,d* = User-defined cracking progression parameters.

The regression fitting parameters of the above equation (*a* and *b*) are a function of the effective HMA overlay thickness (H_{eff}), the type of existing pavement, and for PCC pavements, load transfer at joints and cracks, as shown below. The effective HMA overlay thickness is provided in Table 24. The user-defined cracking progression parameters can be used by the user to accelerate or delay the amount of reflection cracks, which also are included in Table 24. Non-unity cracking progression parameters (*c* and *d*) could be used with caution, after they have been calibrated locally.

$$a = 3.5 + 0.75\left(H_{eff}\right) \tag{28}$$

$$b = -0.688684 - 3.37302\left(H_{eff}\right)^{-0.915469} \tag{29}$$

The MEPDG predicts the total amount of cracking by combining the reflection cracks with the fatigue cracks predicted in the HMA overlay. Thus, the reflection cracking regression equation is not calibrated separately, but is calibrated concurrently with the other cracking transfer functions based on total cracking measured at the surface of the overlay. Table 2 listed those sections with HMA overlays (the SPS-5 test sections and sections 1031, 4112, 4096, 4113, and 4420).

Table 24—Reflection Cracking Model Regression Fitting Parameters

Pavement Type	Fitting and User-Defined Parameters			
	a and b	C	D	
	H_{eff} of Equations 13.b and 13.c		Delay Cracking by 2 years	Accelerate Cracking by 2 years
Flexible	$H_{eff} = H_{HMA}$	---	---	---
Rigid-Good Load Transfer	$H_{eff} = H_{HMA} - 1$	---	---	---
Rigid-Poor Load Transfer	$H_{eff} = H_{HMA} - 3$	---	---	---
Effective Overlay Thickness, H_{eff}, inches	---	---	---	---
<4	---	1.0	0.6	3.0
4 to 6	---	1.0	0.7	1.7
>6	---	1.0	0.8	1.4

NOTES:
1. Minimum recommended H_{HMA} is 2 inches for existing flexible pavements, 3 inches for existing rigid pavements with good load transfer, and 4 inches for existing rigid pavements with poor load transfer.

As noted in the previous section on the thermal cracking transfer function, sections 4092, 4093, 4096, and 4420 are semi-rigid pavements that have exhibited the higher lengths of transverse cracking. These measured cracks are probably reflection cracks from the CTB layer. Unfortunately, the cracking (fatigue or shrinkage) in the CTB layer is unknown, so predicting the reflection of unknown amounts of cracks in the existing layers is difficult. In addition, the flexible or rigid pavements with HMA overlays (sections 1031 and 7028) have also exhibited transverse cracks which are probably reflection cracks from the cracks or joints in the existing HMA and PCC pavements, respectively.

Table 23 summarized the bias of the total area of fatigue cracking for the HMA overlays. The bias was found to be low, but only because many of the test sections have exhibited no to low areas of fatigue cracking (less than 5 percent). It was observed that the MEPDG under predicted the total area of cracking measured on these sections (see Figure 37 and Table 23). It is expected that additional roadway segments with higher amounts of cracking need to be included in the sampling matrix for recalibration.

3.6 IRI or Smoothness Regression Equation – Flexible Pavements and HMA Overlays

The following equations were developed from data collected within the LTPP program and are used to predict IRI over time for HMA-surfaced pavements.

Equation for New HMA Pavements and HMA Overlays of Flexible Pavements:

$$IRI = IRI_o + 0.0150(SF) + 0.400(FC_{Total}) + 0.0080(TC) + 40.0(RD) \qquad (30)$$

Where:

IRI_o = Initial IRI after construction, in/mi.
SF = Site factor; as defined below.
FC_{Total} = Area of fatigue cracking (combined alligator, longitudinal, and reflection cracking in the wheel path), percent of total lane area. All load related cracks are combined on an area basis – length of cracks is multiplied by 1 foot to convert length into an area basis.
TC = Length of transverse cracking (including the reflection of transverse cracks in existing HMA pavements), ft/mi.
RD = Average rut depth, in.

The site factor (SF) is calculated in accordance with the following equation.

$$SF = Age\left(0.02003(PI+1) + 0.007947(Precip+1) + 0.000636(FI+1)\right) \quad (31)$$

Where:

Age = Pavement age, years.
PI = Percent plasticity index of the soil.
FI = Average annual freezing index, degree F days.
$Precip$ = Average annual precipitation or rainfall, in.

<u>Equation for HMA Overlays of Rigid Pavements:</u>

$$IRI = IRI_o + 0.00825(SF) + 0.575(FC_{Total}) + 0.0014(TC) + 40.8(RD) \quad (32)$$

Figure 38 includes a comparison of the predicted and measured IRI values for the Georgia LTPP sites. As shown, there is a significant bias in the predicted IRI values. However, the IRI values are predicted using the other predicted distresses (fatigue cracking, rutting, and thermal cracking). If the other distress transfer functions exhibit a significant bias, then it is likely that the IRI regression equation will exhibit bias. Thus, the IRI regression equation should be revised only after the other flexible pavement transfer functions have been recalibrated to eliminate any bias and improve on the goodness-of-fit.

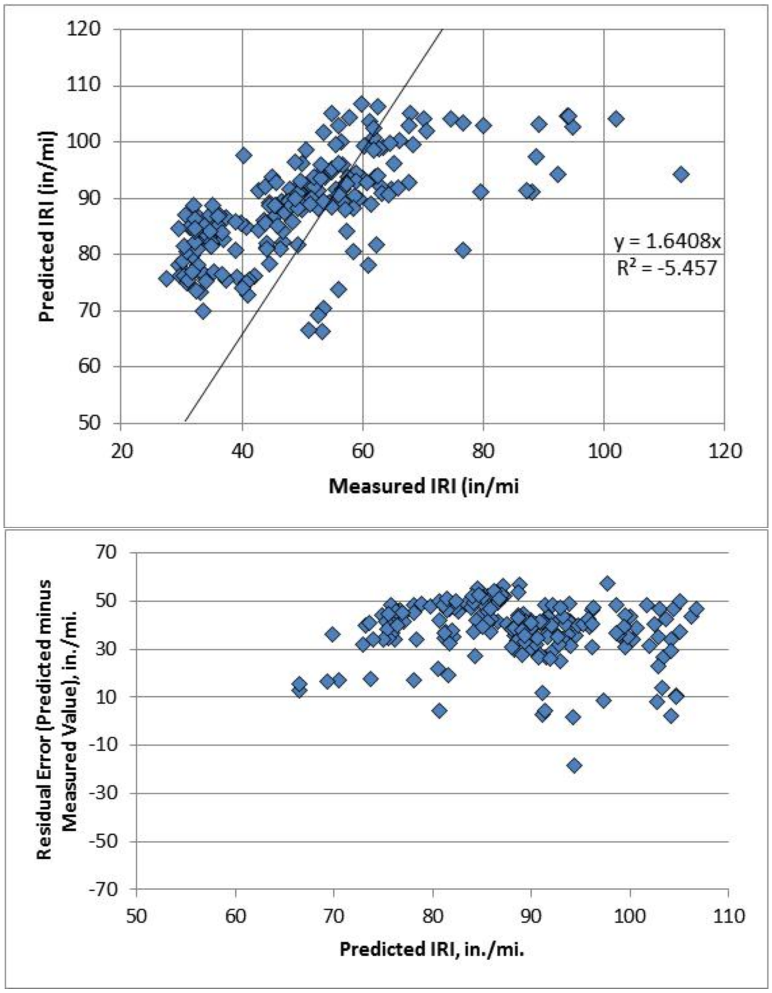

Figure 38—Predicted versus Measured IRI for the Flexible Pavements, Semi-Rigid Pavements and HMA Overlays

IV. PREDICTED DISTRESSES – RIGID PAVEMENTS AND PCC OVERLAYS

Verification of the MEPDG "global" calibration coefficient of the rigid pavement transfer functions for Georgia conditions consisted of running the *M-E Pavement* for the LTPP test sections and evaluating goodness of fit and bias. The global model coefficients utilized were those developed under the recently completed NCHRP project 20-07 to reflect corrections made to the global concrete CTE values that were used in NCHRP project 1-37A. The corrected CTE values used in the NCHRP project 20-07 were used in evaluating and judging the accuracy of the transfer functions for the Georgia LTPP rigid test sections.

Table 3 under section 2 grouped the 11 LTPP rigid pavement test sections by structural features. Nine of the sites are JPCP and two are CRCP. Two of the JPCP have been rehabilitated. One of the JPCP test sections (7028) was overlaid with HMA and the other was overlaid with a CRCP layer (4118).

Different design criteria through the transfer functions are used to design JPCP and CRCP and must be considered as two separate groups in evaluating or judging the applicability of the global calibration coefficients to Georgia conditions (see Table 22). Although IRI is the common design criteria between JPCP and CRCP, two different regression equations are used to predict IRI over time. This section of the interim report compares the predicted distress and smoothness to the measured values.

4.1 JPCP Fatigue Cracking or Mid-Slab Cracking Transfer Function

Two key models are involved with the verification of transverse slab cracking. The following equation estimates the fatigue life (N) of PCC when subjected to repeated stress for a given flexural strength. Calibration factors C_1 and C_2 could be modified but since they are based on substantial laboratory and field testing data, the MEPDG Manual of Practice does not recommend changing these coefficients since they are based on extensive field data.

$$\log\left(N_{i,j,k,l,m,n}\right) = C_1 \cdot \left(\frac{MR_i}{\sigma_{i,j,k,l,m,n}}\right)^{C_2} \tag{33}$$

The transfer function with appropriate coefficients is the S-shaped curve giving the relationship between field measured cracking and accumulated fatigue damage (DF) at top and bottom of the JPCP slabs. Parameters C_4 and C_5 in the following equation are the ones to adjust to remove bias and improve the goodness of fit with field data.

$$CRK = \frac{1}{1 + C_4\left(DI_F\right)^{C_5}} \tag{34}$$

The analysis utilized the Georgia database to establish the goodness of fit and bias in the MEPDG transverse cracking model. Figure 39 shows the predicted versus measured slab cracking for the global calibration coefficients. The plot shows poor goodness of fit along with bias.

The majority of JPCP sections have little to no measured transverse fatigue cracking (see Figure 23 in section 2). Figure 39 compares the predicted and measured percent slabs cracked, while Figure 40 compares the calculated concrete fatigue damage index accumulated over time to the measured percent slabs cracked. Predicted cracking versus the residual error (predicted minus measured values) are included in Figure 41 and confirms bias in the model. The main cause of for poor goodness of fit and bias in the global model, however, is probably due to a lack of measured cracking data in the higher range as illustrated in Figure 40.

In addition, some measured data show significant increase in transverse cracking over a short time interval, while the transfer function (predicted cracking) does not exhibit this increase. As a result, the transfer function significantly under predicts transverse cracking. A few measured data are believed to be outliers or considered suspicious data. An example of suspicious data point is illustrated in Figure 40. Forensic evaluation of those pavement sections may reveal the actual cause of the high amount of cracking or identify the measurement as an error. This large difference between the measured and predicted values is another reason why more test sections need to be included in the local calibration process so that one data point does not have a significant impact on the local calibration factors, if an outlier or suspicious data point cannot be explained.

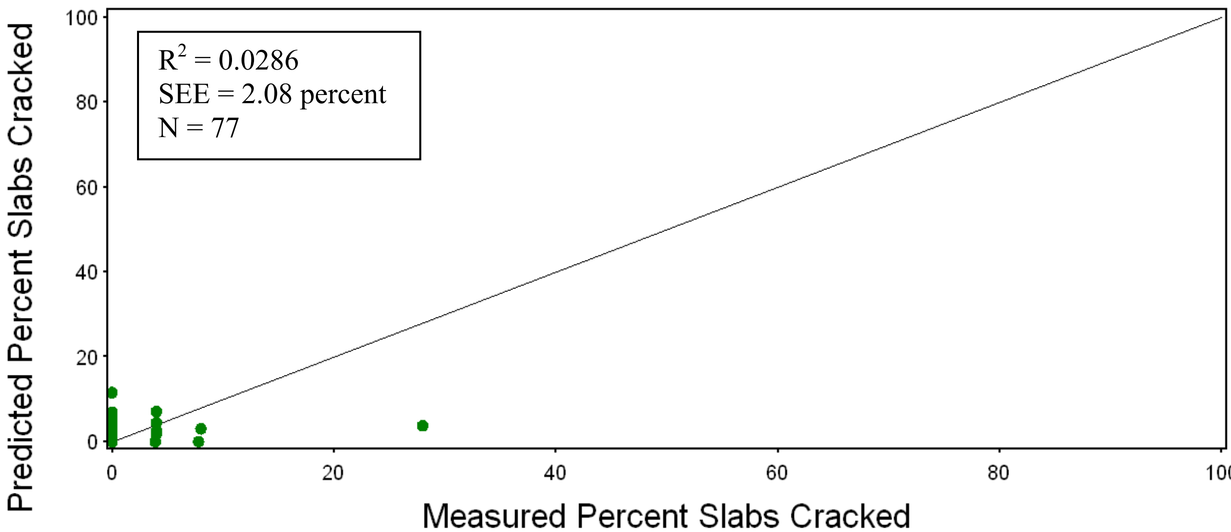

Figure 39—Predicted versus Measured Percent Slabs Cracked

Table 25 summarizes the statistical analysis between the predicted and measured cracking data. It should be noted that the amount of cracking is very low for the majority of the LTPP sites in Georgia, so the standard error of the estimate is only representative of these low amounts of measured cracking. Non-LTPP test sections will be needed that exhibit higher amounts of cracking for use in calibrating the transfer function, unless the policy of the Department is to rehabilitate or replace the pavements when a low amount of cracked slabs are observed. The results are summarized as follows, for the LTPP rigid pavement test sections with low amounts of cracked slabs:

- The intercept of the y= x curve was 1.418 (ranging from 0.928 to 1.907) with a corresponding p-value of <0.0001. The p-value less than 0.05 means the Test 1 null hypothesis was rejected. Thus, the MEPDG predicted cracking did exhibit this aspect of bias.
- The slope of the y equals x curve was 0.199. The corresponding p-value was <0.0001. Thus, the Test 2 null hypothesis was rejected, indicating that the predicted cracking does not equal the measured cracking, and this difference is significant. MEPDG cracking estimates cannot be extrapolated beyond the key inputs used for calibration.
- Finally, the p-value from paired t-test value compares predicted cracking from the MEPDG to the measured cracking value. The t-test value was 0.1836, and suggests the difference between the pairs is not significant.

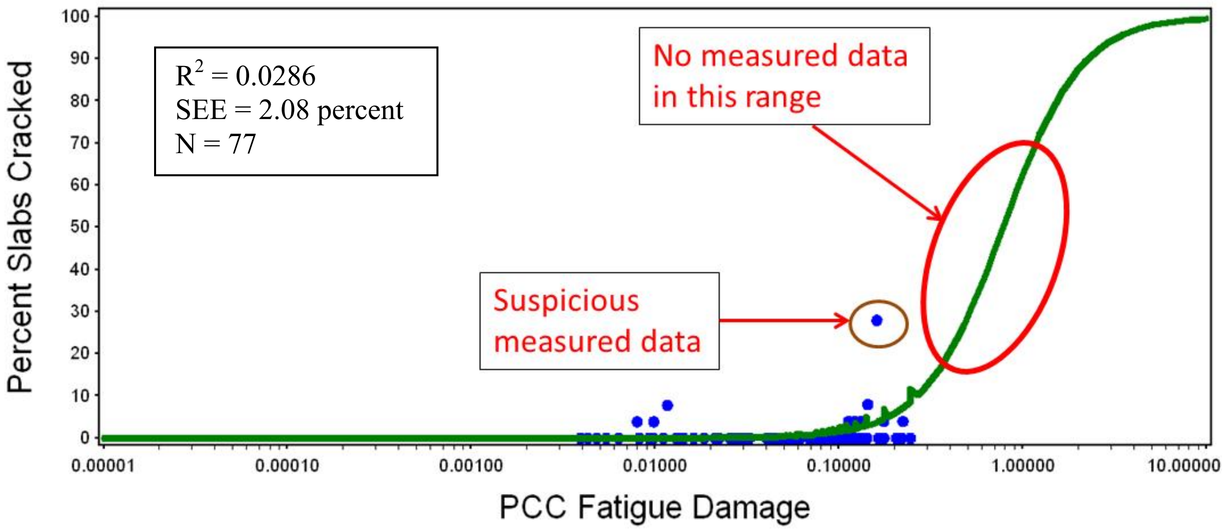

Figure 40—Measured Fatigue Transverse Cracking versus Concrete Fatigue Damage for all Georgia LTPP JPCP Sections

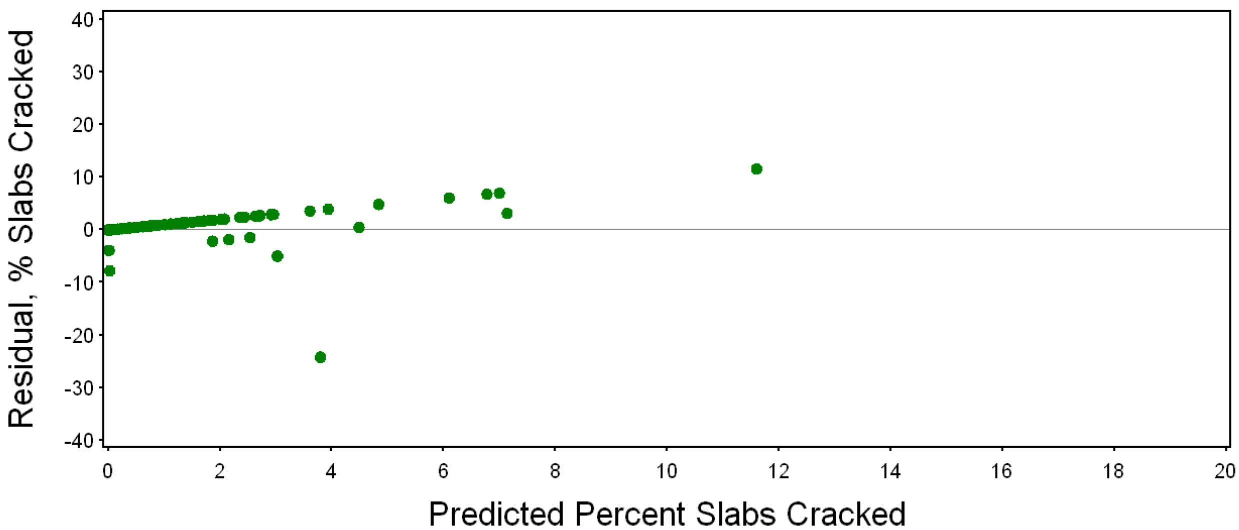

Figure 41—Predicted versus Residuals (Predicted – Measured Value) for Percent Slabs Cracked

Table 25 Statistical Comparison of Measured and MEPDG Predicted Transverse Cracking

Hypothesis Testing and T-Test				Goodness of Fit	
Test Type	**Value**	**Range**	**p-value**	**R^2**	**SEE, percent**
Hypothesis Test (1): Intercept = 0	1.418	0.928 to 1.907	<0.0001	0.0286	2.08
Hypothesis Test (2): Slope = 1	0.199	0.004 to 0.355	<0.0001		
Paired t-test	—	—	0.1836		

4.2 JPCP Faulting Transfer Function

The mean transverse joint faulting is predicted using a complex incremental approach. A detailed description of the faulting prediction process is presented in the MEPDG Manual of Practice. MEPDG faulting is predicted using the models presented below:

$$Fault_m = \sum_{i=1}^{m} \Delta Fault_i \tag{35}$$

$$\Delta Fault_i = C_{34} * (FAULTMAX_{i-1} - Fault_{i-1})^2 * DE_i \tag{36}$$

$$FAULTMAX_i = FAULTMAX_0 + \mathrm{C}_7 * \sum_{j=1}^{m} DE_j * Log(1 + \mathrm{C}_5 * 5.0^{EROD})^{C_6} \tag{37}$$

$$FAULTMAX_0 = \mathrm{C}_{12} * \delta_{\mathrm{curling}} * \left[Log(1 + C_5 * 5.0^{EROD}) * Log(\frac{P_{200} * WetDays}{p_s}) \right]^{C_6} \tag{38}$$

Where:

$Fault_m$	=	mean joint faulting at the end of month m, in
$\Delta Fault_i$	=	incremental change (monthly) in mean transverse joint faulting during month *i*, in
$FAULTMAX_i$	=	maximum mean transverse joint faulting for month *i*, in
$FAULTMAX_0$	=	initial maximum mean transverse joint faulting, in
EROD	=	base/subbase erodibility factor
DE_i	=	differential deformation energy accumulated during month *i*.
Computed		
		using various inputs including joint LTE and dowel damage
EROD	=	base/subbase erodibility factor
$\delta_{curling}$	=	maximum mean monthly slab corner upward deflection PCC due to temperature curling and moisture warping.
P_S	=	overburden on subgrade, lb
P_{200}	=	percent subgrade soil material passing No. 200 sieve
WetDays	=	average annual number of wet days (greater than 0.1 in rainfall)

$$\mathrm{C}_{12} = \mathrm{C}_1 + \mathrm{C}_2 * FR^{0.25} \tag{39}$$

$$\mathrm{C}_{34} = \mathrm{C}_3 + \mathrm{C}_4 * FR^{0.25} \tag{40}$$

FR	=	base freezing index defined as percentage of time the top base temperature is below freezing (32°F) temperature.

Dowel joint damage accumulated for the current month is determined from the following equation:

$$\Delta DOWDAM_{tot} = \sum_{j=1}^{N} C_8 * F_j \frac{n_j}{d\, f_c^*} \tag{41}$$

Where:

$\Delta DOWDAM_{tot}$ = Cumulative dowel damage for the current month

n_i = Number of axle load applications for current increment and load group *j*

N = Number of load categories

f_c^* = PCC compressive stress estimated

C_8 = Calibration constant

F_j = Effective dowel shear force induced by axle loading of load category j.

C_1 through C_8 are calibration constants to be established based on field performance.

Faulting model calibration involved determination of the calibration parameters C_1 through C_7 from the above equations and the rate of dowel deterioration parameter, C_8, from the above equation, which minimize the error function, ERR, defined as:

$$ERR(C_1, C_2, ..., C_8) = \sum_{ob=1}^{Nob} \left(FaultPredicted_{ob} - FaultMeasured_{ob}\right)^2 \qquad (42)$$

Where:

ERR = error function

$C_1, C_2, ..., C_8$ = calibration parameters

$FaultPredicted_{ob}$ = predicted faulting for observation *ob* in the calibration database

$FaultMeasured_{ob}$ = measured faulting for observation *ob* in the calibration database

Nob = number of observation in the calibration database

Global calibration coefficients from NCHRP 20-07,

C1	=	0.51040
C2	=	0.00838
C3	=	0.00147
C4	=	0.008345
C5	=	5999
C6	=	0.8404
C7	=	5.9293
C8	=	400

Figure 42 shows the predicted versus measured faulting using the global calibration coefficients. The plot shows poor goodness of fit along with bias. The predicted faulting versus the residual faulting error (predicted minus measured value) is included in Figure 43 and shows a tread that confirms bias in the model. However, the magnitude of faulting is very low, significantly lower than the threshold value normally used in design. The reason for the low faulting values is the Department has been doweling JPCP since the 1970's.

There were no obvious causes for poor goodness of fit and bias in the global faulting model. Selecting pavements with a wide range of measured faulting may improve the model. As noted above, however, the Department has been doweling JPCP since the 1970's. Thus, finding non-LTPP roadway segments with higher faulting may not be possible. From the results, the global calibration coefficients are inappropriate for Georgia conditions, and hence, there is a need for local calibration. Calibrating the faulting transfer function, however, is considered a low priority because the Department's policy is to continue using doweled JPCP in the future.

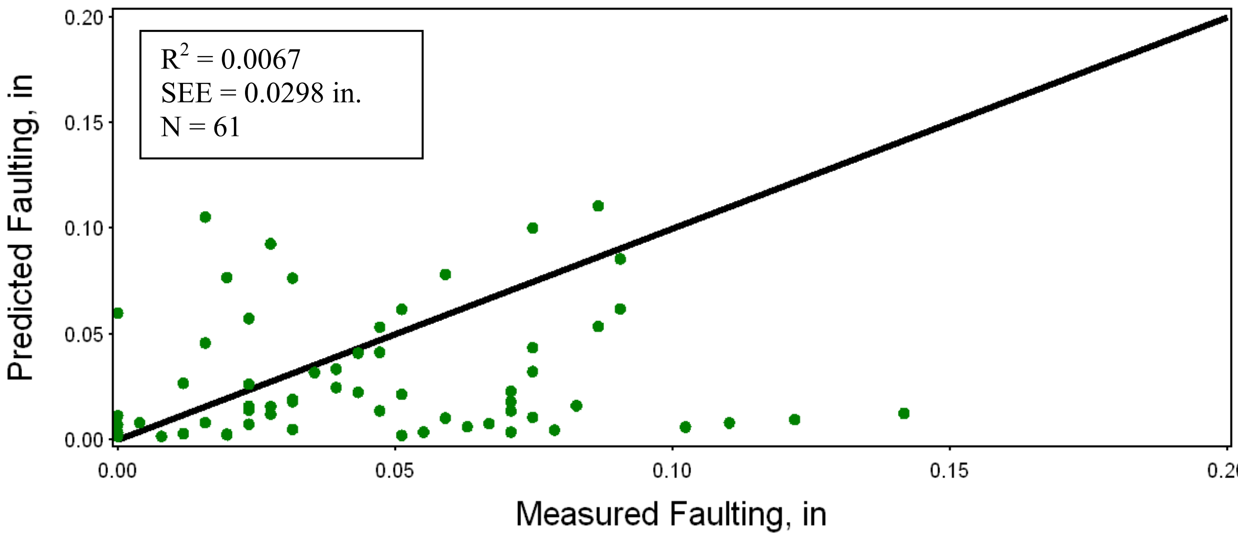

Figure 42—Predicted versus Measured Joint Faulting

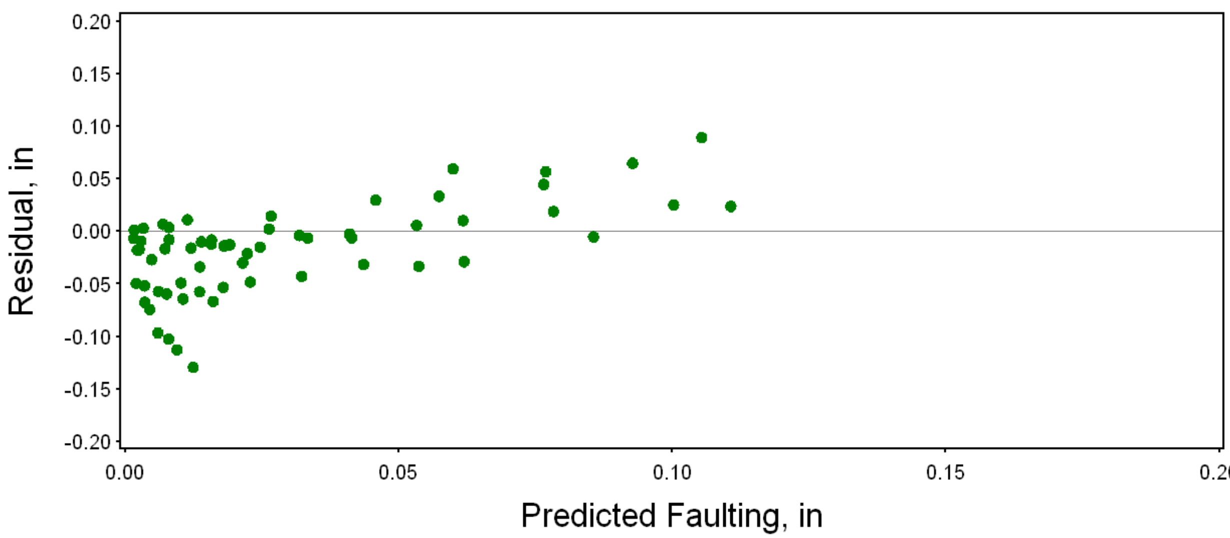

Figure 43—Predicted versus Residuals (Predicted minus Measured Value) for Joint Faulting

Table 26 present results of the statistical analysis performed in comparing the predicted faulting and measured values. The results are summarized as follows:

- The intercept of the y= x curve was 0.0259 (ranging from 0.013 to 0.039) with a corresponding p-value of 0.0003. The p-value less than 0.05 implied the Test 1 null hypothesis is rejected. Thus, the MEPDG transfer function for faulting does exhibit bias.
- The slope of the y= x curve was 0.448. The corresponding p-value was <0.0001. Thus, the Test 2 null hypothesis was rejected, indicating the predicted MEPDG faulting is

unequal to the measured faulting, and is significant. MEPDG faulting estimates cannot be extrapolated beyond or outside of the key inputs used for calibration.

- Finally, the p-value from paired t-testing comparing faulting estimated with MEPDG and measured faulting was 0.0023. This shows that this aspect of bias was significant.

Table 26—Statistical Comparison of Measured and MEPDG Predicted Faulting

Hypothesis Testing and T-Test				**Goodness of Fit**	
Test Type	**Value**	**Range**	**p-value**	R^2	**SEE, in**
Hypothesis Test (1): Intercept = 0	0.259	0.013 to 0.039	0.0003	0.0067	0.0298
Hypothesis Test (2): Slope = 1	0.448	0.299 to 0.597	<0.0001		
Paired t-test	—	—	0.1836		

4.3 JPCP IRI or Smoothness Regression Equation

IRI is predicted using the following regression equation:

$$IRI = IRI_I + J1*CRK + J2*SPALL + J3*FAULT + J4*SF \qquad (43)$$

Where:

IRI_I	=	Initial IRI
CRK	=	JPCP transverse cracking
SPALL	=	JPCP joint spalling
FAULT	=	JPCP mean joint faulting
SF	=	Sire factor

A plot of predicted and measured IRI for the Georgia LTPP sites is shown in Figure 44, while the predicted IRI versus the residual error of IRI (predicted minus measured value) are included in Figure 45. The residual error versus the predicted value suggests bias in the regression equation.

These results indicate that goodness of fit was poor and the model predictions were biased and thus local calibration with Georgia data is required. However, the IRI values are predicted using the values from the other predicted distresses. If the other distress transfer function exhibit a significant bias, then it is likely that the IRI regression equation will exhibit bias. Thus, the IRI regression equation should be revised only after the other JPCP transfer functions have been recalibrated to eliminate any bias and improve on the goodness-of-fit.

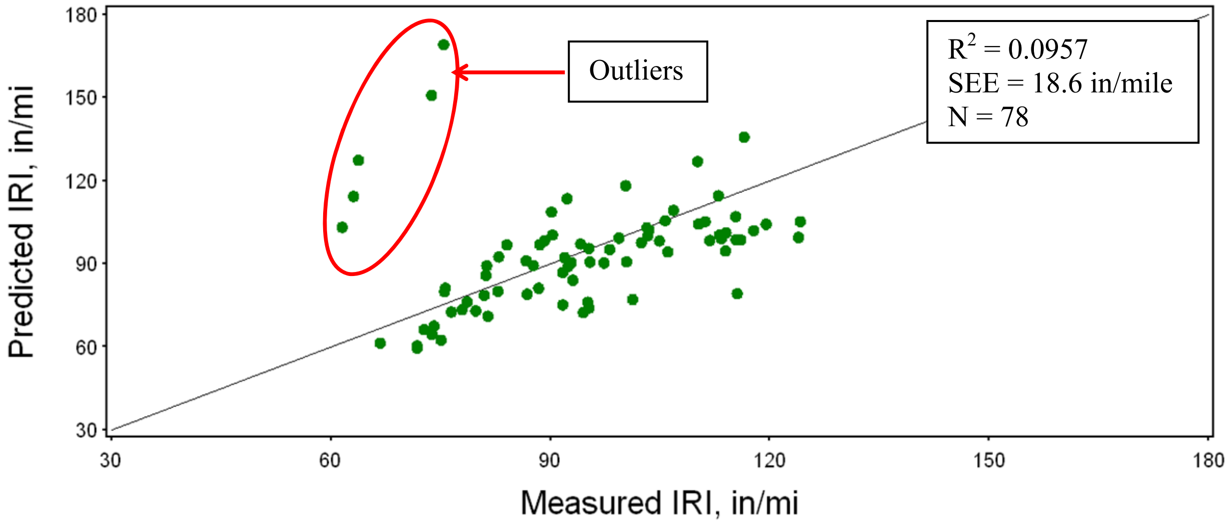

Figure 44—Predicted versus Measured IRI for Georgia LTPP JPCP Sections

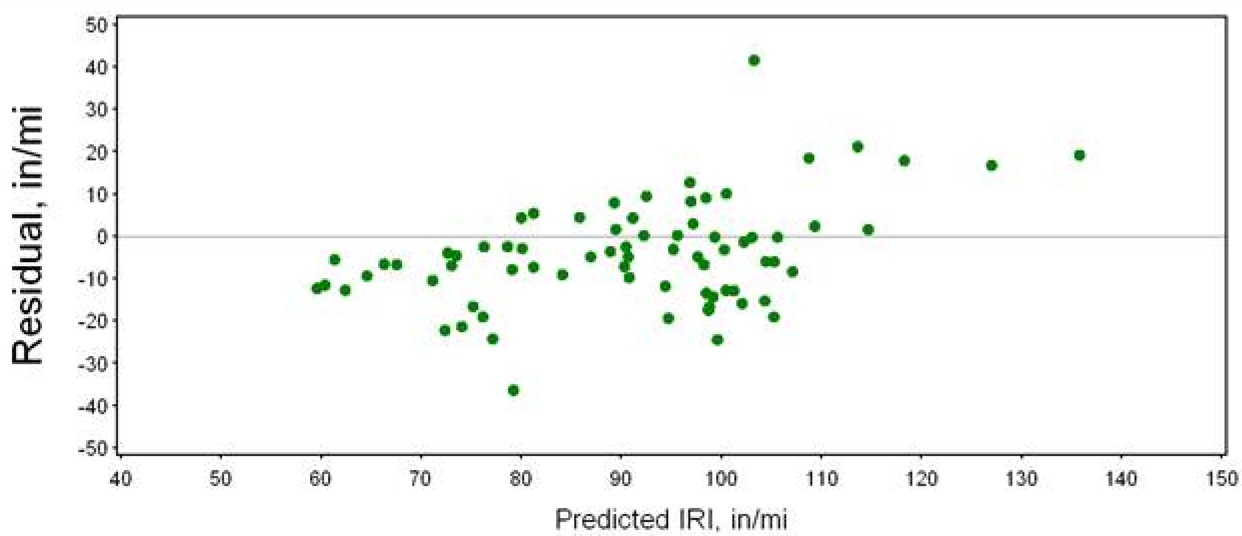

Note: The five data points identified as potential outliers in Figure 44 are not shown in this figure, because the scales for the predicted IRI was set to 150 in./mi. and the maximum residual set at 50 in./mi.

Figure 45—Predicted versus Residuals (Predicted Minus Measured Values) for IRI for Georgia LTPP JPCP Sections

There were no obvious causes for poor goodness of fit and bias in the global model. Table 27 summarizes the statistical analysis performed for comparing predicted IRI and measured IRI values. The results are summarized as follows:

- The intercept of the y= x curve was 58.2 (ranging from 32.9 to 83.4) with a corresponding p-value of <0.0001. The p-value less than 0.05 implied the Test 1 null hypothesis was rejected. Thus, the MEPDG predicted IRI does exhibit bias.
- The slope of the y= x curve was 0.981. The corresponding p-value was 0.4389. Thus, the Test 2 null hypothesis is accepted, indicating the predicted IRI can be considered equal to the measured values. For this case, the MEPDG IRI estimates can be extrapolated beyond the key inputs used for calibration.
- Finally, the p-value from the paired t-test comparison of predicted IRI and measured IRI. The t-test value was 0.9313 and is considered significant.

Table 27—Statistical Comparison of Measured and Predicted IRI

Hypothesis Testing and T-Test				**Goodness of Fit**	
Test Type	**Value**	**Range**	**p-value**	**R^2**	**SEE, in/mile**
Hypothesis Test (1): Intercept = 0	58.2	32.9 to 83.4	<0.0001	0.0067	0.0298
Hypothesis Test (2): Slope = 1	0.981	0.937 to 1.03	0.4389		
Paired t-test	—	—	0.9313		

4.4 CRCP Punchouts Transfer Function

The following globally calibrated model predicts CRCP punchouts as a function of accumulated fatigue damage due to top-down stresses in the transverse direction. A complete explanation and discussion of the punchout transfer function is included in the MEPDG Manual of Practice.

$$PO = \frac{A_{PO}}{1 + \alpha_{PO} \cdot DI_{PO}^{\beta_{PO}}} \tag{44}$$

Where:

PO = Total predicted number of medium and high severity punchouts per mile.
DI_{PO} = Accumulated fatigue damage (due to slab bending in the transverse direction) at the end of y^{th} year.
$A_{PO}, \alpha_{PO}, \beta_{PO}$ = Calibration constants (85, 1.4149, -0.8061, respectively) from NCHRP 20-07.

No punchouts were predicted for the CRCP LTPP test sections while punchouts were measured along both CRCP test sections. As such, there is bias in the transfer function, but only two test sections is simply too few to make any judgment or assessment of the transfer function. More test sections need to be included in the comparison prior to making or recommending any adjustments to the global calibration coefficients.

4.5 CRCP IRI or Smoothness Regression Equation

Key distresses affecting the IRI for CRCP include punchouts. The global IRI model for CRCP is given as follows:

$$IRI = IRI_I + C_1 \bullet PO + C_2 \bullet SF \tag{45}$$

Where:

IRI_I = Initial IRI, in/mi.
PO = Number of medium and high severity punchouts per mile.
C_1 = 3.15
C_2 = 28.35
SF = Site factor

$$SF = AGE \bullet (1 + 0.556\ FI) \bullet (1 + P_{200}) * 10^{-6} \tag{46}$$

Where:
AGE = Pavement age, yr.
FI = Freezing index, °F days.
P_{200} = Percent subgrade material passing No. 200 sieve.

There are too few IRI measured values to determine if the regression equation exhibits bias and needs to be recalibrated. As for other IRI regression equations (JPCP and HMA), however, the punchout transfer function should be validated and/or recalibrated prior to making any changes to the IRI regression equation.

V. SUMMARY AND CONCLUSIONS

5.1 Major and Appropriate Findings – Accuracy and Precision of Transfer Functions

The number of Georgia LTPP sites and their developed level of distress are inadequate for the validation or confirmation process of the global calibration coefficients from a statistical perspective. The Local Calibration Guide includes a general recommendation for a minimum of 18 and 21 flexible and the same for rigid pavement projects. The following summarizes some findings relative to the number of sites.

- The flexible pavements and HMA overlays have a sufficient number of test sections in total, but the SPS-5 project (15 test sections) exhibit significantly different performance characteristics than the other GPS sites located in Georgia. The rutting, fatigue cracking, and longitudinal cracking measured on these sections are believed to be the result of moisture damage or some other material anomaly. These sections, however, can be used but should be considered separately in the calibration process and the condition of the HMA confirmed through the use of cores and other destructive sampling techniques. Additional flexible pavement test sections need to be added to the sampling matrix to be considered under Task 3 of the next phase.

- The rigid pavements and PCC overlays have an insufficient number of test sections for validation and confirmation – a total of 11 were available and considered under Task 2 for this interim report. More importantly, the magnitudes of distresses developed for the rigid pavements is considered too low relative to the design criteria to accurately establish or adjust the global calibration coefficients. Additional rigid pavement test sections need to be added to the sampling matrix to be considered under Task 3 of the next phase.

The following are some of the other findings:

- Plots of measured versus predicted distress illustrate a general poor correlation and bias for the transfer functions for both flexible and rigid pavements. Many of the flexible and rigid pavement test sections exhibit distresses much lower than the design criteria and thus are not sufficient to provide predictions at this level of distress. Tables 20 and 21 provided the range and median values of distress. The median value is near 0 or significantly less than the design criteria recommended for use in the MEPDG Manual of Practice. If these LTPP test sections are not representative of typical roadway segments, sections with higher distresses should be included in the latter tasks for calibration and validation of the transfer functions.

- Use of the backcalculated elastic layer modulus values significantly reduced the bias of the rut depth transfer function in comparison to the use of laboratory resilient modulus values. Other agencies have reported this same observation. A similar comparison was made between the use of the GDOT default NALS and the global NALS. The use of the GDOT NALS did not significantly lower or increase the bias and standard error of the predicted distresses indicating other factors have a significant impact on performance and the occurrence of distress.

- The resilient modulus of the aggregate base layers is relatively low in comparison to the MEPDG default values for the LTPP test sections. These values should be checked against other aggregate base materials and crushed stones specified in Georgia.

- The AASHTO C-factor determined for the LTPP subgrade under conventional flexible pavement structures in Georgia are similar to the values recommended for use in the AASHTO Manual of Practice. Conversely, the c-factors for the other materials and structures are significantly different from the c-factors listed in the MEPDG Manual of Practice (see Table 18).

- The backcalculated mean k-value and the month of measurement for JPCP and CRCP were used iteratively to obtain the input resilient modulus. This input resilient modulus varies between 5,500 to 11,300 psi.

- Another important finding regarding the LTPP sites is that the number of LTPP sites result in an unbalanced factorial (see Tables 2 and 3). Thus, other pavement sections with appropriate design features need to be included for balancing the sampling factorial.

5.2 Gaps – Site Condition and Design Features

Tables 2 and 3 provided a category of the Georgia LTPP projects. As noted in section 2, there are missing areas within those categories. Based on the findings and results from the comparison of the predicted and measured distresses, preliminary sampling matrices or factorials were prepared for the flexible and rigid pavements. These preliminary factorials are provided in Tables 28 and 29. The sampling templates basically represent the current/past GDOT practices presented above, and were prepared to fill in some of those gaps.

The first step in project identification and selection is to identify as many potential projects as possible that could be used to satisfy the recommendations presented above and populating the sampling template presented in Tables 28 and 29. Table 28 for new JPCP pavements has 30 cells, while Table 29 for new flexible and rehabilitated pavements consists of 46 cells. The following summarizes the items that will have a significant impact on the calibration and were not included in the features of the LTPP test sections.

- Polymer modified asphalt or mixtures and mixtures with varying amount of RAP. GDOT typically uses less than 20 percent RAP. Half of the SPS-5 test sections included mixtures with 30 percent RAP, but it is expected that finding non-LTPP roadway segments with that amount of RAP will be difficult. Thus, it was not included as a primary factor in the sampling matrix or template.

- Pavement preservation treatments were not included on any of the LTPP test sections for both types of pavements. Georgia DOT has implemented and used pavement preservation program to extend pavement service life for PCC and HMA pavements. The program was found to be very beneficial. Calibration of the MEPDG should consider or include this benefit, but the MEPDG does not have the capability to directly consider the impact of different pavement preservation methods. Most preservation methods do not add structural value to the existing pavement. Thus, another calibration issue is how to handle the extended use of different pavement preservation treatment methods in Georgia.

  Montana DOT is the only agency where pavement preservation methods were considered within the calibration process to date. It is expected that a similar type of procedure be used to eliminate bias in the predictions of distress and consider the impact of preservation methods on enhancing performance. The Michigan DOT is another agency that is identifying methods to account for the benefit of using aggressive preservation programs in terms of the MEPDG. The Arizona DOT has sufficient performance data and information on the preservation methods used to determine local calibration coefficients. The key issue is how to determine the standard error of the estimate when these methods are placed at different times under different existing pavement conditions. The issue is not related to missing data or information, but rather how to use and apply that information in validating or calibrating transfer functions.

Table 28—Preliminary Sampling Template or Matrix for Validation of New JPCP Transfer Functions

PCC Thickness, in	Doweled Pavement	Edge Support	Subgrade Type: Coarse (A-1 through A-3)			Subgrade Type: Fine (A-4 through A-7)		
			Base Type					
			Aggr. Base	**Chemically Stabilized***	**Asphalt Interlayer**	**Aggr. Base**	**Chemically Stabilized***	**Asphalt Interlayer**
≤ 10	Non-doweled	None		3017		3019	3018	
		Tied PCC and or widened lanes						
	Doweled	None		3020		3007		
		Tied PCC and or widened lanes						
> 10	Non-doweled	None		3011				
		Tied PCC and or widened lanes						
	Doweled	None		3015				
		Tied PCC and or widened lanes						3016

Dark Shaded Cells – Indicate these designs are not used on State Routes.
*Chemically stabilized base = lean concrete base, soil cement, or cement treated base
X – Identifies cells to be filled for a partial or fractional factorial.

Table 29—Preliminary Sampling Template or Matrix for Validation of New and Rehabilitated Flexible Pavements and HMA Overlays

HMA Thickness	Binder Type	Soil Type		Pavement Structure: New Construction			Pavement Structure: Rehabilitation (see Note 1) — HMA Overlay with & without Milling		
				Flexible; Conv.	Deep Strength	Semi-Rigid	Flexible Conv.	Deep Strength	Semi-Rigid
<7	Neat	Coarse-Grained			Cells not likely found.	4092; 4093; 4094; 4096; 4420		Cells not likely found.	4096; 4420
		Fine-Grained	None	1004					
			Stabilized						
	PMA	Coarse-Grained							
		Fine-Grained	None						
			Stabilized						
7 to 10	Neat	Coarse-Grained		1005					
		Fine-Grained	None	1001; 4111					
			Stabilized						
	PMA	Coarse-Grained							
		Fine-	None						

HMA Thickness	Binder Type	Soil Type		Pavement Structure					
				New Construction			Rehabilitation (see Note 1)		
							HMA Overlay with & without Milling		
				Flexible; Conv.	Deep Strength	Semi-Rigid	Flexible Conv.	Deep Strength	Semi-Rigid
		Grained	Stabilized						
>10	Neat	Coarse-Grained			0501; 1031; 4112; 4113			SPS-5; 1031; 4112; 4113	
		Fine-Grained	None		4119				
			Stabilized						
	PMA	Coarse-Grained							
		Fine-Grained	None						
			Stabilized						

Dark Shaded Cells – Indicate that these designs are not used on State Routes or the primary system.
Conv. = Conventional; flexible pavements with a relatively thin HMA surface and thick crushed stone or aggregate base layer.
Deep Strength = For this sampling matrix, deep-strength asphalt pavements include very thick asphalt base mixtures with relatively thin aggregate base layers and also includes the category of full-depth HMA pavements.
Semi-Rigid = Includes HMA pavements with a soil-cement subgrade or cement treated base layer.
NOTE 1: Three categories of overlay thickness will be included; less than 2.5 inches, 2.5 to 5 inches, and greater than 5.0 inches.

- Various design features for JPCP were not adequately covered from the LTPP sections. Gaps between these LTPP sections and current Georgia design practice were noted in joint spacing, use of dowels, base types, and shoulders. Asphalt interlayers are used in JPCP construction. Of the 11 LTPP rigid pavement test sections, however, test section 3016 was the only one with an asphalt interlayer.

- CRCP was included for only two projects. Additional projects are needed to conduct a validation and calibration.

- Unbonded PCC overlays of JPCP. There was only one unbonded overlay, so additional unbonded overlay projects are needed for validation. However, there are very few roadway segments available for this family of pavements, so it was excluded as a primary factor in the sampling matrix.

5.3 Conclusion

It is recommended that GDOT proceed with the next phase of the study and select projects to fill in the many key gaps so that the calibration process can be used to adjust the calibration coefficients for each distress.

The following flexible pavement and material types and overlays currently used in Georgia:

- Conventional pavement structures – HMA over an aggregate base layer with and without a stabilized subgrade soil. The aggregate base material was found to have

relatively low resilient modulus values. Roadway segments need to be selected with the use of higher strength base materials.
- Full-depth asphalt concrete pavements; primarily used in South Georgia.
- Semi-Rigid pavements consisting of HMA placed over cement treated base or soil cement. Some of the LTPP test sections fall within this group of pavements, but most roadway segments are located below the fault line in South Georgia. However, it was included as a family of pavements in the sampling matrix.
- Asphalt binder: GDOT uses both neat and polymer modified binders. None of the LTPP test sections included the use of polymer modified mixtures or binders. From other studies, it has been concluded that the MEPDG does not accurately account for the benefit and impact on the use of polymer modified binders. Thus, they were included in the sampling matrix.

The following full depth rigid pavement types are currently used in Georgia:
- Jointed Portland Cement Concrete Pavements (JPCP). The design features are typically used in Georgia includes:
    - Steel tie bars are generally used at longitudinal joints to prevent joint opening.
    - Dowel bars are used to assist in load transfer between adjacent slabs at planned and transverse contraction joints in the pavement. Typically, 1½ inch diameter dowels are used.
    - 15 foot joint spacing is used for Interstates, higher duty facilities, and State routes; 20 feet joint spacing is rarely used.
    - Asphalt interlayers are used along interstates, but are not always used on State routes.
- Continuously Reinforced Concrete Pavements (CRCP) are used on Interstates and higher duty facilities.
- Unbonded Concrete Overlays consists of a new concrete overlay of an existing concrete pavement or an existing HMA/JPCP composite pavement. A few of these need to be added to validate the global calibration coefficients.

Apart from conventional rigid pavements, the following thinner concrete overlays are also used by GDOT on intersection improvement projects:
- Conventional Whitetopping is a new concrete overlay that ranges from 4 inches to 8 inches in thickness. It is placed directly onto an existing distressed asphalt pavement for rehabilitation purposes. This can be designed using the MEPDG.
- Ultra-Thin Whitetopping (UTW) is an asphalt pavement rehabilitation method that uses a thin layer of high strength concrete with the depth of rehabilitation between 2 and 4 inches. The remaining asphalt concrete pavement should be in relatively good condition, adequate in thickness (> 3 inches). This cannot be designed using the MEPDG.

Projects for populating the sampling templates are based on recommendations presented in the AASHTO MEPDG Local Calibration Guide as follows:

- Projects should be representative of Georgia pavement design and construction practices.

- Projects should be representative of typical pavement condition (i.e., poor, moderate, and good).
- Project age should span the range typical of Georgia practice (newly constructed, older existing, rehabilitated).
- Projects must be well distributed (located) throughout the state.

Regarding the type of additional sites or projects to be considered to fill the gaps within the next task are listed below.

- States such as Arizona, Colorado, Missouri, Montana, Utah, and Mississippi have supplemented with sections from their pavement management system (PMS) inventory to augment the confirmation process. Use of other roadway segments should be considered in filling out a partial factorial of the sampling matrix. Wyoming, Mississippi and other agencies have included LTPP sites in neighboring states that are located near their boundaries. There are additional flexible and rigid LTPP sites located near the border between Georgia and adjacent states. Care should be taken that these sites share similar climate, material types, truck traffic, and construction practices to ensure a meaningful validation process. For example, Montana found that their LTPP and research test sections had consistently lower air voids and higher densities of hot mix asphalt (HMA) mixtures than the LTPP sites in surrounding states. Montana also has a much more aggressive pavement preservation program. Both of these factors resulted in consistently lower amounts of cracking and rutting than in the surrounding states.
- Rigid pavement gaps that need to be filled include a spread of joint spacing, base types of interest to GDOT, tied PCC shoulders, and use of large dowel bars. Sections with these features are provided in the field section matrix selection below.

This page left blank intentionally.

Appendix A
Pavement Cross Section and Structure for the LTPP Sites Located in Georgia

Table A.1—New Flexible and Semi-Rigid Pavement Structures for the Georgia LTPP Sites

Section ID	Layer No.	Layer Type	Material Code & Description	Layer Thickness, in.
13-0502	5	Surface	2 – Porous Friction Course	0.9
	4	HMA	1 – Dense Graded HMA	1.9
	3	Stabilized Base	319 – Dense Graded HMA Base	11.2
	2	Aggregate Base	308 – Soil Aggregate Mix; Coarse-Grained; A-1-b	13
	1	Subgrade	215 – Silty Sand with Gravel; A-4	102
13-0503	5	Surface	2 – Porous Friction Course	0.7
	4	HMA	1 – Dense Graded HMA	2.0
	3	Stabilized Base	319 – Dense Graded HMA Base	11.4
	2	Aggregate Base	308 – Soil Aggregate Mix; Coarse-Grained; A-1-b	13
	1	Subgrade	215 – Silty Sand with Gravel; A-4	234
13-0504	5	Surface	2 – Porous Friction Course	0.7
	4	HMA	1 – Dense Graded HMA	2.2
	3	Stabilized Base	319 – Dense Graded HMA Base	11.3
	2	Aggregate Base	308 – Soil Aggregate Mix; Coarse-Grained; A-1-b	13.1
	1	Subgrade	215 – Silty Sand with Gravel; A-4	66
13-0505	5	Surface	2 – Porous Friction Course	1.0
	4	HMA	1 – Dense Graded HMA	2.4
	3	Stabilized Base	319 – Dense Graded HMA Base	11.3
	2	Aggregate Base	308 – Soil Aggregate Mix; Coarse-Grained; A-1-b	13.1
	1	Subgrade	215 – Silty Sand with Gravel; A-4	66
13-0506	5	Surface	2 – Porous Friction Course	0.8
	4	HMA	1 – Dense Graded HMA	2.2
	3	Stabilized Base	319 – Dense Graded HMA Base	11.4
	2	Aggregate Base	308 – Soil Aggregate Mix; Coarse-Grained; A-1-b	13.1
	1	Subgrade	215 – Silty Sand with Gravel; A-4	66
13-0507	5	Surface	2 – Porous Friction Course	0.7
	4	HMA	1 – Dense Graded HMA	2.4
	3	Stabilized Base	319 – Dense Graded HMA Base	11.6
	2	Aggregate Base	308 – Soil Aggregate Mix; Coarse-Grained; A-1-b	13.0
	1	Subgrade	215 – Silty Sand with Gravel; A-4	66
13-0508	5	Surface	2 – Porous Friction Course	0.7
	4	HMA	1 – Dense Graded HMA	1.7
	3	Stabilized Base	319 – Dense Graded HMA Base	11.4
	2	Aggregate Base	308 – Soil Aggregate Mix; Coarse-Grained; A-1-b	13.1
	1	Subgrade	215 – Silty Sand with Gravel; A-4	---

Table A.1—New Flexible and Semi-Rigid Pavement Structures for the Georgia LTPP Sites (Continued)

13-0509	5	Surface	2 – Porous Friction Course	0.7
	4	HMA	1 – Dense Graded HMA	1.8
	3	Stabilized Base	319 – Dense Graded HMA Base	11.3
	2	Aggregate Base	308 – Soil Aggregate Mix; Coarse-Grained; A-1-b	13.0
	1	Subgrade	215 – Silty Sand with Gravel; A-4	---
13-0560	5	Surface	2 – Porous Friction Course	0.7
	4	HMA	1 – Dense Graded HMA	1.6
	3	Stabilized Base	319 – Dense Graded HMA Base	15.2
	2	Aggregate Base	308 – Soil Aggregate Mix; Coarse-Grained; A-1-b	15.5
	1	Subgrade	215 – Silty Sand with Gravel; A-4	---
13-0561	5	Surface	2 – Porous Friction Course	0.7
	4	HMA	1 – Dense Graded HMA	1.8
	3	Stabilized Base	319 – Dense Graded HMA Base	15.6
	2	Aggregate Base	308 – Soil Aggregate Mix; Coarse-Grained; A-1-b	15.5
	1	Subgrade	215 – Silty Sand with Gravel; A-4	---
13-0562	5	Surface	2 – Porous Friction Course	0.7
	4	HMA	1 – Dense Graded HMA	1.8
	3	Stabilized Base	319 – Dense Graded HMA Base	15.2
	2	Aggregate Base	308 – Soil Aggregate Mix; Coarse-Grained; A-1-b	15.5
	1	Subgrade	215 – Silty Sand with Gravel; A-4	---
13-0563	5	Surface	2 – Porous Friction Course	0.8
	4	HMA	1 – Dense Graded HMA	2.2
	3	Stabilized Base	319 – Dense Graded HMA Base	15.1
	2	Aggregate Base	308 – Soil Aggregate Mixture; Coarse-Grained	15.5
	1	Subgrade	215 – Silty Sand with Gravel; A-4	36
13-0564	5	Surface	2 – Porous Friction Course	0.7
	4	HMA	1 – Dense Graded HMA	1.7
	3	Stabilized Base	319 – Dense Graded HMA Base	15.2
	2	Aggregate Base	308 – Soil Aggregate Mix; Coarse-Grained; A-1-b	15.5
	1	Subgrade	215 – Silty Sand with Gravel; A-4	---
13-0565	5	Surface	2 – Porous Friction Course	1.0
	4	HMA	1 – Dense Graded HMA	2.0
	3	Stabilized Base	319 – Dense Graded HMA Base	15.6
	2	Aggregate Base	308 – Soil Aggregate Mix; Coarse-Grained; A-1-b	15.5
	1	Subgrade	215 – Silty Sand with Gravel; A-4	60
13-0566	5	Surface	2 – Porous Friction Course	0.6
	4	HMA	1 – Dense Graded HMA	1.7
	3	Stabilized Base	319 – Dense Graded HMA Base	14.4
	2	Aggregate Base	308 – Soil Aggregate Mix; Coarse-Grained; A-1-b	15.5
	1	Subgrade	215 – Silty Sand with Gravel; A-4	---

Table A.1—New Flexible and Semi-Rigid Pavement Structures for the Georgia LTPP Sites (Continued)

13-1001	4	HMA	1 – Dense Graded HMA	1.7
	3	HMA	1 – Dense Graded HMA	6.4
	2	Aggregate Base	304 – Crushed Gravel	8.6
	1	Subgrade	145 – Sandy Silt; A-7-6	---
13-1004	4	HMA	1 – Dense Graded HMA	1.9
	3	HMA	1 – Dense Graded HMA	4.9
	2	Aggregate Base	308 – Soil Aggregate Mix; Coarse-Grained; A-1-b	7.6
	1	Subgrade	114 – Sandy Lean Clay; A-5	---
13-1005	4	HMA	1 – Dense Graded HMA	1.4
	3	HMA	1 – Dense Graded HMA	6.2
	2	Aggregate Base	308 – Soil Aggregate Mix; Coarse-Grained; A-1-a	8.8
	1	Subgrade	216 – Clayey Sand; A-4	---
13-1031	5	Surface	2 – Porous Friction Course	0.6
	4	HMA	1 – Dense Graded HMA	2.4
	3	HMA	1 – Dense Graded HMA	8.2
	2	Embankment	309 – Fined-Grained Soil; A-2-4	8.8
	1	Subgrade	214 – Silty Sand; A-1-b	---
13-4092	4	HMA	1 – Dense Graded HMA	1.2
	3	HMA	1 – Dense Graded HMA	4.5
	2	Stabilized Soil	339 – Soil Cement	8.3
	1	Subgrade	216 – Clayey Sand; A-2-4	---
13-4093	4	HMA	1 – Dense Graded HMA	1.2
	3	HMA	1 – Dense Graded HMA	4.6
	2	Stabilized Soil	339 – Soil Cement	7.8
	1	Subgrade	216 – Clayey Sand; A-2-4	156
13-4096	4	HMA	1 – Dense Graded HMA	1.3
	3	HMA	1 – Dense Graded HMA	2.8
	2	Stabilized Soil	339 – Soil Cement	6.3
	1	Subgrade	216 – Clayey Sand; A-3	---
13-4111	4	Surface	2 – Porous Friction Course	0.7
	3	HMA	1 – Dense Graded HMA	8.1
	2	Aggregate Base	308 – Soil Aggregate Mix; Coarse-Grained; A-1-a	8.2
	1	Subgrade	113 – Sandy Clay; A-6	---
13-4112	4	Surface	72 – Slurry Seal Coat	0.1
	3	HMA	1 – Dense Graded HMA	3.1
	2	HMA	319 – Dense Graded HMA Base	12.7
	1	Subgrade	202 – Poorly Graded Sand; A-3	---

Table A.1—New Flexible and Semi-Rigid Pavement Structures for the Georgia LTPP Sites (Continued)

13-4113	4	Surface	71 – Chip Seal/Seal Coat	0.1
	3	HMA	1 – Dense Graded HMA	3.6
	2	Stablized Base	321 – Asphalt Stabilized/Treated Base	11.5
	1	Subgrade	204 – Poorly Graded Sand with Silt; A-3	---
13-4119	5	Surface	2 – Porous Friction Course	0.8
	4	HMA	1 – Dense Graded HMA	1.8
	3	HMA	319 – Dense Graded HMA Base	13.8
	2	Aggregate Base	308 – Soil Aggregate Mix; Coarse-Grained; A-1-a	16.4
	1	Subgrade	145 – Sandy Silt; A-4	48
13-4420	4	HMA	1 – Dense Graded HMA	1.7
	3	HMA	1 – Dense Graded HMA	2.9
	2	Stabilized Soil	339 – Soil Cement	7.9
	1	Subgrade	214 – Silty Sand; A-2-4	---

Table A.2—Rehabilitated Flexible and Semi-Rigid Pavement Structures for the Georgia LTPP Sites
[NOTE: The layers for the existing pavement structure are provided in Table A.1; the information included in this table is only for the rehabilitation.]

Section ID	Layer No.	Layer Type	Material Code & Description	Layer Thickness, in.
13-0502	7	Overlay	2 – Porous Friction Course	1.0
	6	Overlay	1 – Dense Graded HMA with RAP	1.6
			No milling of the existing pavement structure	---
13-0503	8	Overlay	2 – Porous Friction Course	1.1
	7	Overlay	1 – Dense Graded HMA with RAP	1.4
	6	Overlay	1 – Dense Graded HMA with RAP	3.8
			Milling used to remove surface	---
	5	Surface	2 – Porous Friction Course	0.0
	4	HMA	1 – Dense Graded HMA	1.4
13-0504	8	Overlay	2 – Porous Friction Course	0.9
	7	Overlay	1 – Dense Graded HMA	1.4
	6	Overlay	1 – Dense Graded HMA	3.9
			Milling used to remove surface	---
	5	Surface	2 – Porous Friction Course	0.0
	4	HMA	1 – Dense Graded HMA	1.6
13-0505	7	Overlay	2 – Porous Friction Course	1.0
	6	Overlay	1 – Dense Graded HMA	1.4
			Milling used to remove surface	---
	5	Surface	2 – Porous Friction Course	0.0
	4	HMA	1 – Dense Graded HMA	1.8
13-0506	8	Overlay	2 – Porous Friction Course	1.0
	7	Overlay	1 – Dense Graded HMA	1.8
	6	Overlay	1 – Dense Graded HMA	2.4
			Milling used to remove surface	---
	5	Surface	2 – Porous Friction Course	0.0
	4	HMA	1 – Dense Graded HMA	0.0
13-0507	8	Overlay	2 – Porous Friction Course	0.8
	7	Overlay	1 – Dense Graded HMA	1.3
	6	Overlay	1 – Dense Graded HMA	4.6
			Milling used to remove surface	---
	5	Surface	2 – Porous Friction Course	0.0
	4	HMA	1 – Dense Graded HMA	1.6
13-0508	8	Overlay	2 – Porous Friction Course	0.9
	7	Overlay	1 – Dense Graded HMA with RAP	1.3
	6	Overlay	1 – Dense Graded HMA with RAP	5.4
			Milling used to remove surface	---
	5	Surface	2 – Porous Friction Course	0.0
	4	HMA	1 – Dense Graded HMA	0.0

Table A.2—Rehabilitated Flexible and Semi-Rigid Pavement Structures for the Georgia LTPP Sites (Continued)
[NOTE: The layers for the existing pavement structure are provided in Table A.1; the information included in this table is only for the rehabilitation.]

13-0509	8	Overlay	2 – Porous Friction Course	1.0
	7	Overlay	1 – Dense Graded HMA with RAP	2.0
	6	Overlay	1 – Dense Graded HMA with RAP	2.1
			Milling used to remove surface	---
	5	Surface	2 – Porous Friction Course	0.0
	4	HMA	1 – Dense Graded HMA	0.4
13-0560	8	Overlay	2 – Porous Friction Course	0.7
	7	Overlay	1 – Dense Graded HMA with RAP	1.2
	6	Overlay	1 – Dense Graded HMA with RAP	1.1
			Milling used to remove surface	---
	5	Surface	2 – Porous Friction Course	0.0
	4	HMA	1 – Dense Graded HMA	1.3
13-0561	8	Overlay	2 – Porous Friction Course	1.1
	7	Overlay	1 – Dense Graded HMA with RAP	1.1
	6	Overlay	1 – Dense Graded HMA with RAP	1.9
			Milling used to remove surface	---
	5	Surface	2 – Porous Friction Course	0.0
13-0562	8	Overlay	2 – Porous Friction Course	0.9
	7	Overlay	1 – Dense Graded HMA	1.4
	6	Overlay	1 – Dense Graded HMA	2.1
			Milling used to remove surface	---
	5	Surface	2 – Porous Friction Course	0.0
	4	HMA	1 – Dense Graded HMA	1.6
13-0563	7	Overlay	2 – Porous Friction Course; Inlay	1.1
	6	Overlay	1 – Dense Graded HMA; Inlay	2.3
			Milling used to remove surface	---
	5	Surface	2 – Porous Friction Course	0.0
	4	HMA	1 – Dense Graded HMA	0.0
13-0564	7	Overlay	1 – Dense Graded HMA with RAP; Inlay	1.0
	6	Overlay	1 – Dense Graded HMA with RAP; Inlay	2.3
			Milling used to remove surface	---
	5	Surface	2 – Porous Friction Course	0.0
	4	HMA	1 – Dense Graded HMA	0.0
13-0565	8	Overlay	2 – Porous Friction Course	0.9
	7	Overlay	1 – Dense Graded HMA; with RAP; Inlay	1.2
	6	Overlay	1 – Dense Graded HMA; with RAP; Inlay	3.3
			Milling used to remove surface	---
	5	Surface	2 – Porous Friction Course	0.0
	4	HMA	1 – Dense Graded HMA	1.9

Table A.2—Rehabilitated Flexible and Semi-Rigid Pavement Structures for the Georgia LTPP Sites (Continued)
[NOTE: The layers for the existing pavement structure are provided in Table A.1; the information included in this table is only for the rehabilitation portion.]

13-0566	8	Overlay	2 – Porous Friction Course	0.8
	7	Overlay	1 – Dense Graded HMA; Inlay	1.3
	6	Overlay	1 – Dense Graded HMA; Inlay	4.2
			Milling used to remove surface	---
	5	Surface	2 – Porous Friction Course	0.0
	4	HMA	1 – Dense Graded HMA	0.0
13-1001			Maintenance activity applied.	
13-1004			Maintenance activity applied.	
13-1005			Maintenance activity applied.	
13-1031	6	Overlay	2 – Porous Friction Course	0.9
			Milling used to remove surface	---
	5	Surface	2 – Porous Friction Course	0.0
13-4092			Maintenance activity applied.	
13-4093			Maintenance activity applied.	
13-4096	6	Overlay	13 – RAP Overlay; Plant Produced	1.4
	5	Overlay	71 – Seal Coat/Chip Seal	0.3
13-4112			Maintenance activity applied.	
13-4113	5	Overlay	1 – Dense Graded HMA	1.8
13-4119			Maintenance activity applied.	
13-4420	6	Overlay	1 – Dense Graded HMA	1.1
	5	Overlay	1 – Dense Graded HMA	0.7

Table A.3—New Rigid Pavement Structures for the Georgia LTPP Sites

Section ID	Layer No.	Layer Type	Material Code & Description	Layer Thickness, in.
13-3007	3	PCC	4 – Jointed Plain Concrete	9.3
	2	Aggregate Base	308 – Soil Aggregate Mix; Coarse-Grained; A-1-b	9.0
	1	Subgrade	145 – Sandy Silt; A-2-4	---
13-3011	4	PCC	4 – Jointed Plain Concrete	10.1
	3	Treated Base	319 – Dense Graded HMA Base	0.9
	2	Treated Soil	339 – Soil Cement	4.7
	1	Subgrade	214 – Silty Sand; A-2-4	---
13-3015	4	PCC	4 – Jointed Plain Concrete	10.0
	3	Treated Base	78 – Asphalt Concrete Inerlayer	1.0
	2	Treated Soil	339 – Soil Cement	5.7
	1	Subgrade	202 – Poorly Graded Sand; A-2-4	---
13-3016	4	PCC	4 – Jointed Plain Concrete	11.1
	3	Treated Base	319 – Dense Graded HMA Base	1.4
	2	Aggregate Base	308 – Soil Aggregate Mix; Coarse-Grained; A-1-a	5.0
	1	Subgrade		60
13-3017	3	PCC	4 – Jointed Plain Concrete	9.9
	2	Treated Base	331 – Cement Treated Base	6.1
	1	Subgrade	214 – Silty Sand; A-5	144
13-3018	3	PCC	4 – Jointed Plain Concrete	9.9
	2	Treated Base	331 – Cement Treated Base	5.8
	1	Subgrade	216 – Clayey Sand; A-4	---
13-3019	3	PCC	4 – Jointed Plain Concrete	9.1
	2	Aggregate Base	308 – Soil Aggregate Mix; Coarse-Grained; A-1-a	7.2
	1	Subgrade	114 – Sandy Lean Clay; A-7-5	---
13-3020	3	PCC	4 – Jointed Plain Concrete	9.1
	2	Treated Soil	339 – Soil Cement	5.4
	1	Subgrade	216 – Clayey Sand; A-6	---
13-4118	2	PCC	4 – Jointed Plain Concrete	7.8
	1	Subgrade	216 – Clayey Sand; A-4	---
13-5023	3	PCC	6 – Continuously Reinforced Concrete	8.4
	2	Treated Soil	339 – Soil Cement	5.5
	1	Subgrade	202 – Poorly Graded Sand; A-3	---

Table A.4—Rehabilitated Rigid Pavement Structures for the Georgia LTPP Sites
[NOTE: The layers for the existing pavement structure are provided in Table A.3; the information included in this table is only for the rehabilitation.]

Section ID	Layer No.	Layer Type	Material Code & Description	Layer Thickness, in.
13-3017			Maintenance activity applied.	
13-3020			Maintenance activity applied.	
13-4118	3	Overlay, PCC	6 – Continuously Reinforced Concrete	8.4
13-7028	This PCC pavement already had an HMA overlay when it was included in the LTPP database			
13-7028	7	Overlay	1 – Dense Graded HMA	3.4
	6	Overlay	72 – Chip Seal/Seal Coat	0.1
	5	Overlay	1 – Dense Graded HMA	2.6
	4	PCC	4 – Jointed Plain Concrete	9.1
	3	Treated Base	321 – Asphalt Treated Base	3.1
	2	Aggregate Base	310 – Other Base Material; A-1-b	3.9
	1	Subgrade	216 – Clayey Sand; A-4	---
13-7028			Maintenance activity applied.	
13-7028	8	2nd Overlay	1 – Dense Graded HMA	2.5
			Milling used to remove surface	---
	7	Overlay	1 – Dense Graded HMA	1.9

This page left blank intentionally.

Appendix B
Graphs of Average Annual Daily Truck Traffic Reported Over Time for the Georgia LTPP Sites

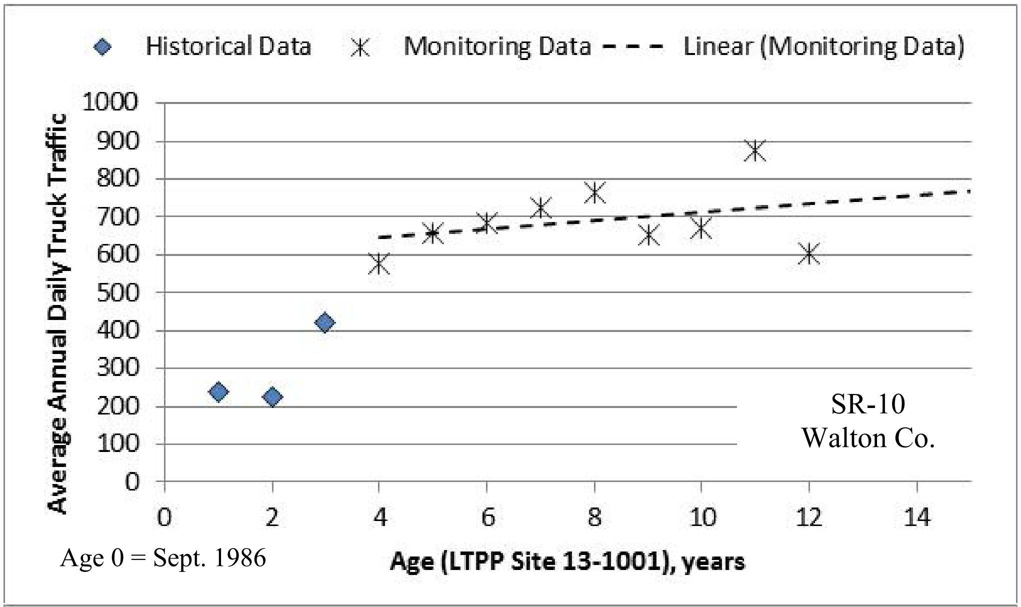

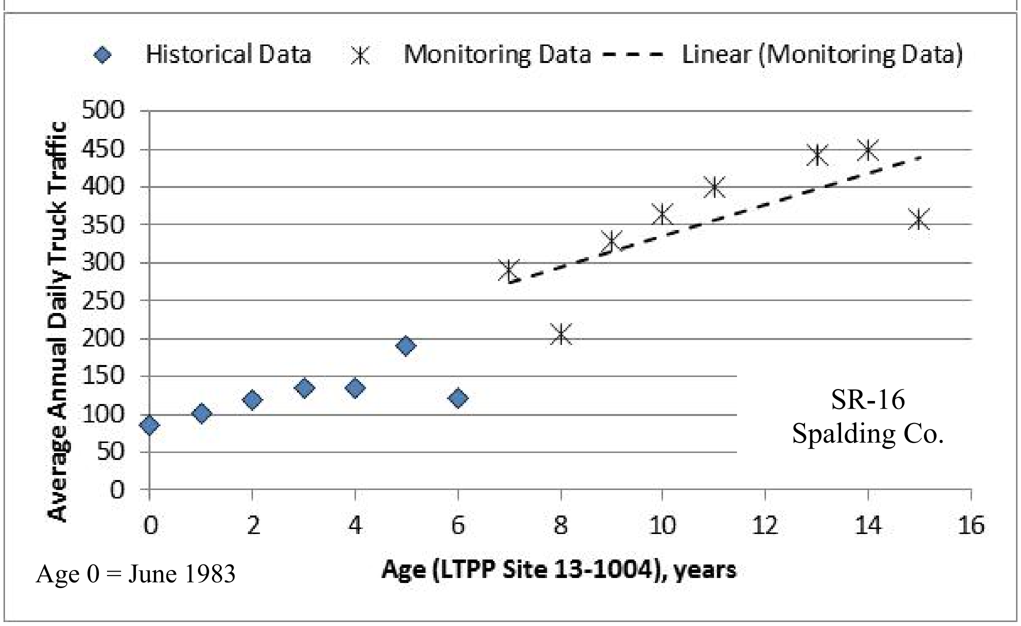

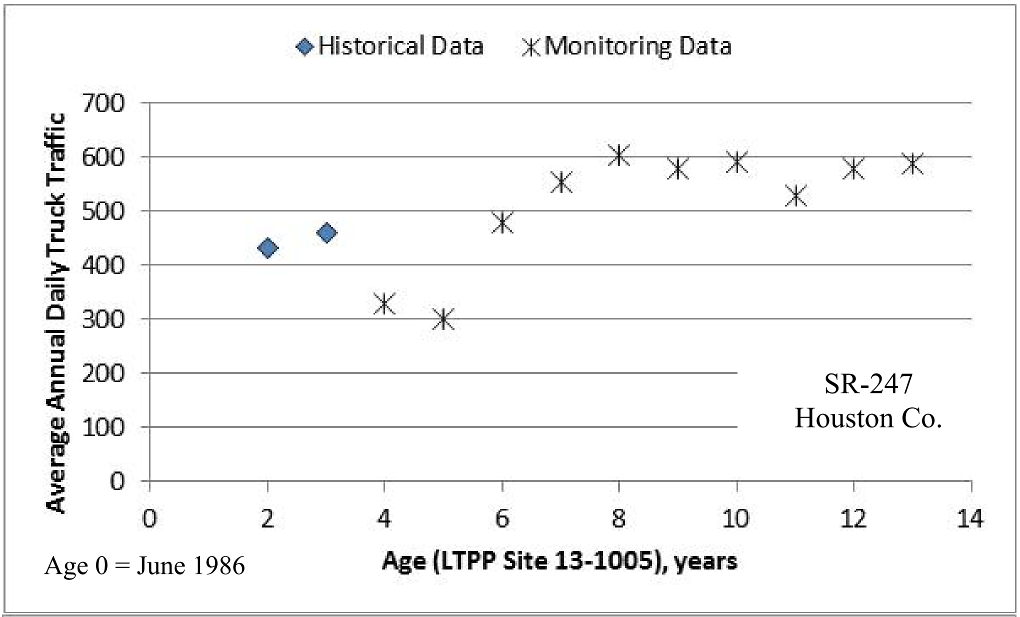
Historical Data
Monitoring Data
Average Annual Daily Truck Traffic
700
600
500
400
300
200
100
0
0
2
4
6
8
10
12
14
SR-247
Houston Co.
Age 0 = June 1986
Age (LTPP Site 13-1005), years

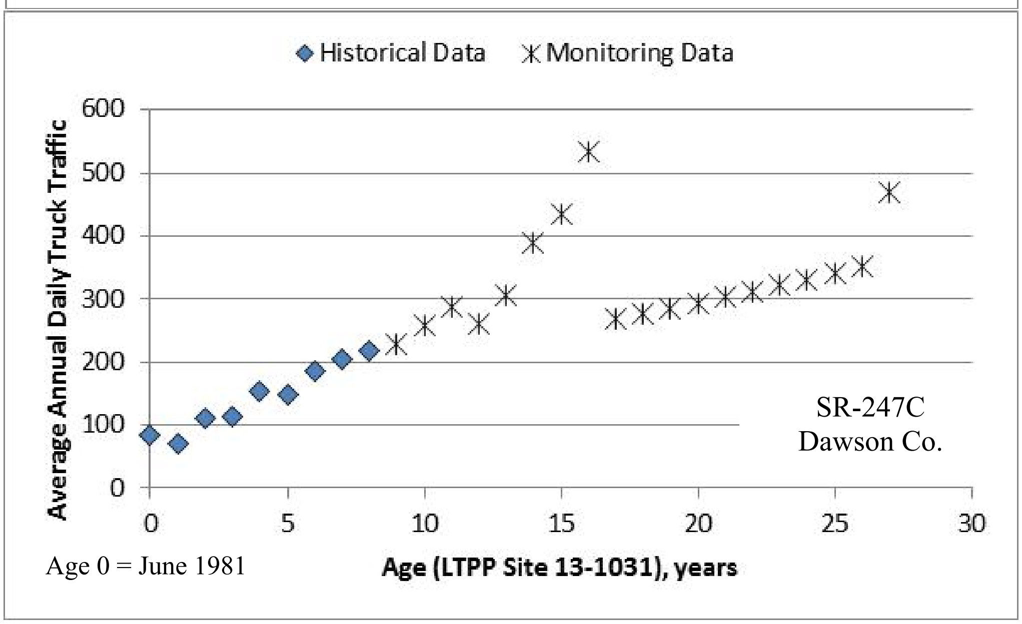
Historical Data
Monitoring Data
Average Annual Daily Truck Traffic
600
500
400
300
200
100
0
0
5
10
15
20
25
30
SR-247C
Dawson Co.
Age 0 = June 1981
Age (LTPP Site 13-1031), years

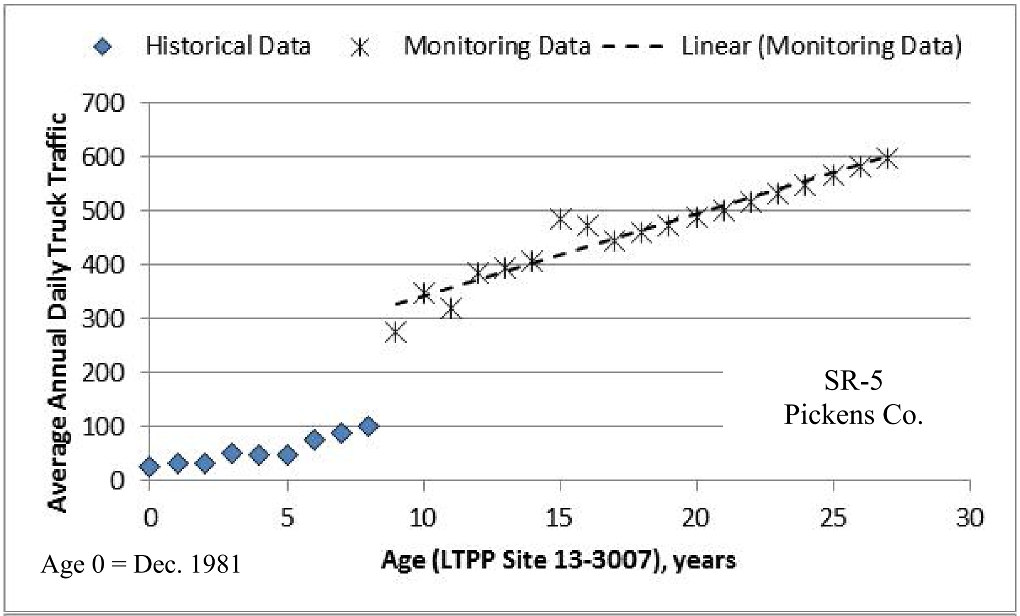

Historical Data
Monitoring Data
Linear (Monitoring Data)
Average Annual Daily Truck Traffic
700
600
500
400
300
200
100
0
0
5
10
15
20
25
30
SR-5
Pickens Co.
Age 0 = Dec. 1981
Age (LTPP Site 13-3007), years

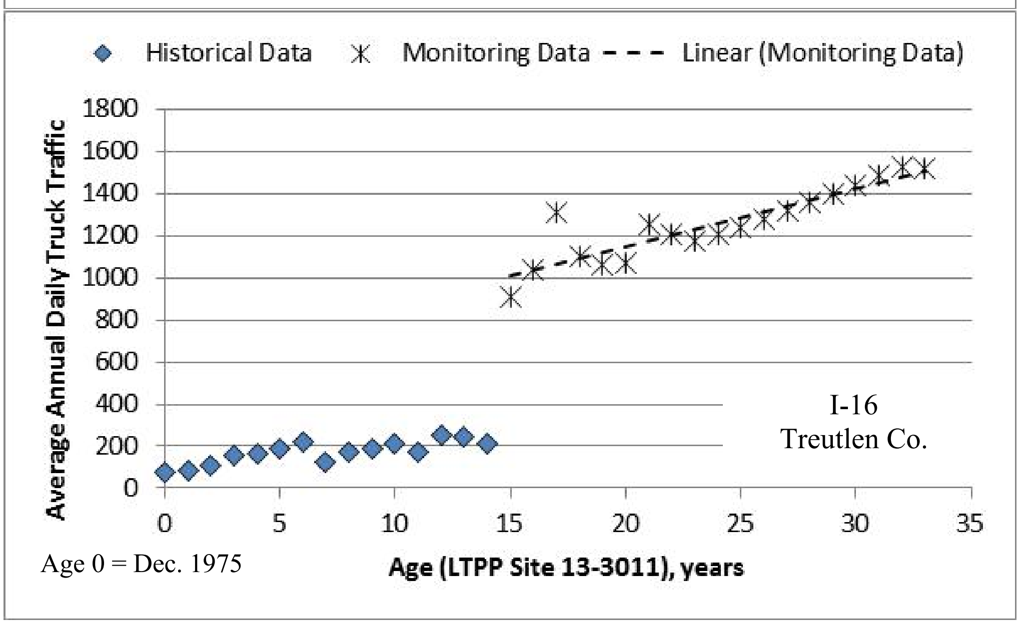

Historical Data
Monitoring Data
Linear (Monitoring Data)
Average Annual Daily Truck Traffic
1800
1600
1400
1200
1000
800
600
400
200
0
0
5
10
15
20
25
30
35
I-16
Treutlen Co.
Age 0 = Dec. 1975
Age (LTPP Site 13-3011), years

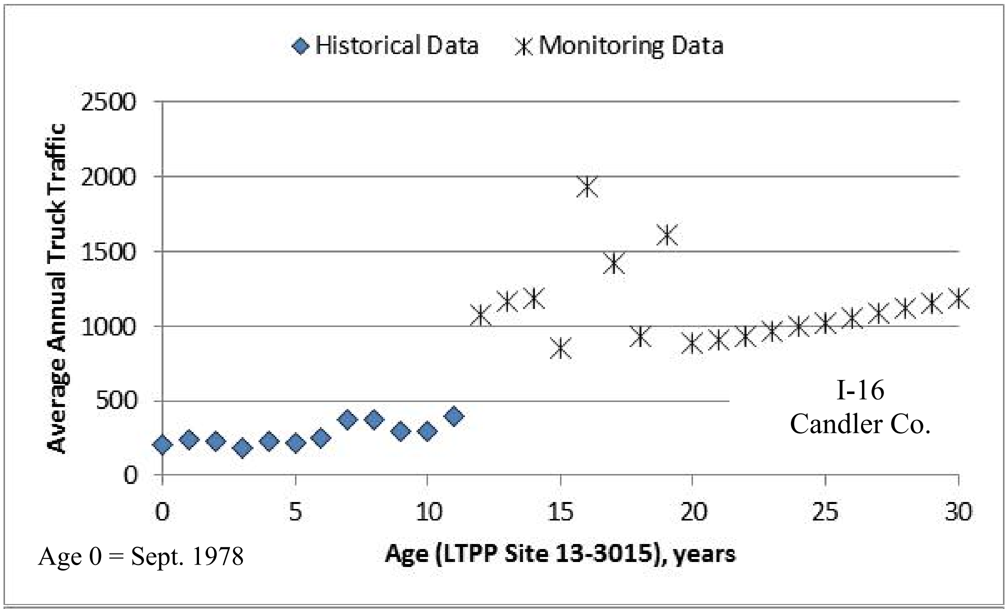
Historical Data
Monitoring Data
Average Annual Truck Traffic
2500
2000
1500
1000
500
0
0
5
10
15
20
25
30
I-16
Candler Co.
Age 0 = Sept. 1978
Age (LTPP Site 13-3015), years

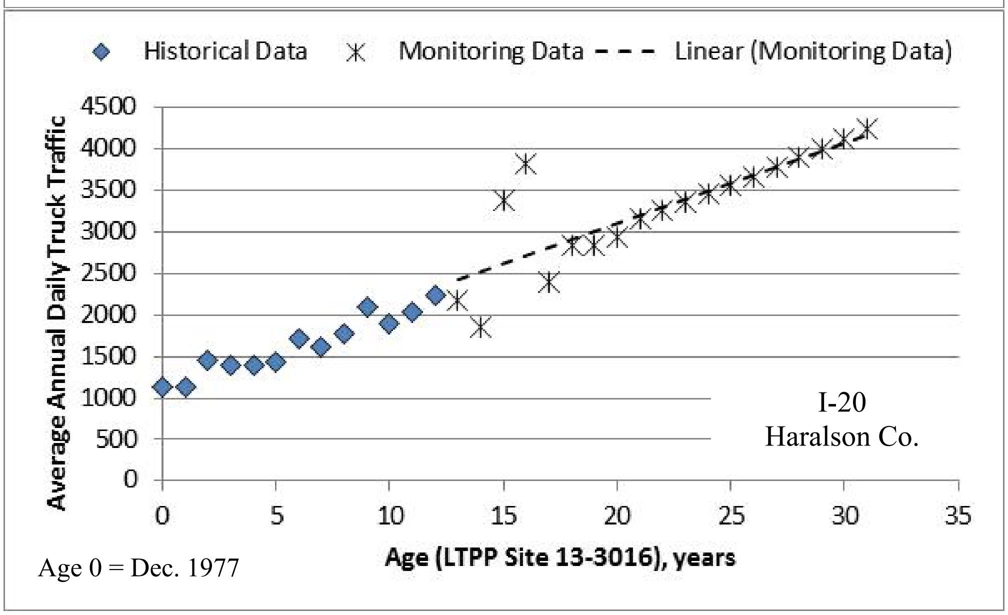
Historical Data
Monitoring Data
Linear (Monitoring Data)
Average Annual Daily Truck Traffic
4500
4000
3500
3000
2500
2000
1500
1000
500
0
0
5
10
15
20
25
30
35
I-20
Haralson Co.
Age 0 = Dec. 1977
Age (LTPP Site 13-3016), years

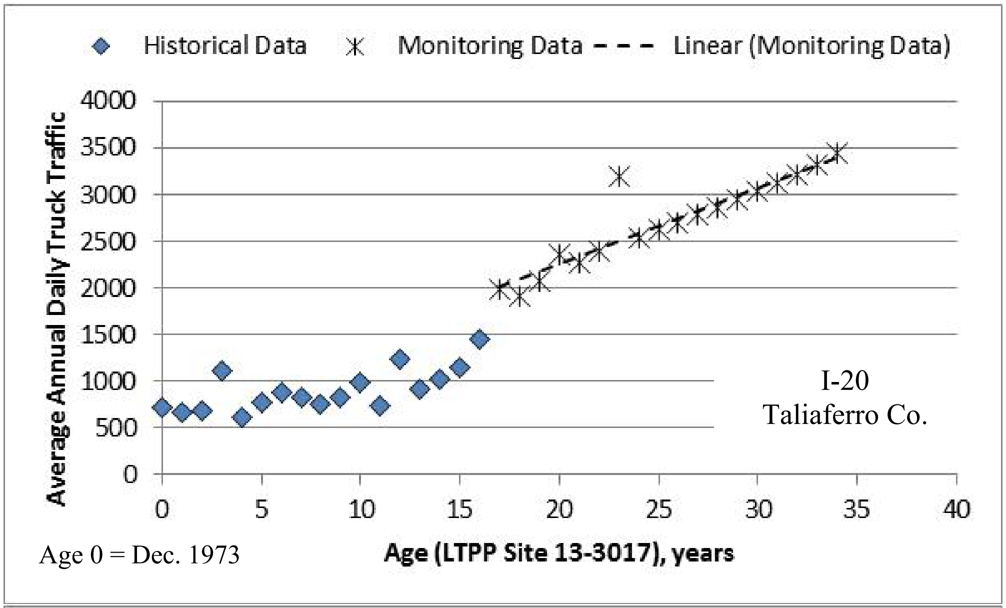
Historical Data
Monitoring Data
Linear (Monitoring Data)
Average Annual Daily Truck Traffic
4000
3500
3000
2500
2000
1500
1000
500
0
0
5
10
15
20
25
30
35
40
I-20
Taliaferro Co.
Age 0 = Dec. 1973
Age (LTPP Site 13-3017), years

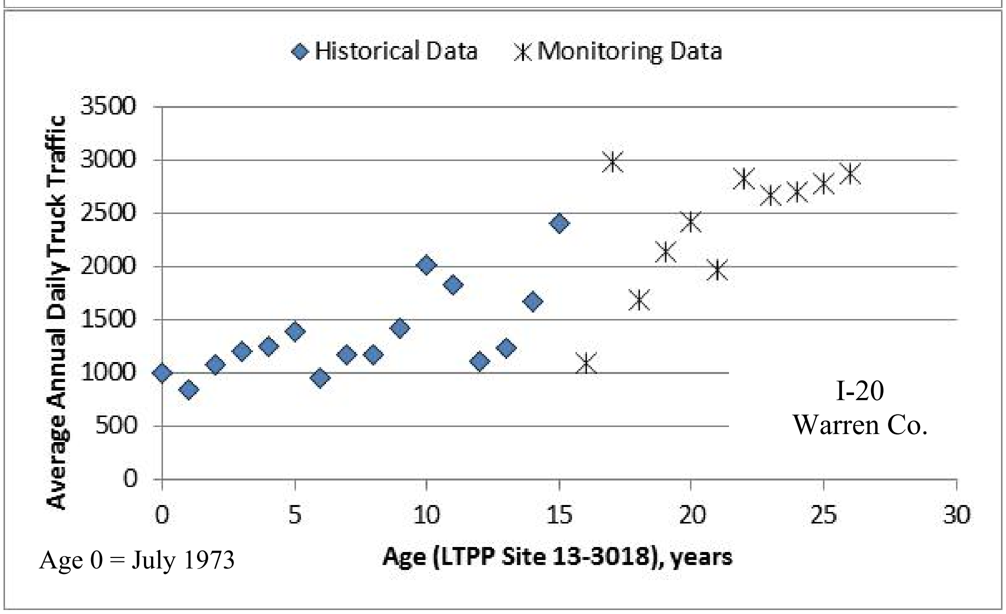
Historical Data
Monitoring Data
Average Annual Daily Truck Traffic
3500
3000
2500
2000
1500
1000
500
0
0
5
10
15
20
25
30
I-20
Warren Co.
Age 0 = July 1973
Age (LTPP Site 13-3018), years

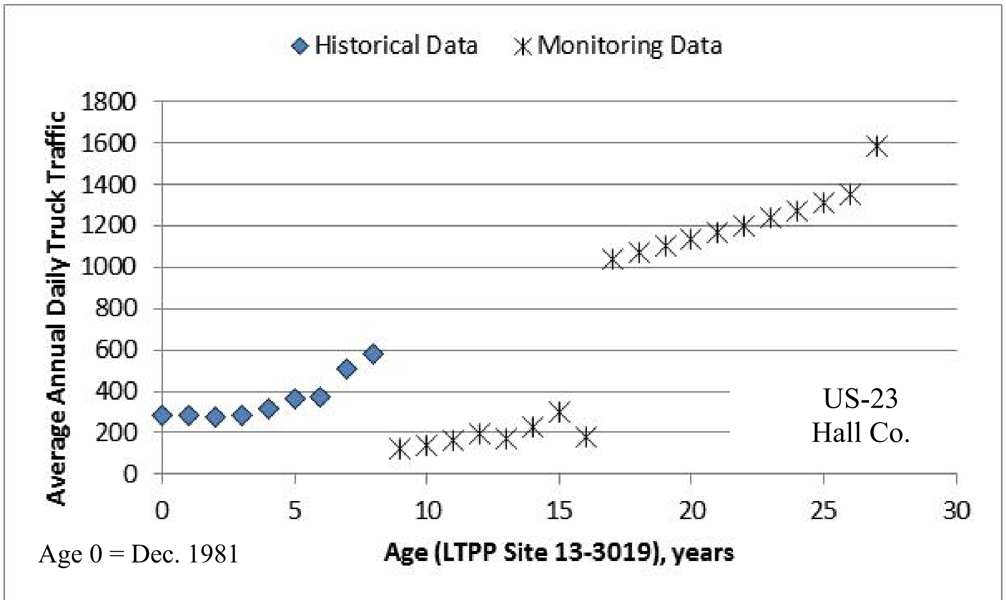
Historical Data
Monitoring Data
Average Annual Daily Truck Traffic
1800
1600
1400
1200
1000
800
600
400
200
0
0
5
10
15
20
25
30
US-23
Hall Co.
Age 0 = Dec. 1981
Age (LTPP Site 13-3019), years

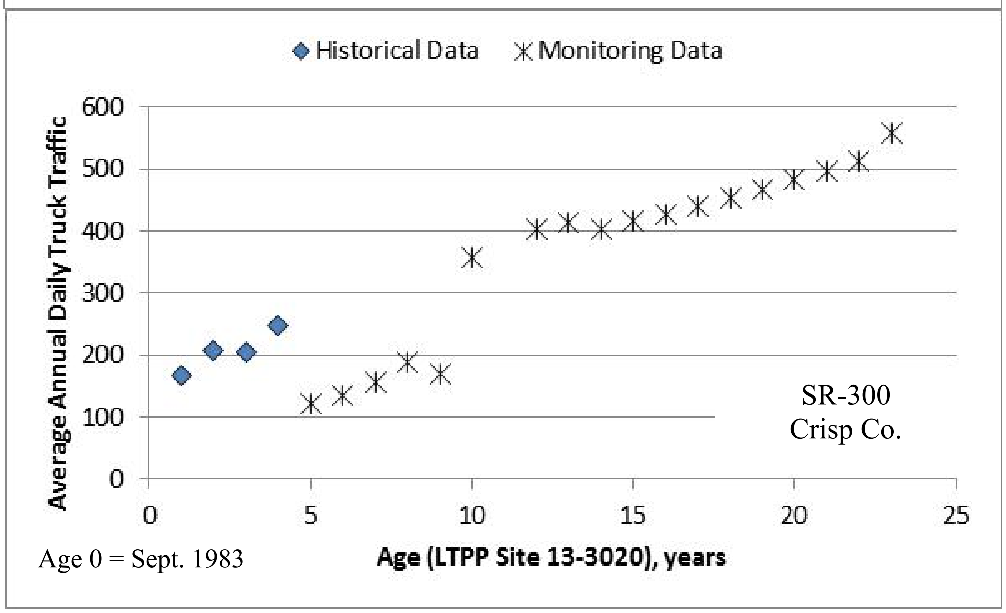
Historical Data
Monitoring Data
Average Annual Daily Truck Traffic
600
500
400
300
200
100
0
0
5
10
15
20
25
SR-300
Crisp Co.
Age 0 = Sept. 1983
Age (LTPP Site 13-3020), years

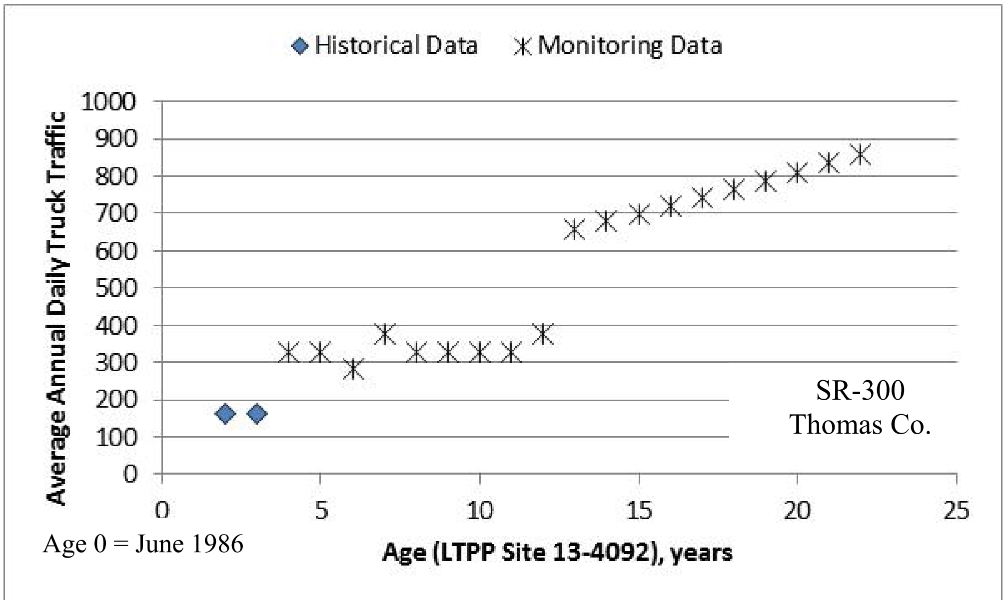
Historical Data
Monitoring Data
Average Annual Daily Truck Traffic
1000
900
800
700
600
500
400
300
200
100
0
0
5
10
15
20
25
SR-300
Thomas Co.
Age 0 = June 1986
Age (LTPP Site 13-4092), years

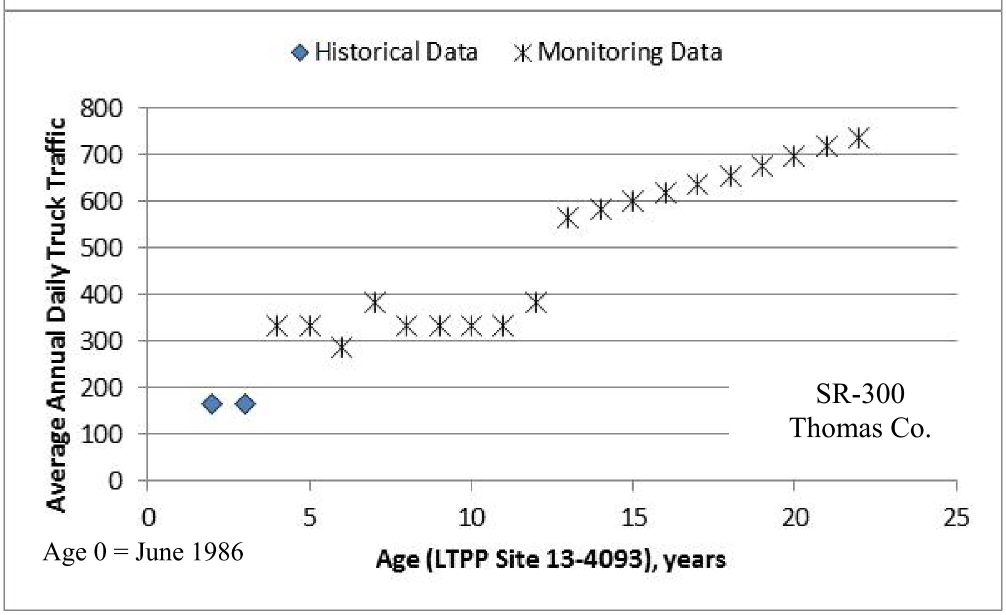
Historical Data
Monitoring Data
Average Annual Daily Truck Traffic
800
700
600
500
400
300
200
100
0
0
5
10
15
20
25
SR-300
Thomas Co.
Age 0 = June 1986
Age (LTPP Site 13-4093), years

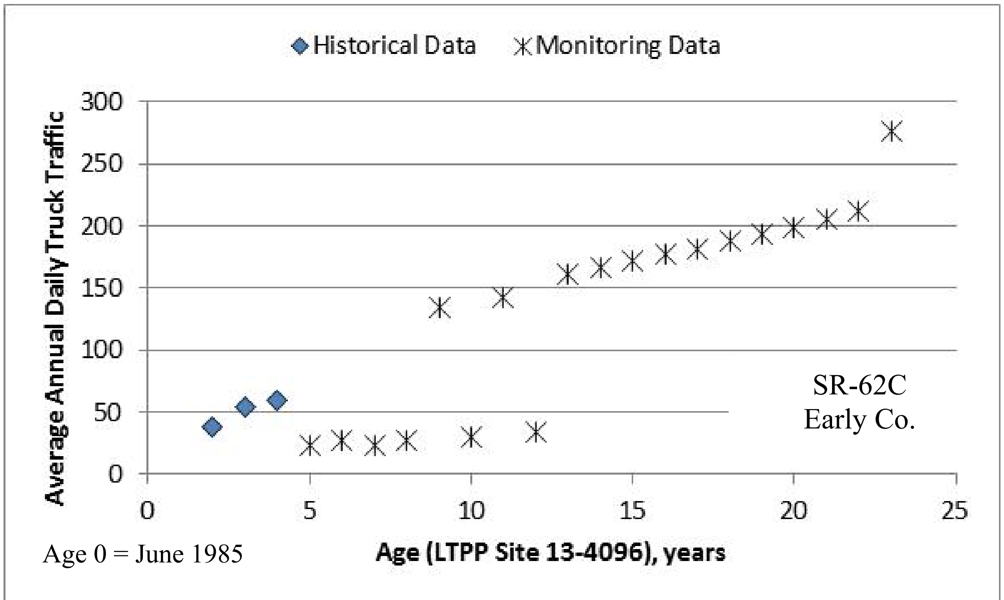
Historical Data
Monitoring Data
Average Annual Daily Truck Traffic
300
250
200
150
100
50
0
0
5
10
15
20
25
SR-62C
Early Co.
Age 0 = June 1985
Age (LTPP Site 13-4096), years

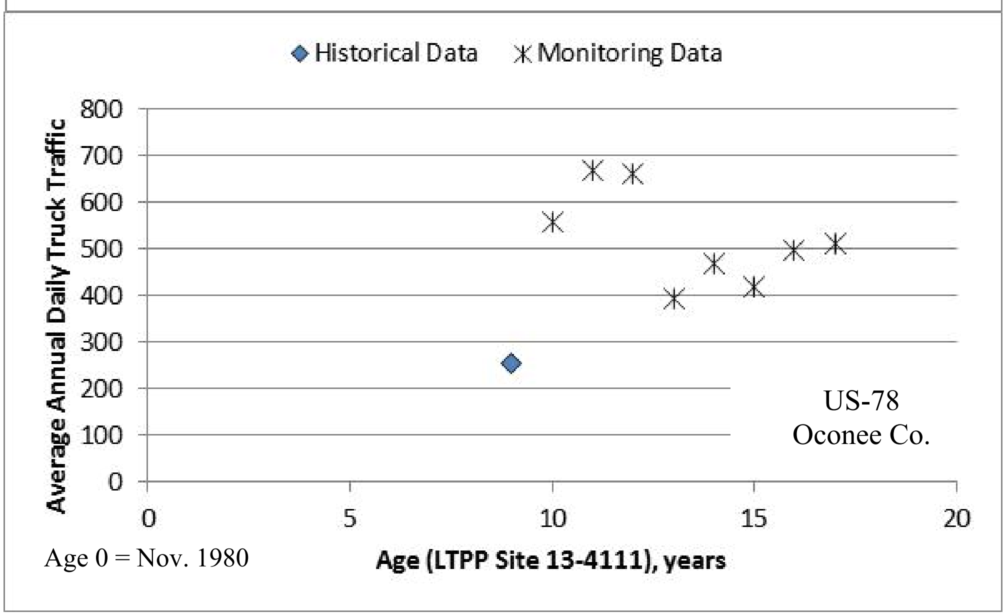
Historical Data
Monitoring Data
Average Annual Daily Truck Traffic
800
700
600
500
400
300
200
100
0
0
5
10
15
20
US-78
Oconee Co.
Age 0 = Nov. 1980
Age (LTPP Site 13-4111), years

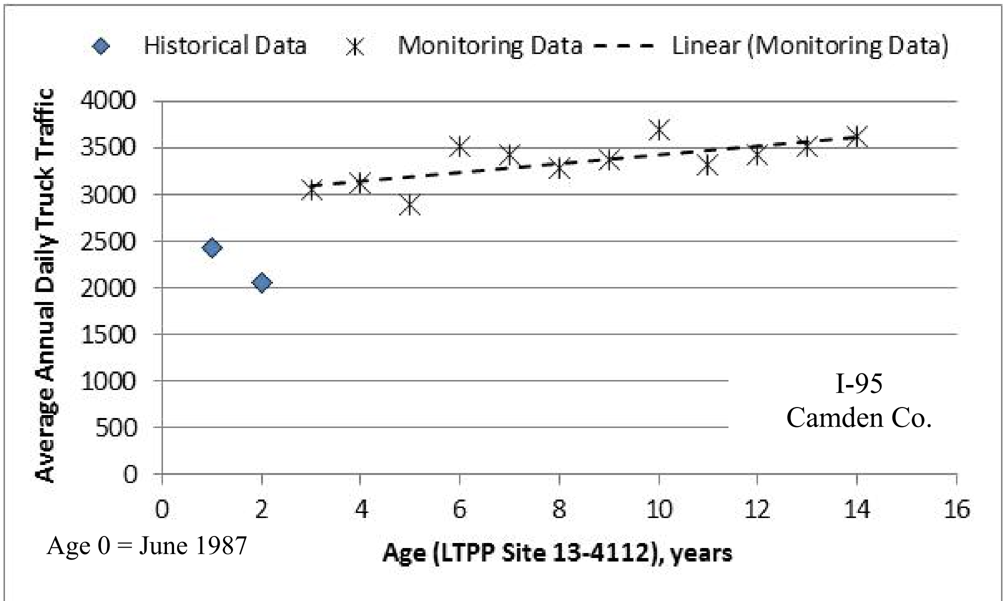
Historical Data
Monitoring Data
Linear (Monitoring Data)
Average Annual Daily Truck Traffic
4000
3500
3000
2500
2000
1500
1000
500
0
0
2
4
6
8
10
12
14
16
I-95
Camden Co.
Age 0 = June 1987
Age (LTPP Site 13-4112), years

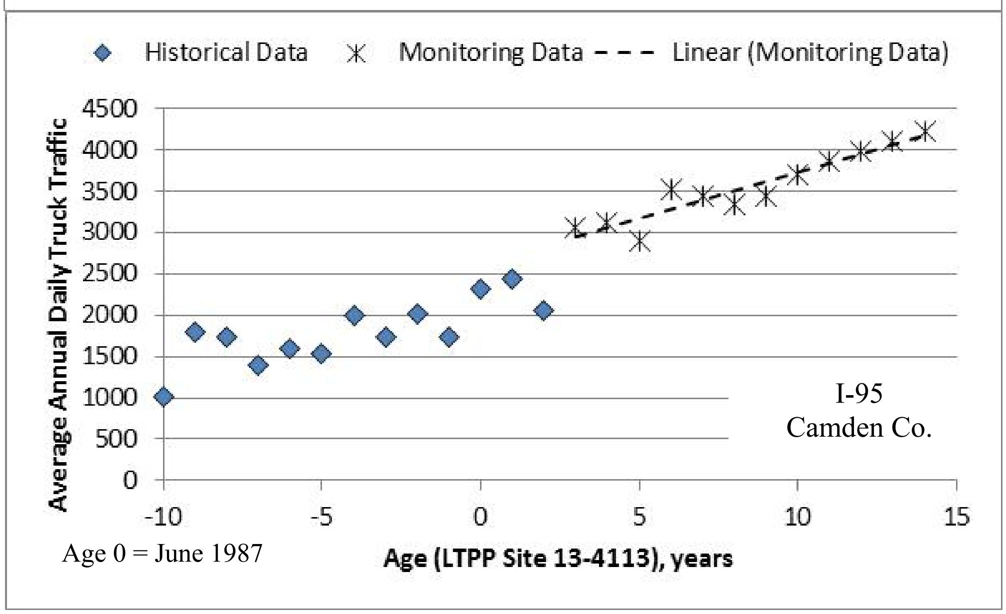
Historical Data
Monitoring Data
Linear (Monitoring Data)
Average Annual Daily Truck Traffic
4500
4000
3500
3000
2500
2000
1500
1000
500
0
-10
-5
0
5
10
15
I-95
Camden Co.
Age 0 = June 1987
Age (LTPP Site 13-4113), years

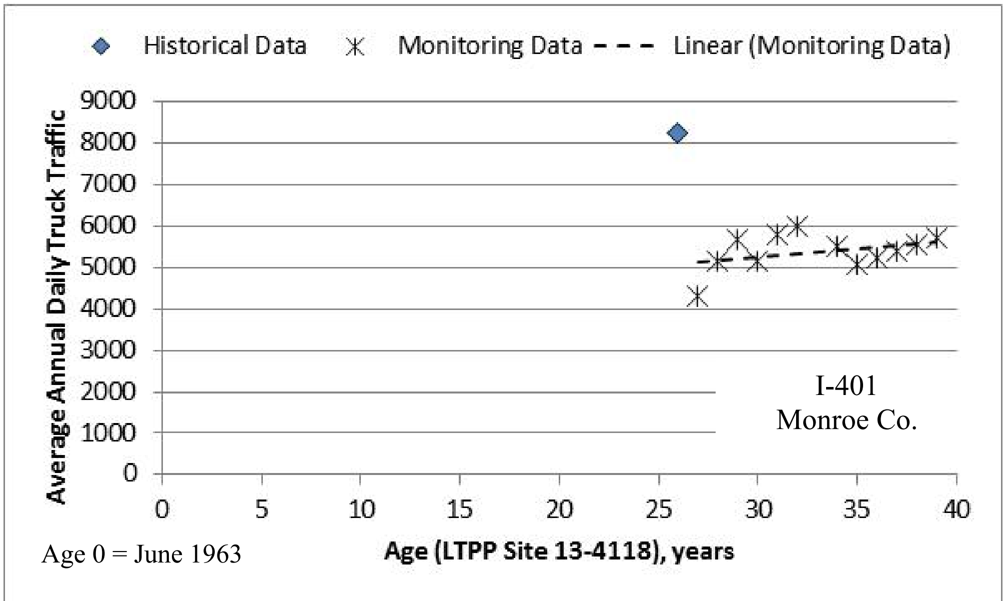
Historical Data
Monitoring Data
Linear (Monitoring Data)
Average Annual Daily Truck Traffic
9000
8000
7000
6000
5000
4000
3000
2000
1000
0
0
5
10
15
20
25
30
35
40
I-401
Monroe Co.
Age 0 = June 1963
Age (LTPP Site 13-4118), years

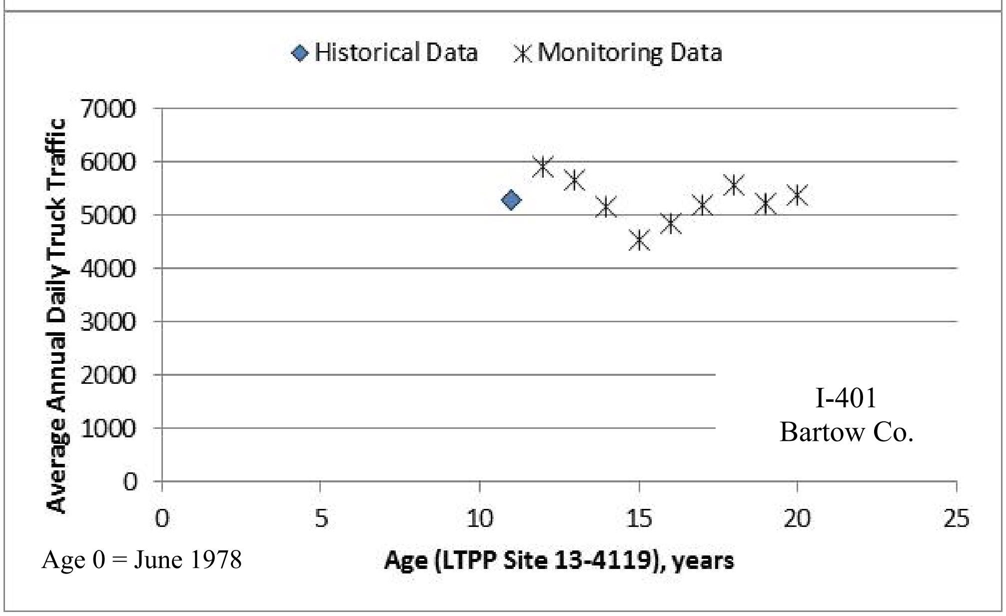
Historical Data
Monitoring Data
Average Annual Daily Truck Traffic
7000
6000
5000
4000
3000
2000
1000
0
0
5
10
15
20
25
I-401
Bartow Co.
Age 0 = June 1978
Age (LTPP Site 13-4119), years

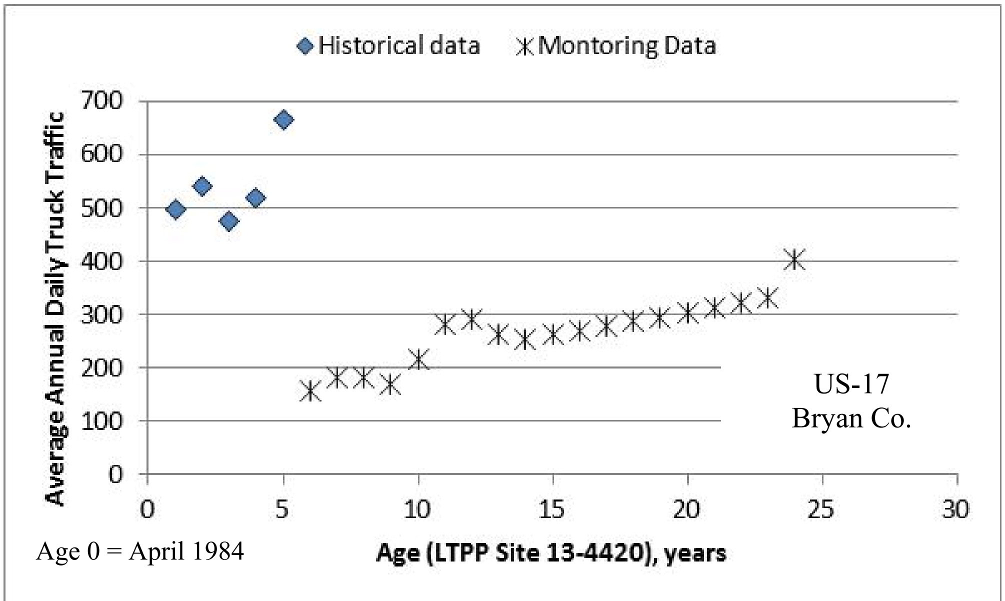
Historical data
Montoring Data
Average Annual Daily Truck Traffic
0
100
200
300
400
500
600
700
0
5
10
15
20
25
30
US-17
Bryan Co.
Age 0 = April 1984
Age (LTPP Site 13-4420), years

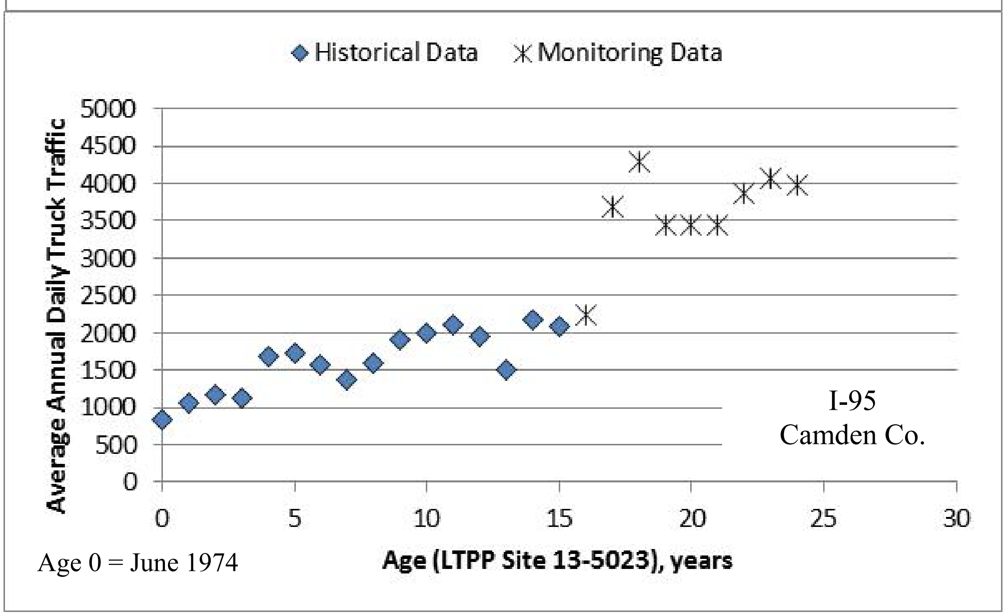
Historical Data
Monitoring Data
Average Annual Daily Truck Traffic
0
500
1000
1500
2000
2500
3000
3500
4000
4500
5000
0
5
10
15
20
25
30
I-95
Camden Co.
Age 0 = June 1974
Age (LTPP Site 13-5023), years

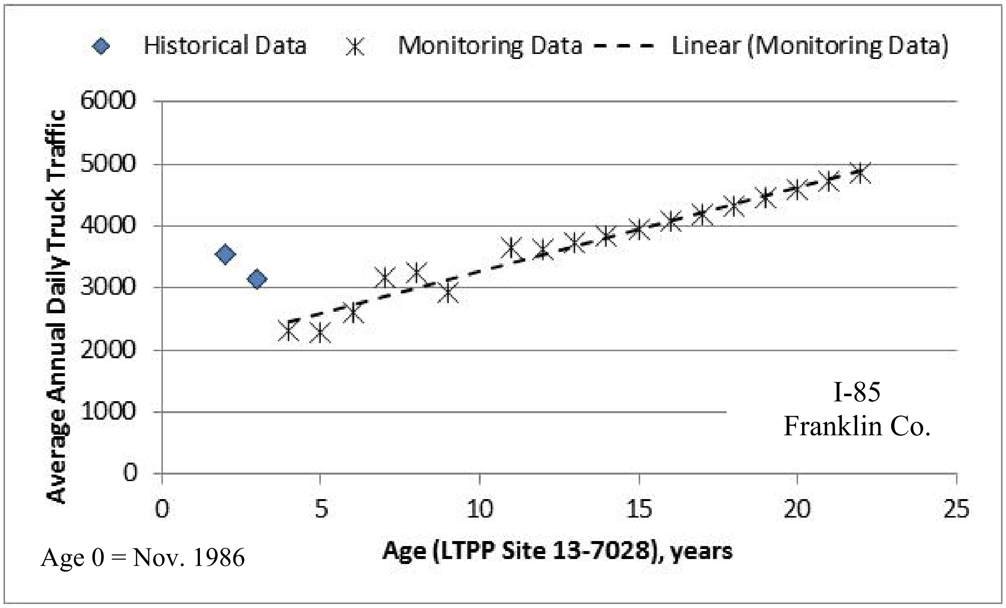
Historical Data
Monitoring Data
Linear (Monitoring Data)
6000
5000
4000
3000
2000
1000
0
Average Annual Daily Truck Traffic
0
5
10
15
20
25
Age (LTPP Site 13-7028), years
Age 0 = Nov. 1986
I-85
Franklin Co.

Appendix C
Monthly Volume Distribution Factors

SHRP ID	Month	Vehicle/Truck Class									
		4	5	6	7	8	9	10	11	12	13
1031	1	1.08	1.17	0.9	1	0.99	0.9	0.9	0	1	1.66
1031	2	1.08	0.9	0.81	1	0.72	0.9	0.45	0	1	0.81
1031	3	0.72	0.72	1.08	1	0.81	0.99	0.9	0	1	0.81
1031	4	0.72	0.72	0.9	1	0.9	0.99	1.23	1.5	1	0.81
1031	5	0.9	0.81	1.35	1	1.08	1.08	1.24	1.5	1	0.81
1031	6	1.08	0.81	1.08	1	1.17	1.17	1.24	1.5	1	1.67
1031	7	1.08	0.81	0.81	1	1.26	0.99	0.9	1.5	1	0.81
1031	8	1	1	1	1	1	1	1	1	1	1
1031	9	1	1	1	1	1	1	1	1	1	1
1031	10	1	1	1	1	1	1	1	1	1	1
1031	11	1.17	1.62	1.17	1	1.08	0.99	0.9	1.5	1	0.81
1031	12	1.17	1.44	0.9	1	0.99	0.99	1.24	1.5	1	0.81
3007	1	0.66	0.55	0.65	0.94	0.64	1.07	1.03	0.4	0.52	0.79
3007	2	0.66	0.66	0.7	0.86	0.75	1.07	0.9	0.33	0.52	1.54
3007	3	0.85	0.79	0.82	0.86	0.93	1.06	1.06	0.55	0.52	0.95
3007	4	0.94	0.9	1.2	1.06	1.13	1.07	1.14	0.82	1.13	1.02
3007	5	1	0.86	1.47	1.53	1.24	1.05	1.04	1.17	1.12	1.25
3007	6	0.93	0.97	1.33	1.48	1.33	1.12	1.13	1.55	1.12	1.34
3007	7	0.8	0.87	1.16	1.29	1.26	1.2	1.28	1.23	1.16	1.17
3007	8	1.21	1.2	1.04	0.86	1.11	0.84	0.84	1.19	1.12	1.01
3007	9	1.29	1.28	1.17	0.81	1.1	0.9	0.95	1.19	1.12	0.99
3007	10	1.28	1.51	1.02	1.07	0.93	0.79	0.84	1.19	1.12	0.82
3007	11	1.27	1.37	0.75	0.62	0.79	0.78	0.72	1.19	1.43	0.75
3007	12	1.11	1.04	0.69	0.62	0.79	1.05	1.07	1.19	1.12	0.37
3011	1	0.82	1.06	0.86	0.39	0.86	0.97	0.76	0.84	0.91	0.91
3011	2	0.87	1.33	1.04	1.19	0.98	0.99	1.05	0.89	1.24	0.74
3011	3	0.93	1	0.98	1.18	1.03	0.93	0.99	0.83	0.83	1.53
3011	4	0.66	0.62	0.68	1.26	1.07	0.97	0.95	1.29	1.42	2.21
3011	5	0.86	0.82	0.79	1.34	1.04	0.99	0.99	1.24	1.32	1.67
3011	6	1.21	1.11	0.93	0.82	1.1	1.05	1.02	1.29	1.22	1.16
3011	7	1.47	1.46	1.39	1.03	0.89	0.99	1.12	0.78	0.69	0.69
3011	8	1.13	0.82	1.16	0.66	0.96	1.13	1	0.89	0.88	0.67
3011	9	1.16	0.93	1.15	0.81	0.99	1.1	1.06	1.01	0.92	0.73
3011	10	1.18	0.92	1.21	1.1	1.06	1.03	1.1	1.02	0.92	0.56
3011	11	0.96	1.12	1.02	1.2	1.05	0.87	0.95	0.7	0.66	0.67
3011	12	0.75	0.81	0.79	1.02	0.97	0.98	1.01	1.22	0.99	0.46

SHRP ID	Month	Vehicle/Truck Class									
		4	5	6	7	8	9	10	11	12	13
3017	1	0.16	0.12	0.66	1.05	0.24	0.2	1.29	0.11	0.39	0.82
3017	2	0.2	0.04	0.59	1.01	0.24	0.36	1.37	0.39	0.63	0.49
3017	3	0.72	0.57	0.83	0.58	0.84	0.76	1.16	0.6	0.72	0.55
3017	4	1.49	1.41	1.27	0.39	1.36	1.4	0.86	1.29	1.08	0.6
3017	5	1.61	1.67	1.23	0.2	1.55	1.53	0.95	1.75	1.48	2.13
3017	6	1.6	1.94	1.31	3.2	1.58	1.63	1.04	1.82	1.51	2.13
3017	7	1.52	1.97	1.24	0.14	1.42	1.46	0.62	1.54	1.3	0.55
3017	8	0.94	1.27	0.72	1.05	1.06	1.03	0.48	0.94	0.85	0.57
3017	9	1.53	1.32	1.19	0.36	1.57	1.58	0.91	1.75	1.68	0.6
3017	10	1.3	0.9	1.16	0.77	1.2	1.16	1.01	1.03	1.15	1.37
3017	11	0.52	0.4	0.97	1.86	0.53	0.51	1.25	0.46	0.7	1.06
3017	12	0.41	0.39	0.83	1.39	0.41	0.38	1.06	0.32	0.51	1.13
3018	1	0.17	0.11	0.79	1.6	0.22	0.22	1.94	0.16	0.51	1.12
3018	2	0.23	0.06	0.74	1.53	0.28	0.39	2.06	0.39	0.67	0.65
3018	3	0.74	0.56	0.91	0.89	0.91	0.84	1.42	0.74	0.86	0.74
3018	4	1.41	1.26	1.08	0.6	1.29	1.34	0.65	1.28	1.07	0.81
3018	5	1.71	1.65	1.08	0.12	1.51	1.45	0.36	1.61	1.26	0.57
3018	6	1.54	1.97	1.08	0.12	1.53	1.5	0.24	1.72	1.32	0.57
3018	7	1.49	2.14	1.02	0.12	1.4	1.4	0.19	1.46	1.07	0.65
3018	8	1.41	1.95	1.19	0.12	1.52	1.63	0.25	1.63	1.3	0.96
3018	9	1.46	1.2	1.03	0.56	1.54	1.55	0.42	1.61	1.56	1.11
3018	10	1.29	0.78	1.15	1.19	1.18	1.17	1	1.01	1.13	2.18
3018	11	0.33	0.16	1.08	2.87	0.39	0.34	1.93	0.28	0.79	1.28
3018	12	0.22	0.16	0.85	2.28	0.23	0.17	1.54	0.11	0.46	1.36
3020	1	0.55	0.47	0.64	2.85	0.56	0.65	0.56	0.43	0.43	0
3020	2	0.87	0.62	1	0	0.95	1	0.72	0.86	0.54	0
3020	3	1.08	0.77	1.08	0	0.99	1.01	1.01	1.01	0.4	0
3020	4	1.08	0.95	1.06	0	1.25	1.21	1.04	1.33	0.4	0
3020	5	1.65	1.03	1.24	4.7	1.37	1.57	1.61	1.75	4.35	4.7
3020	6	1.33	1.14	1.01	2.21	1.07	1.08	0.95	1.06	0.88	3.45
3020	7	0.8	1.34	0.86	0	0.86	0.78	0.77	0.67	0.79	0
3020	8	1.16	1.66	1.15	0.64	1.15	0.99	0.98	1.17	0.92	0.54
3020	9	1.08	1.48	1.27	0.97	1.48	1.37	1.29	1.72	1.39	2.21
3020	10	0.86	1.06	0.9	0.63	0.78	0.72	1.22	0.76	0.91	1.1
3020	11	0.9	0.84	0.95	0	0.9	0.91	1.27	0.69	0.58	0
3020	12	0.64	0.64	0.84	0	0.64	0.71	0.58	0.55	0.41	0

SHRP ID	Month	Vehicle/Truck Class									
		4	5	6	7	8	9	10	11	12	13
4112	1	0.6	0.84	1.56	0.96	0.96	1.06	1.32	0.96	1.08	1.32
4112	2	0.72	0.96	1.2	0.96	1.08	1.06	1.2	0.96	1.14	0.96
4112	3	0.96	1.08	0.96	0.6	1.08	1.06	0.96	0.96	1.14	0.96
4112	4	1.44	1.2	0.96	0.48	1.08	0.96	0.96	0.96	1.08	0.84
4112	5	1.08	0.96	0.84	0.48	1.08	0.96	0.96	0.96	0.84	0.48
4112	6	1.08	1.08	0.72	0.6	1.08	0.96	0.96	1.08	0.96	0.6
4112	7	0.72	0.84	1.08	1.08	0.96	0.84	0.84	0.96	0.84	0.6
4112	8	0.84	0.72	0.96	1.32	1.08	0.96	0.84	1.08	0.96	0.84
4112	9	0.84	0.84	0.84	1.32	0.84	0.96	0.96	1.08	0.96	0.84
4112	10	1.44	1.32	0.96	1.44	0.96	1.06	0.96	1.08	1.08	1.32
4112	11	1.32	1.2	0.96	1.44	0.96	1.06	0.96	0.96	1.08	1.44
4112	12	0.96	0.96	0.96	1.32	0.84	1.06	1.08	0.96	0.84	1.8
4113	1	0.6	0.84	1.56	0.96	0.96	1.08	1.68	0.96	1.2	1.32
4113	2	0.72	0.96	1.2	0.84	1.08	1.08	1.08	0.96	1.2	0.96
4113	3	0.96	1.08	0.96	0.72	1.08	1.08	0.84	1.08	1.44	0.96
4113	4	1.32	1.2	0.96	0.48	1.26	0.96	0.96	0.96	1.08	0.84
4113	5	1.08	0.96	0.84	0.48	1.26	0.96	0.96	0.96	0.84	0.48
4113	6	0.96	1.08	0.72	0.48	0.96	0.84	1.08	0.96	0.84	0.48
4113	7	0.6	0.84	0.96	0.84	0.72	0.6	0.96	0.72	0.6	0.48
4113	8	1.2	0.72	0.96	1.32	0.96	0.96	0.72	1.08	0.84	1.32
4113	9	0.84	0.84	0.84	1.32	0.96	0.96	0.96	1.08	0.96	0.72
4113	10	1.56	1.32	0.96	1.68	0.96	1.08	0.84	1.2	1.08	1.32
4113	11	1.32	1.2	0.96	1.56	0.96	1.32	0.84	1.08	1.08	1.44
4113	12	0.84	0.96	1.08	1.32	0.84	1.08	1.08	0.96	0.84	1.68
4118	1	0.55	1.1	0.44	0.22	1.1	1.21	0.44	1.32	1.1	1.65
4118	2	0.77	1.21	0.55	0.22	1.1	0.99	0.33	1.21	1.1	0.66
4118	3	0.99	1.21	0.66	0.22	1.1	0.99	0.33	0.99	0.99	0.66
4118	4	1.21	1.43	0.88	0.22	1.21	0.88	0.33	0.77	0.77	0.44
4118	5	0.66	0.77	0.66	0.11	0.88	1.21	0.33	1.1	1.1	0.44
4118	6	1.1	0.99	0.77	0.22	1.43	1.21	0.55	1.32	1.32	0.44
4118	7	0.99	0.99	1.87	3.19	1.21	1.1	2.42	1.32	1.21	1.54
4118	8	1.21	0.88	1.32	2.09	1.1	1.32	1.98	1.32	1.43	0.88
4118	9	1.1	0.77	1.32	1.43	0.77	0.99	1.65	0.88	0.99	1.21
4118	10	1.43	0.88	1.43	1.65	0.55	0.55	1.43	0.44	0.55	1.43
4118	11	1	1	1	1	1	1	1	1	1	1
4118	12	0.99	0.77	1.1	1.43	0.55	0.55	1.21	0.33	0.44	1.65

SHRP ID	Month	Vehicle/Truck Class									
		4	5	6	7	8	9	10	11	12	13
4119	1	1.08	1.2	0.96	0.72	1.08	0.96	0.84	0.96	1.08	1.2
4119	2	1.2	1.5	0.96	0.6	0.96	0.96	0.6	0.96	1.08	0.96
4119	3	1.38	1.5	1.24	0.96	1.08	1.08	0.84	1.08	1.44	0.96
4119	4	1.2	1.08	1.08	1.44	1.08	0.96	1.08	1.08	1.08	1.08
4119	5	1.08	0.96	0.96	1.2	1.08	1.08	0.96	1.08	1.08	0.84
4119	6	0.84	0.84	1.08	1.44	1.08	1.26	1.32	1.2	0.96	1.2
4119	7	0.48	0.72	0.84	1.2	1.08	0.96	1.08	0.96	0.84	0.96
4119	8	0.96	0.84	1.24	0.84	1.08	1.08	1.08	1.08	0.96	0.96
4119	9	1.38	1.08	1.24	0.72	0.84	1.26	0.96	1.2	1.08	0.72
4119	10	0.96	0.84	0.96	0.96	1.08	1.08	1.2	1.08	1.08	0.96
4119	11	0.84	0.84	0.96	1.44	0.96	0.96	1.56	1.08	1.08	1.56
4119	12	0.6	0.6	0.48	0.48	0.6	0.36	0.48	0.24	0.24	0.6
5023	1	0.6	0.6	0.72	0.84	0.6	0.72	0.72	0.72	0.6	0.84
5023	2	0.84	0.6	0.84	1.32	0.6	0.6	1.08	0.6	0.48	1.32
5023	3	1.56	1.2	0.96	1.56	0.96	0.72	0.96	0.72	0.72	1.44
5023	4	1.92	1.44	0.96	0.72	1.08	0.96	0.6	0.6	0.72	0.36
5023	5	1.68	1.08	0.84	0.6	0.96	0.96	0.6	0.84	0.6	0.24
5023	6	0.96	0.72	0.84	1.2	0.72	0.72	0.84	0.72	0.72	0.84
5023	7	0.84	1.2	1.56	2.28	0.96	0.72	2.04	0.84	0.84	3
5023	8	0.6	1.08	1.2	0.96	1.32	1.32	1.2	1.32	1.56	1.2
5023	9	0.36	0.96	1.08	0.72	1.32	1.44	1.2	1.44	1.68	0.84
5023	10	0.6	0.84	1.08	0.84	1.2	1.32	1.08	1.44	1.56	0.96
5023	11	1.08	1.08	0.84	0.24	1.08	1.2	0.6	1.32	1.2	0.24
5023	12	0.96	1.2	1.08	0.72	1.2	1.32	1.08	1.44	1.32	0.72
7028	1	0.55	0.77	0.44	0.22	1.15	1.1	0.44	1.12	0.99	0.11
7028	2	0.66	0.77	0.55	0.55	1.1	1.1	0.55	1.14	1.1	0.33
7028	3	0.88	1.1	0.77	0.55	0.99	1.1	0.44	1.14	1.1	0.22
7028	4	1.32	1.21	1.21	0.99	0.99	0.88	0.77	0.77	0.66	0.55
7028	5	1.76	1.48	1.21	1.21	0.88	0.88	0.77	0.77	0.66	0.44
7028	6	1.54	1.32	0.88	0.77	0.77	0.88	0.44	0.88	0.77	0.33
7028	7	1	1	1	1	1	1	1	1	1	1
7028	8	1.98	1.49	1.1	1.65	0.77	0.77	0.99	0.77	0.77	0.66
7028	9	0.66	0.77	1.48	1.43	1.1	1.21	1.65	1.14	1.1	1.98
7028	10	0.66	0.77	1.49	1.21	1.16	1.1	1.87	1.14	1.21	2.31
7028	11	0.55	0.77	0.99	1.43	1.1	1.1	1.76	1.14	1.54	2.09
7028	12	0.44	0.55	0.88	0.99	0.99	0.88	1.32	0.99	1.1	1.98

Appendix D
Number of Axles per Truck Class

Section ID	Truck Classification	Number of Axles per Truck Class			
		Single Axles	Tandem Axles	Tridem Axles	Quad Axles
1001	4	1	1	0	0
1001	5	2	0	0	0
1001	6	1	1	0	0
1001	7	1	0.26	0	0
1001	8	2.55	0.45	0	0
1001	9	1.07	1.95	0	0
1001	10	1	2	0	0
1001	11	4.29	0.26	0	0
1001	12	3.52	1.14	0	0
1001	13	2.15	2.13	0	0
1004	4	1	1	0	0
1004	5	2	0	0	0
1004	6	1.02	0.99	0	0
1004	7	1	0.26	0	0
1004	8	2.38	0.67	0	0
1004	9	3	1	0	0
1004	10	1.19	1.09	0	0
1004	11	4.29	0.26	0	0
1004	12	3.52	1.14	0	0
1004	13	2.15	2.13	0	0
3017	4	1.6	0.41	0	0
3017	5	1.75	0	0	0
3017	6	1.01	1	0	0
3017	7	0.64	0	0.17	0.08
3017	8	2.64	0.36	0	0
3017	9	0.54	0.88	0.01	0.01
3017	10	1.26	1.01	0.8	0.01
3017	11	5	0	0	0
3017	12	4	1	0	0
3017	13	2.14	1.75	0.37	0.18

Section ID	Truck Classification	Number of Axles per Truck Class			
		Single Axles	Tandem Axles	Tridem Axles	Quad Axles
3018	4	1.57	0.43	0	0
3018	5	1.43	0	0	0
3018	6	1.01	0.99	0	0
3018	7	0.95	0	0.22	0.15
3018	8	2.63	0.37	0	0
3018	9	0.48	0.79	0.01	0
3018	10	1.27	1	0.78	0.02
3018	11	5	0	0	0
3018	12	4	0.99	0	0
3018	13	2.25	1.83	0.29	0.08
3020	4	1.57	0.44	0	0
3020	5	2	0	0	0
3020	6	1	1	0	0
3020	7	0.15	0	0.05	0.05
3020	8	2.28	0.73	0	0
3020	9	1.06	1.97	0.01	0
3020	10	1.02	1.12	0.87	0.01
3020	11	5	0	0	0
3020	12	3.98	1.01	0	0
3020	13	1.25	2	0.25	0.25
4111	4	1.62	0.39	0	0
4111	5	2	0	0	0
4111	6	1	1	0	0
4111	7	1	0.26	0.83	0
4111	8	2	1	0	0
4111	9	1	2	0	0
4111	10	1.19	1.09	0.89	0
4111	11	4.29	0.26	0.06	0
4111	12	3.52	1.14	0.06	0
4111	13	2.15	2.13	0.35	0

Section ID	Truck Classification	Number of Axles per Truck Class			
		Single Axles	Tandem Axles	Tridem Axles	Quad Axles
4118	4	1.23	0.77	0	0
4118	5	2.04	0	0	0
4118	6	1.09	0.91	0	0
4118	7	1.5	0.24	0.36	0
4118	8	2.72	0.28	0	0
4118	9	1.15	1.92	0	0
4118	10	1.9	1.8	0	0.1
4118	11	5	0	0	0
4118	12	4.37	0.63	0	0
4118	13	2.15	2.13	0.35	0
7028	4	1.11	0.89	0	0
7028	5	2.01	0	0	0
7028	6	1.01	0.99	0	0
7028	7	2.5	0	0.25	0
7028	8	2.29	0.7	0	0
7028	9	1.11	1.94	0	0
7028	10	1.61	1.36	0.36	0
7028	11	4.96	0	0	0
7028	12	3.99	1	0	0
7028	13	2.15	2.13	0.35	0
Average	4	1.3	0.7	0	0
Average	5	2.0	0	0	0
Average	6	1.0	1.0	0	0
Average	7				
Average	8	2.4	0.6	0	0
Average	9	1.2	1.6	0	0
Average	10	1.3	1.3	0.5	0.02
Average	11	4.7	0.1	0.01	0
Average	12	3.9	1.0	0.01	0
Average	13	2.0	2.0	0.20	0.06

This page left blank intentionally.

Appendix E
Air Voids and Asphalt Contents for HMA Layers

Material Type	Section ID	Asphalt Content	Air Voids at Constr.
ATB	502	8.6	8.1
Existing HMA	502	9.2	9.4
FC – Overlay	502	8	15.8
HMA - Overlay - RAP	502	7.6	5.6
ATB	503	8.6	7.2
Existing HMA	503	9.2	8.9
FC – Overlay	503	8	15.1
HMA - Overlay - RAP	503	7.6	4
HMA - Overlay - RAP	503	8.8	3.8
ATB	504	8.6	5
Existing HMA	504	9.2	9.7
FC – Overlay	504	8	16.6
HMA - Overlay - Virgin	504	8.4	3.6
HMA - Overlay - Virgin	504	8.8	3.8
ATB	505	8.6	6
Existing HMA	505	9.2	8.9
FC – Existing	505	7.7	17
FC – Overlay	505	8	15
HMA - Overlay - Virgin	505	8.8	3.8
ATB	506	9.2	6.8
Existing HMA	506	9.2	8.3
FC – Overlay	506	8	15.6
HMA - Overlay - Virgin	506	9	0.9
HMA - Overlay - Virgin	506	9.4	3.4
ATB	507	8.6	6.4
Existing HMA	507	9	10.1
FC – Overlay	507	8	15.8
HMA - Overlay - Virgin	507	9	1.9
HMA - Overlay - Virgin	507	9	3.6

Material Type	Section ID	Asphalt Content	Air Voids at Constr.
ATB	508	8	6.7
Existing HMA	508	9.2	10.2
FC – Overlay	508	8	16
HMA - Overlay - RAP	508	7.6	4.7
HMA - Overlay - RAP	508	8.2	4.4
ATB	509	8	7.1
Existing HMA	509	9.2	10.4
FC – Overlay	509	8	15.3
HMA - Overlay - RAP	509	7.6	6.8
HMA - Overlay - RAP	509	8.2	4.8
ATB	560	8.6	7.3
Existing HMA	560	9.2	6.4
FC – Overlay	560	8	14.8
HMA - Overlay - RAP	560	7.6	8
HMA - Overlay - RAP	560	8.6	0.9
ATB	561	8.6	7
Existing HMA	561	9.2	6.9
FC – Overlay	561	8	16.9
HMA - Overlay - RAP	561	7.6	6.4
HMA - Overlay - RAP	561	8.6	6.1
ATB	562	8.6	7.6
Existing HMA	562	9.2	6.9
FC – Overlay	562	8	16.9
HMA - Overlay - Virgin	562	8.8	4.8
HMA - Overlay - Virgin	562	9	3.7
ATB	563	8.6	8.6
Existing HMA	563	9.2	8.4
FC – Overlay	563	9	16.1
HMA - Overlay - Virgin	563	8.8	1.3
ATB	564	8.6	7.2
Existing HMA	564	9.2	7.9
FC – Overlay	564	8	16
HMA - Overlay - RAP	564	7.6	7.6

Material Type	Section ID	Asphalt Content	Air Voids at Constr.
ATB	565	8.6	6.8
Existing HMA	565	9.2	7.5
FC – Existing	565	8	15.8
FC – Overlay	565	8	15.9
HMA - Overlay - RAP	565	7.6	4.9
HMA - Overlay - RAP	565	8.6	3.3
ATB	566	8.6	8.4
Existing HMA	566	9.2	5.5
FC – Overlay	566	8	16.3
HMA - Overlay - Virgin	566	8.8	2.6
HMA - Overlay - Virgin	566	9	4
Existing HMA	1001	9.5	7.9
Existing HMA	1001	9.5	5.2
Existing HMA – 3	1001	10.7	6.4
Existing HMA	1004	8.5	9.4
Existing HMA	1004	9.6	9.4
Existing HMA – 3	1004	12.9	7.8
Existing HMA	1005	9.6	6.4
Existing HMA	1005	9.1	10
Existing HMA – 3	1005	11.8	7.8
Existing HMA	1031	9.3	8.2
Existing HMA – 3	1031	10.8	8.3
FC – Existing	1031	8	15.5
FC – Overlay	1031	8	15.5
Existing HMA	4092	6.9	6.6
Existing HMA	4092	9.2	6
Existing HMA – 3	4092	11.8	7.1
Existing HMA	4093	9.2	4.6
Existing HMA	4093	10.6	4.9
Existing HMA – 3	4093	11.8	7.1

Material Type	Section ID	Asphalt Content	Air Voids at Constr.
Existing HMA	4096	9.8	9
Existing HMA – 3	4096	11.8	7.3
HMA - Overlay - Virgin	4096	9.3	10.3
Existing HMA – 3	4111	9.7	9.3
FC – Existing	4111	8	15.5
ATB	4112	9.3	9.9
Existing HMA – 3	4112	11.4	6.1
FC – Existing	4112	8	15.5
ATB	4113	8.3	9.3
Existing HMA – 3	4113	10.6	6.9
ATB	4119	9.5	9.9
Existing HMA – 3	4119	11.2	7.8
FC – Existing	4119	8	15.5
Existing HMA	4420	11	7.3
Existing HMA – 3	4420	11.7	6.8
Existing HMA	7028	8.9	5.9
Existing HMA	7028	10.8	4.3

Appendix F
Resilient Modulus Test Results

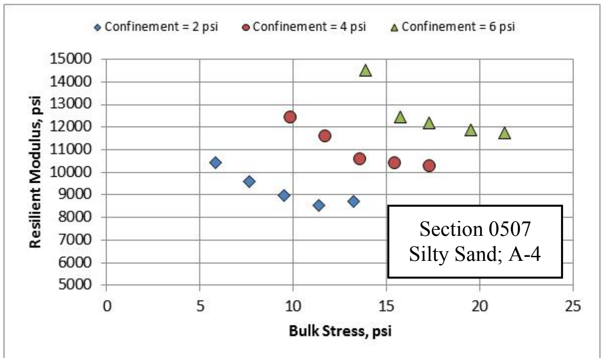

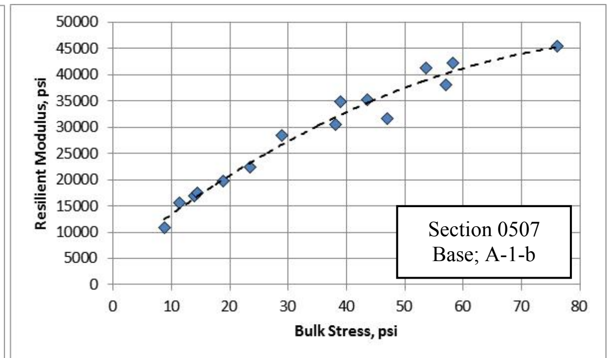

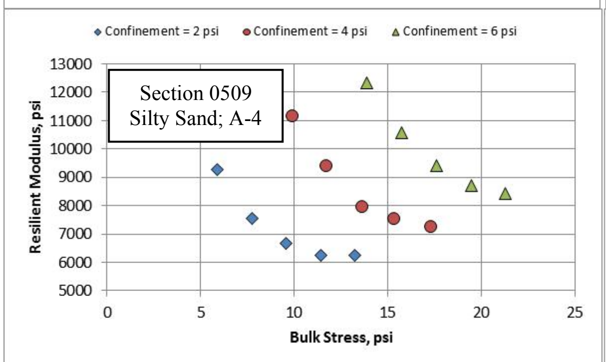

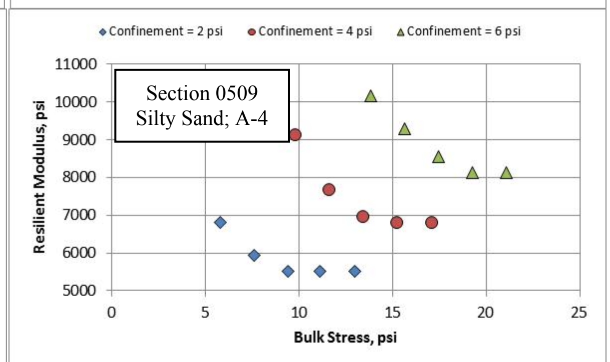

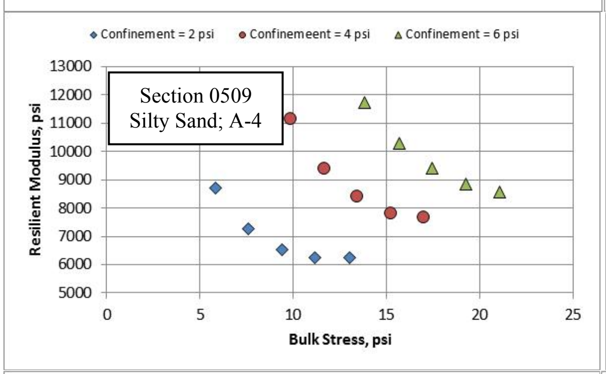

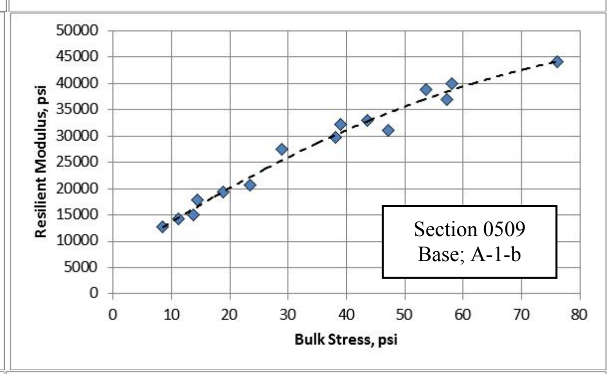

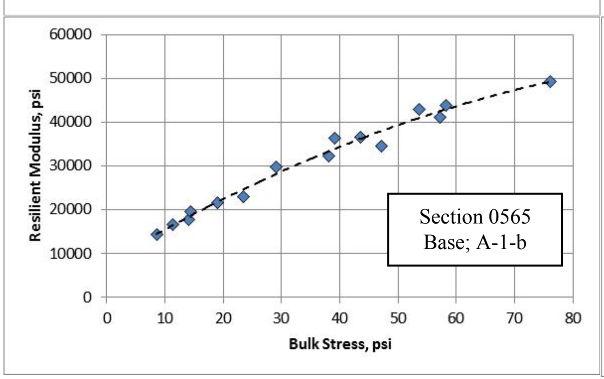

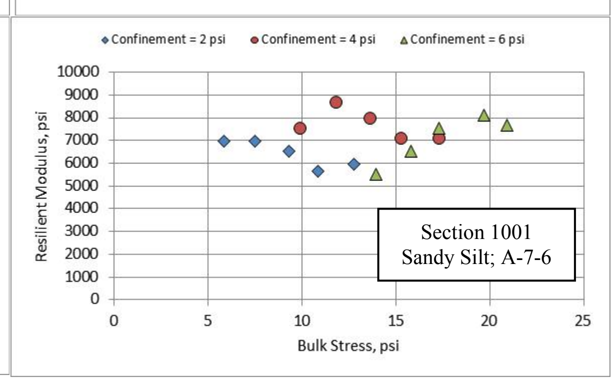

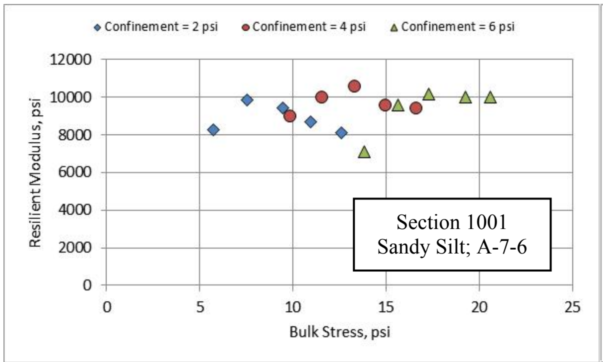
Confinement = 2 psi
Confinement = 4 psi
Confinement = 6 psi
Resilient Modulus, psi
Bulk Stress, psi
Section 1001
Sandy Silt; A-7-6

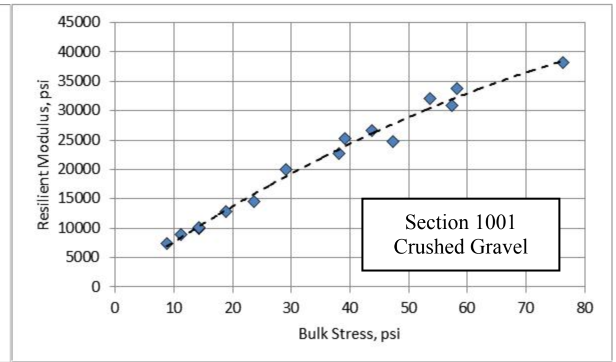
Resilient Modulus, psi
Bulk Stress, psi
Section 1001
Crushed Gravel

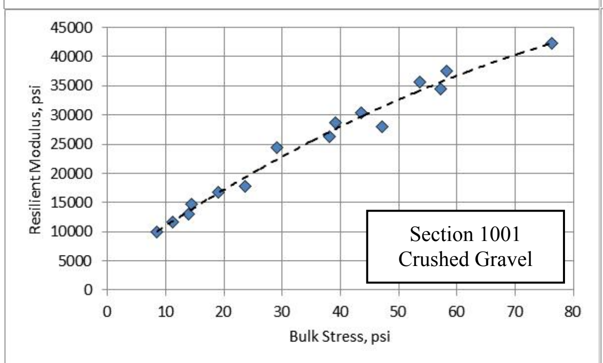
Resilient Modulus, psi
Bulk Stress, psi
Section 1001
Crushed Gravel

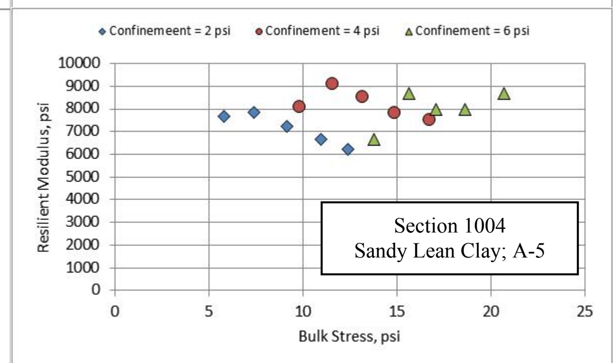
Confinemeent = 2 psi
Confinement = 4 psi
Confinement = 6 psi
Resilient Modulus, psi
Bulk Stress, psi
Section 1004
Sandy Lean Clay; A-5

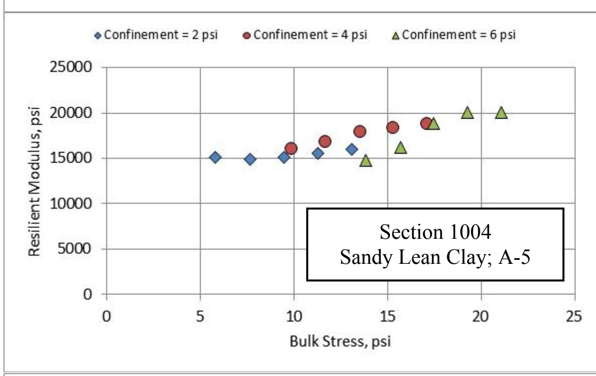
Confinement = 2 psi
Confinement = 4 psi
Confinement = 6 psi
Resilient Modulus, psi
Bulk Stress, psi
Section 1004
Sandy Lean Clay; A-5

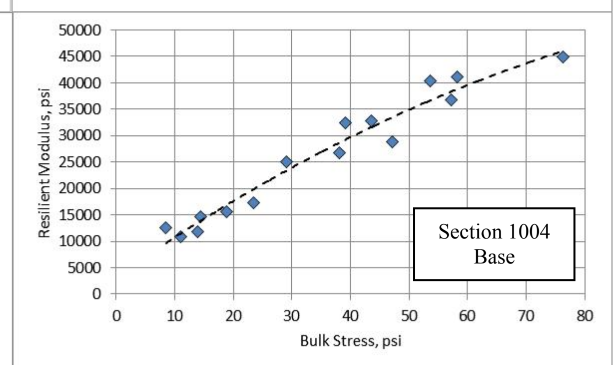
Resilient Modulus, psi
Bulk Stress, psi
Section 1004
Base

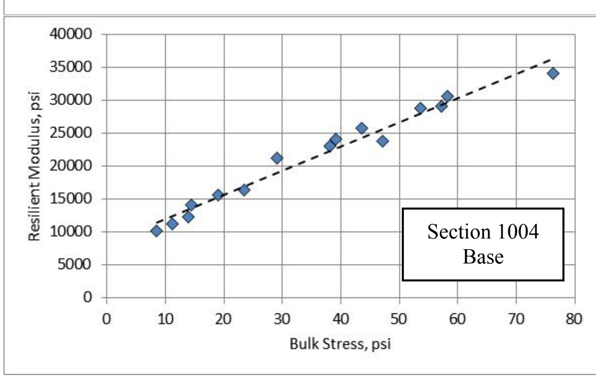
Resilient Modulus, psi
Bulk Stress, psi
Section 1004
Base

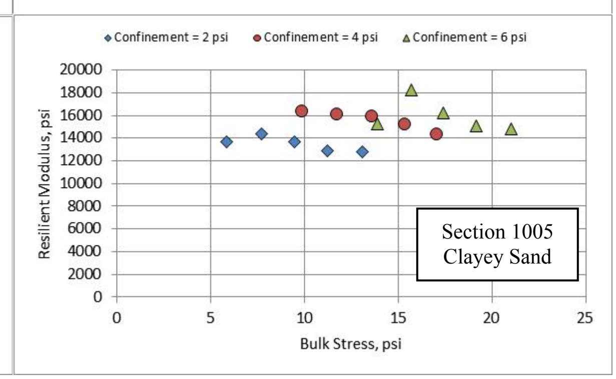
Confinement = 2 psi
Confinement = 4 psi
Confinement = 6 psi
Resilient Modulus, psi
Bulk Stress, psi
Section 1005
Clayey Sand

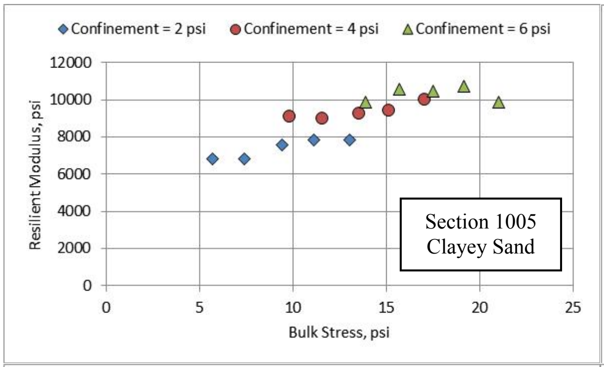
Confinement = 2 psi
Confinement = 4 psi
Confinement = 6 psi
Resilient Modulus, psi
Bulk Stress, psi
Section 1005
Clayey Sand

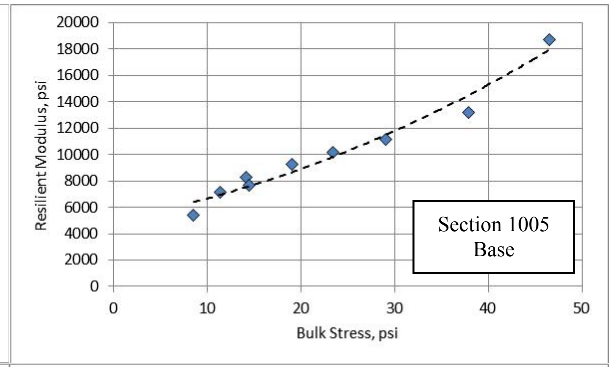
Resilient Modulus, psi
Bulk Stress, psi
Section 1005
Base

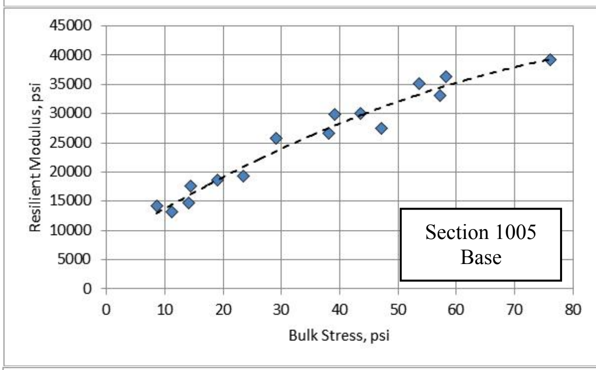
Resilient Modulus, psi
Bulk Stress, psi
Section 1005
Base

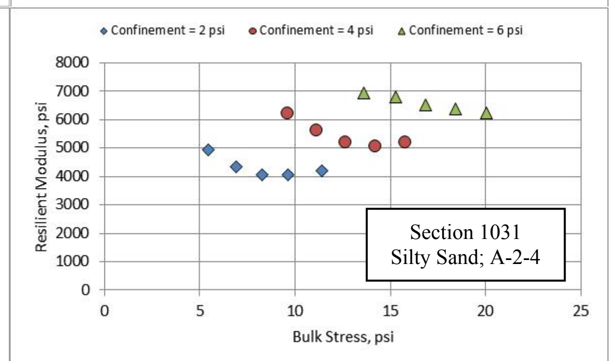
Confinement = 2 psi
Confinement = 4 psi
Confinement = 6 psi
Resilient Modulus, psi
Bulk Stress, psi
Section 1031
Silty Sand; A-2-4

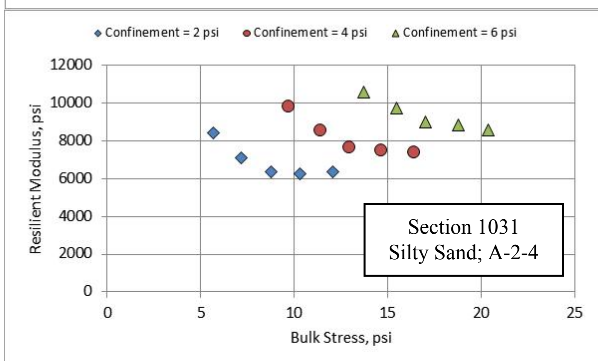
Confinement = 2 psi
Confinement = 4 psi
Confinement = 6 psi
Resilient Modulus, psi
Bulk Stress, psi
Section 1031
Silty Sand; A-2-4

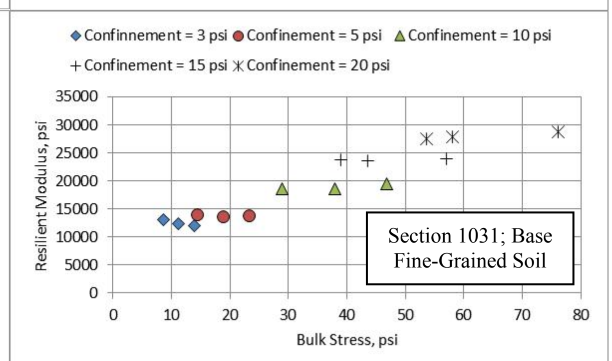
Confinnement = 3 psi
Confinement = 5 psi
Confinement = 10 psi
Confinement = 15 psi
Confinement = 20 psi
Resilient Modulus, psi
Bulk Stress, psi
Section 1031; Base
Fine-Grained Soil

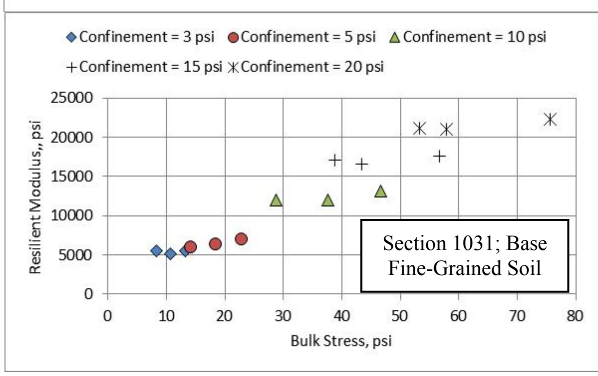
Confinement = 3 psi
Confinement = 5 psi
Confinement = 10 psi
Confinement = 15 psi
Confinement = 20 psi
Resilient Modulus,, psi
Bulk Stress, psi
Section 1031; Base
Fine-Grained Soil

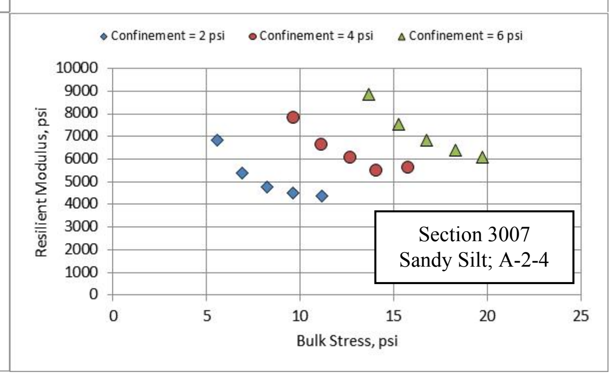
Confinement = 2 psi
Confinement = 4 psi
Confinement = 6 psi
Resilient Modulus, psi
Bulk Stress, psi
Section 3007
Sandy Silt; A-2-4

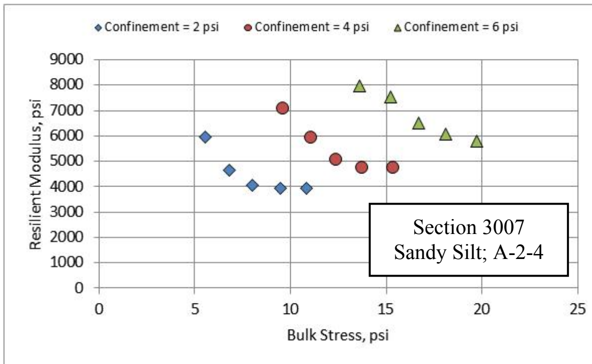
Confinement = 2 psi
Confinement = 4 psi
Confinement = 6 psi
Resilient Modulus, psi
Bulk Stress, psi
Section 3007
Sandy Silt; A-2-4

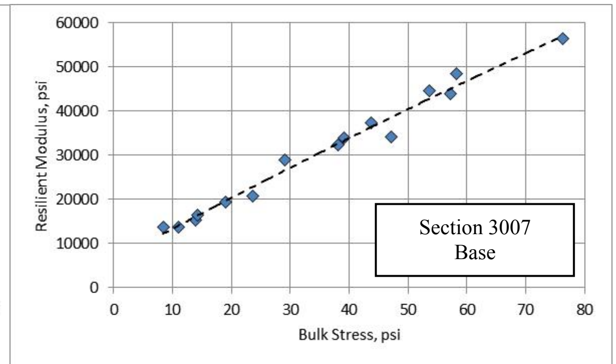
Resilient Modulus, psi
Bulk Stress, psi
Section 3007
Base

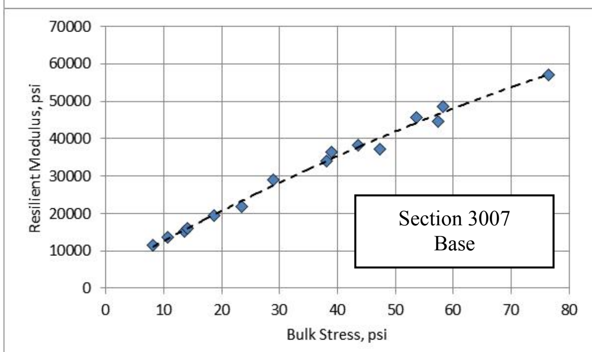
Resilient Modulus, psi
Bulk Stress, psi
Section 3007
Base

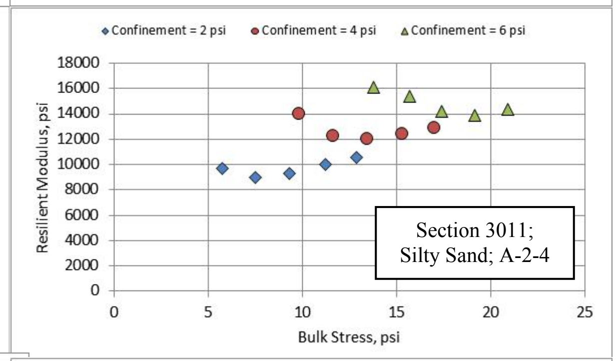
Confinement = 2 psi
Confinement = 4 psi
Confinement = 6 psi
Resilient Modulus, psi
Bulk Stress, psi
Section 3011;
Silty Sand; A-2-4

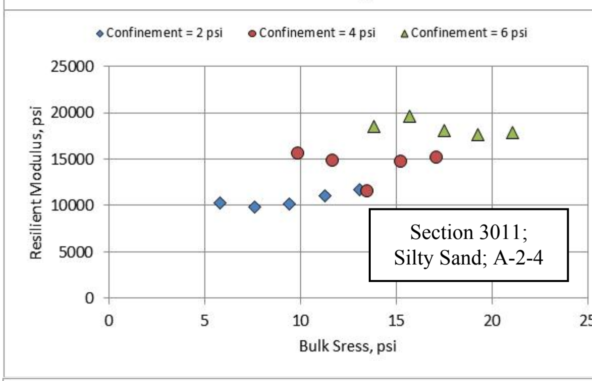
Confinement = 2 psi
Confinement = 4 psi
Confinement = 6 psi
Resilient Modulus, psi
Bulk Sress, psi
Section 3011;
Silty Sand; A-2-4

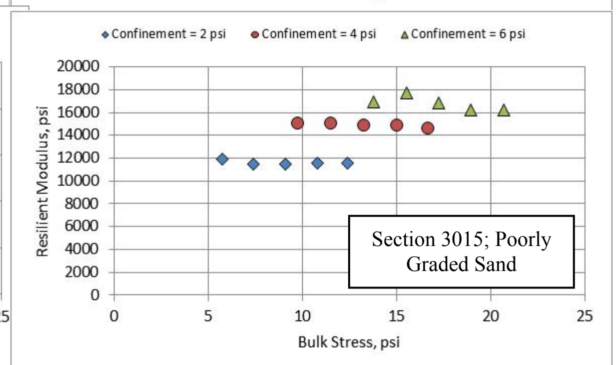
Confinement = 2 psi
Confinement = 4 psi
Confinement = 6 psi
Resilient Modulus, psi
Bulk Stress, psi
Section 3015; Poorly
Graded Sand

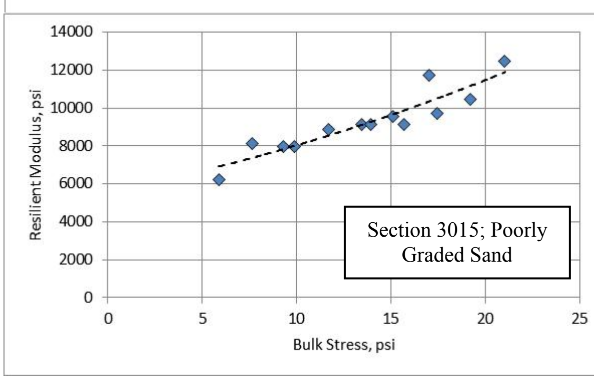
Resilient Modulus, psi
Bulk Stress, psi
Section 3015; Poorly
Graded Sand

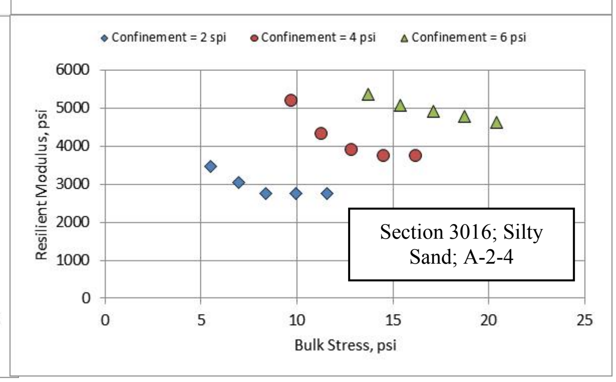
Confinement = 2 spi
Confinement = 4 psi
Confinement = 6 psi
Resilient Modulus, psi
Bulk Stress, psi
Section 3016; Silty
Sand; A-2-4

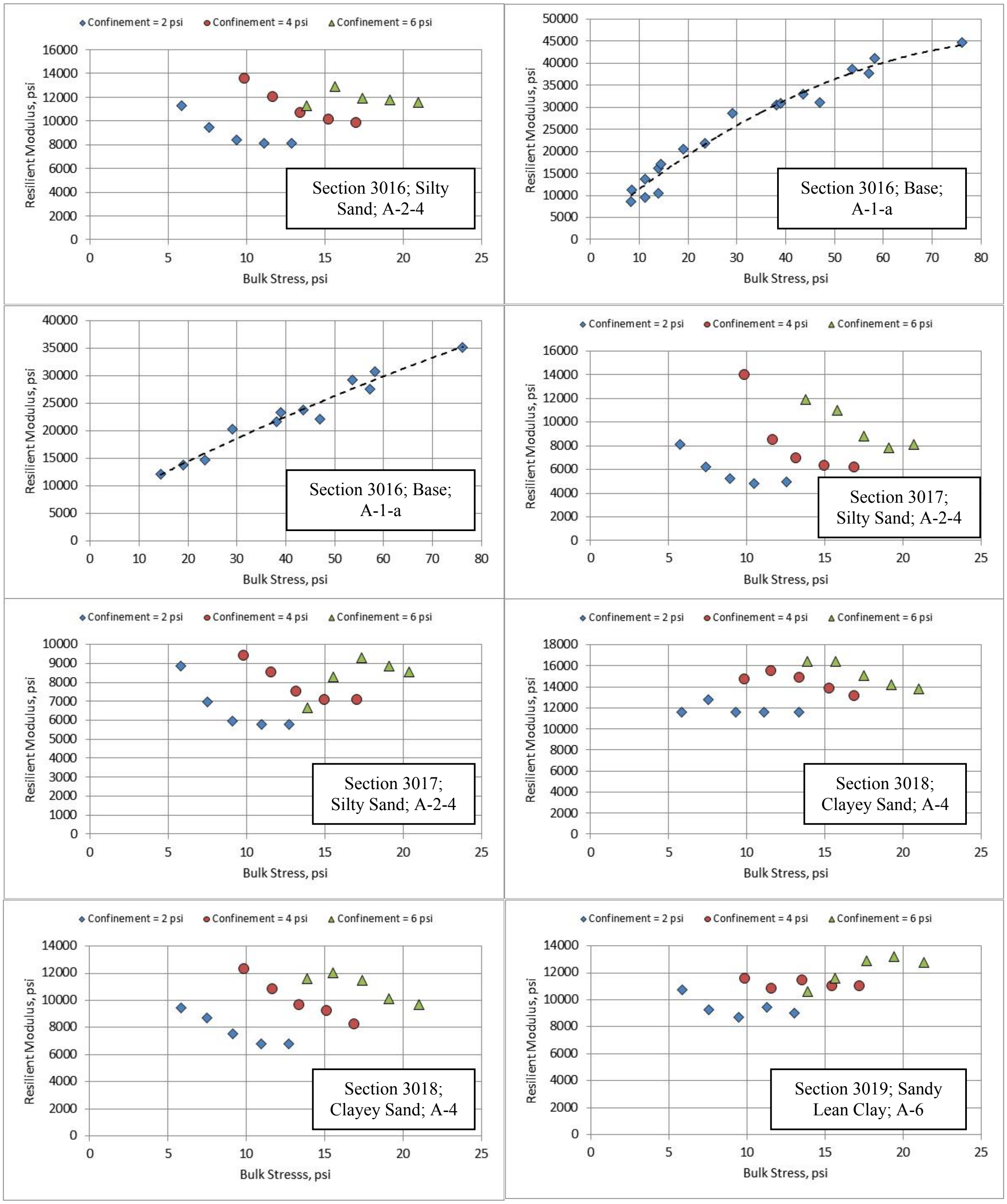
Confinement = 2 psi
Confinement = 4 psi
Confinement = 6 psi
Resilient Modulus, psi
Bulk Stress, psi
Section 3016; Silty Sand; A-2-4
Resilient Modulus, psi
Bulk Stress, psi
Section 3016; Base; A-1-a
Resilient Modulus, psi
Bulk Stress, psi
Section 3016; Base; A-1-a
Confinement = 2 psi
Confinement = 4 psi
Confinement = 6 psi
Resilient Modulus, psi
Bulk Stress, psi
Section 3017; Silty Sand; A-2-4
Confinement = 2 psi
Confinement = 4 psi
Confinement = 6 psi
Resilient Modulus, psi
Bulk Stress, psi
Section 3017; Silty Sand; A-2-4
Confinement = 2 psi
Confinement = 4 psi
Confinement = 6 psi
Resilient Modulus, psi
Bulk Stress, psi
Section 3018; Clayey Sand; A-4
Confinement = 2 psi
Confinement = 4 psi
Confinement = 6 psi
Resilient Modulus, psi
Bulk Stresss, psi
Section 3018; Clayey Sand; A-4
Confinement = 2 psi
Confinement = 4 psi
Confinement = 6 psi
Resilient Modulus, psi
Bulk Stress, psi
Section 3019; Sandy Lean Clay; A-6

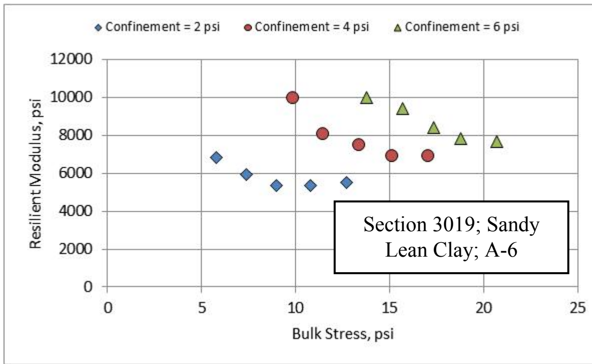
Confinement = 2 psi
Confinement = 4 psi
Confinement = 6 psi
Resilient Modulus, psi
Bulk Stress, psi
Section 3019; Sandy Lean Clay; A-6

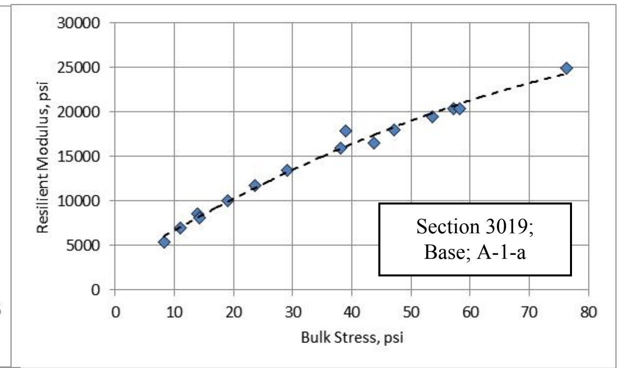
Resilient Modulus, psi
Bulk Stress, psi
Section 3019; Base; A-1-a

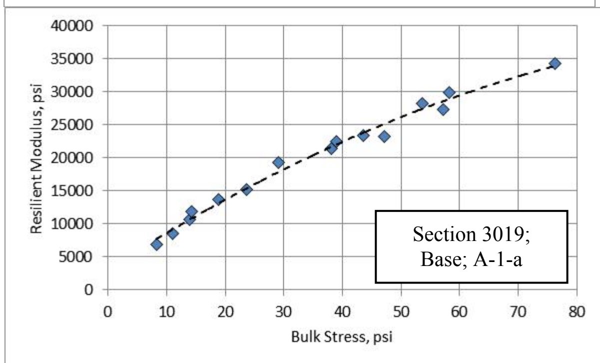
Resilient Modulus, psi
Bulk Stress, psi
Section 3019; Base; A-1-a

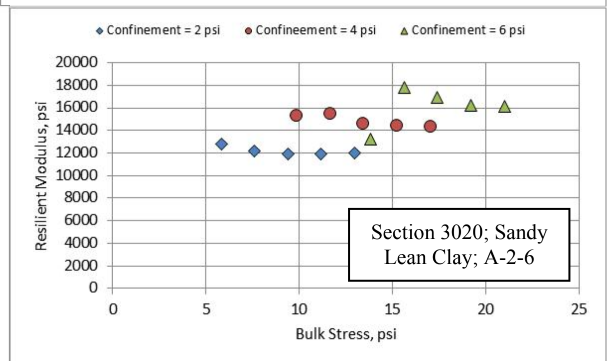
Confinement = 2 psi
Confineement = 4 psi
Confinement = 6 psi
Resilient Modulus, psi
Bulk Stress, psi
Section 3020; Sandy Lean Clay; A-2-6

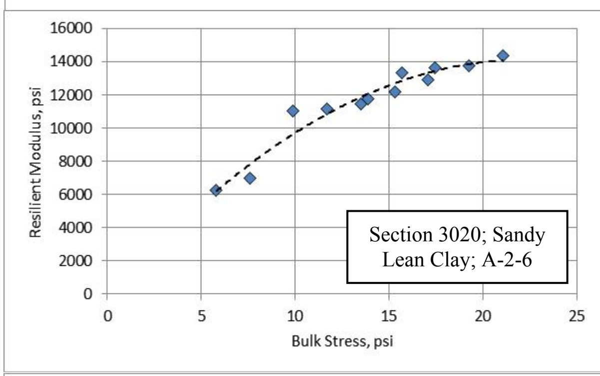
Resilient Modulus, psi
Bulk Stress, psi
Section 3020; Sandy Lean Clay; A-2-6

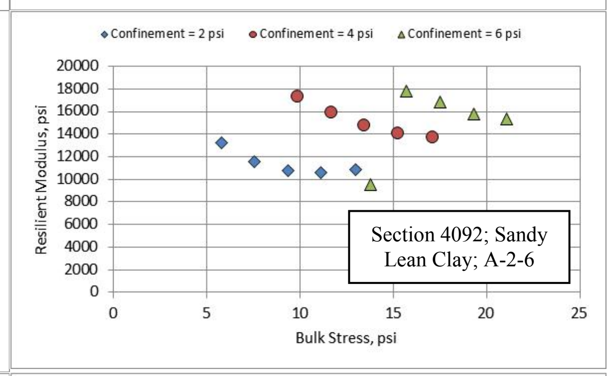
Confinement = 2 psi
Confinement = 4 psi
Confinement = 6 psi
Resilient Modulus, psi
Bulk Stress, psi
Section 4092; Sandy Lean Clay; A-2-6

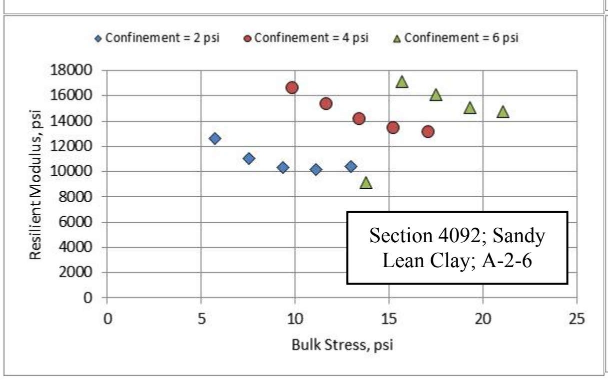
Confinement = 2 psi
Confinement = 4 psi
Confinement = 6 psi
Resilient Modulus, psi
Bulk Stress, psi
Section 4092; Sandy Lean Clay; A-2-6

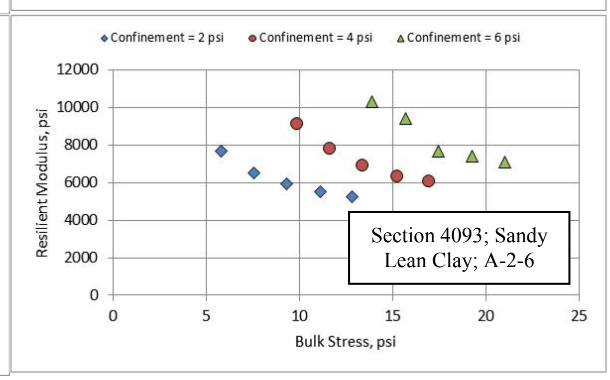
Confinement = 2 psi
Confinement = 4 psi
Confinement = 6 psi
Resilient Modulus, psi
Bulk Stress, psi
Section 4093; Sandy Lean Clay; A-2-6

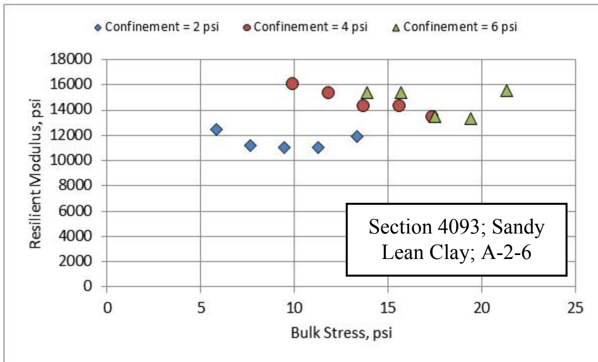
Confinement = 2 psi
Confinement = 4 psi
Confinement = 6 psi
Resilient Modulus, psi
Bulk Stress, psi
Section 4093; Sandy Lean Clay; A-2-6

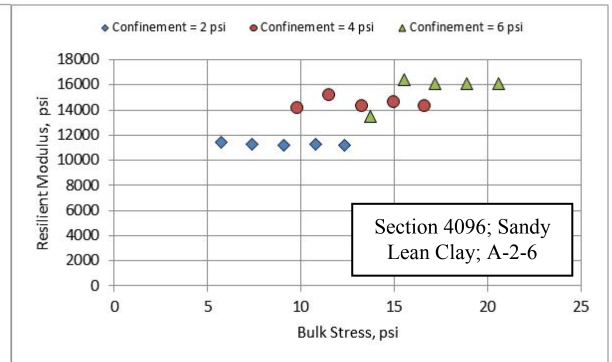
Confinement = 2 psi
Confinement = 4 psi
Confinement = 6 psi
Resilient Modulus, psi
Bulk Stress, psi
Section 4096; Sandy Lean Clay; A-2-6

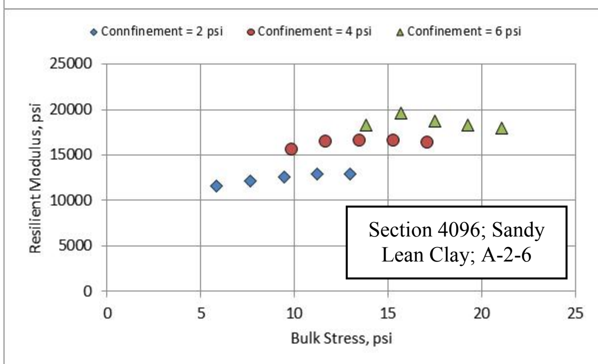
Connfinement = 2 psi
Confinement = 4 psi
Confinement = 6 psi
Resilient Modulus, psi
Bulk Stress, psi
Section 4096; Sandy Lean Clay; A-2-6

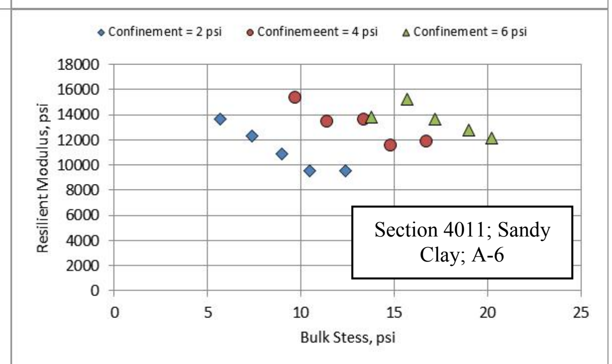
Confinement = 2 psi
Confinemeent = 4 psi
Confinement = 6 psi
Resilient Modulus, psi
Bulk Stess, psi
Section 4011; Sandy Clay; A-6

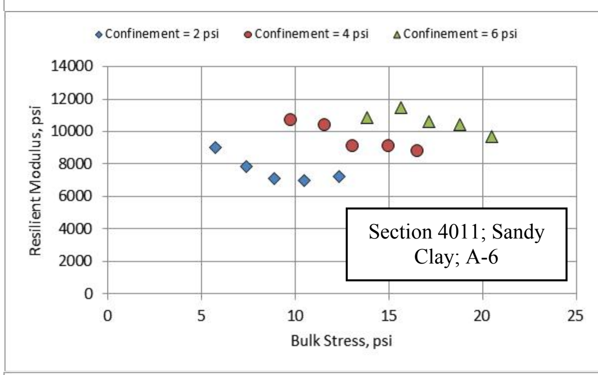
Confinement = 2 psi
Confinement = 4 psi
Confinement = 6 psi
Resilient Modulus, psi
Bulk Stress, psi
Section 4011; Sandy Clay; A-6

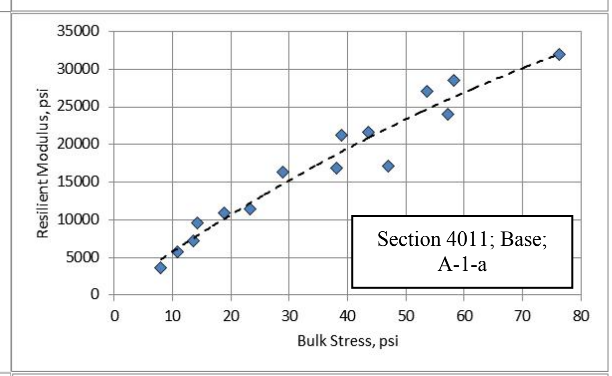
Resilient Modulus, psi
Bulk Stress, psi
Section 4011; Base; A-1-a

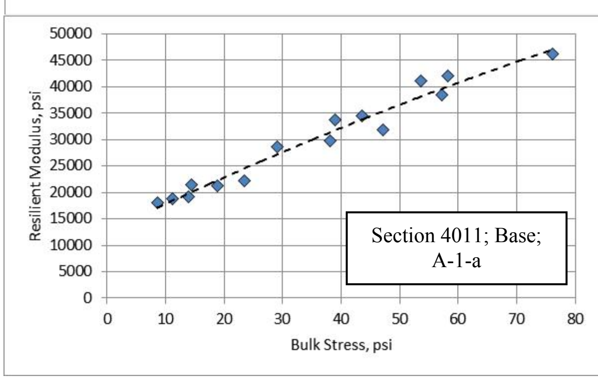
Resilient Modulus, psi
Bulk Stress, psi
Section 4011; Base; A-1-a

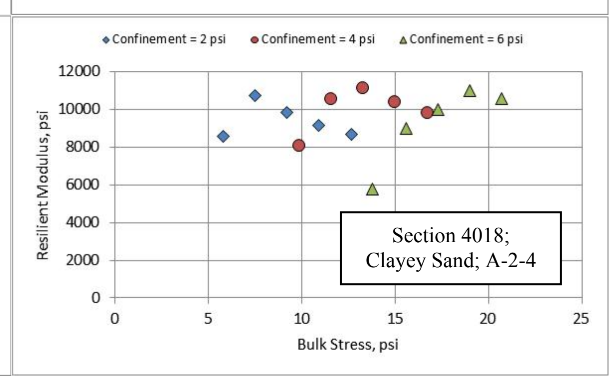
Confinement = 2 psi
Confinement = 4 psi
Confinement = 6 psi
Resilient Modulus, psi
Bulk Stress, psi
Section 4018; Clayey Sand; A-2-4

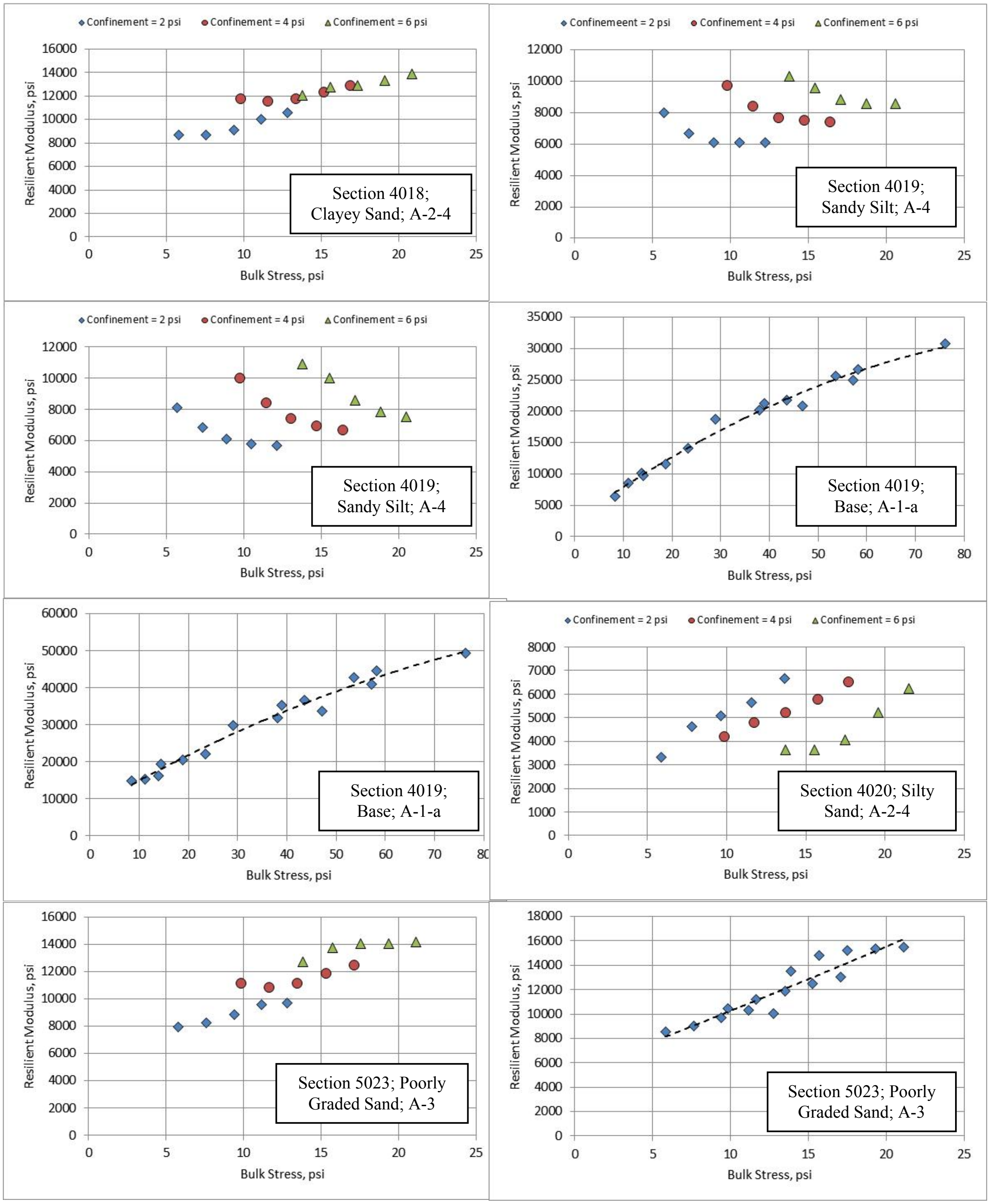
Confinement = 2 psi
Confinement = 4 psi
Confinement = 6 psi
Resilient Modulus, psi
Bulk Stress, psi
Section 4018; Clayey Sand; A-2-4
Confinemeent = 2 psi
Confinement = 4 psi
Confinement = 6 psi
Section 4019; Sandy Silt; A-4
Section 4019; Sandy Silt; A-4
Section 4019; Base; A-1-a
Section 4019; Base; A-1-a
Section 4020; Silty Sand; A-2-4
Section 5023; Poorly Graded Sand; A-3
Section 5023; Poorly Graded Sand; A-3

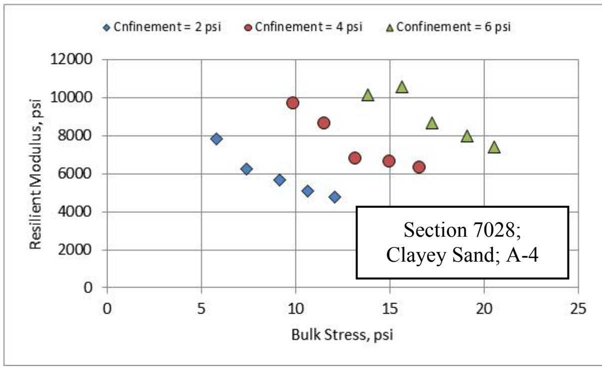
Cnfinement = 2 psi
Cnfinement = 4 psi
Confinement = 6 psi
Resilient Modulus, psi
Bulk Stress, psi
Section 7028;
Clayey Sand; A-4

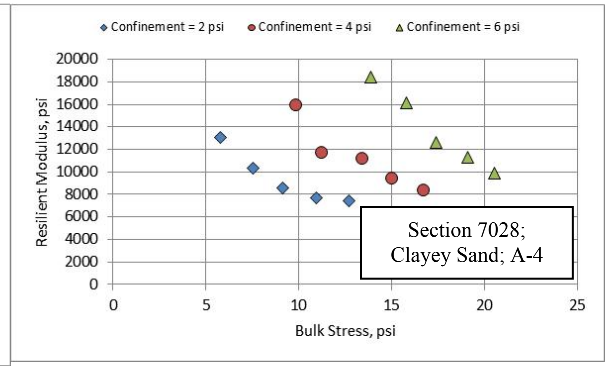
Confinement = 2 psi
Confinement = 4 psi
Confinement = 6 psi
Resilient Modulus, psi
Bulk Stress, psi
Section 7028;
Clayey Sand; A-4

This page left blank intentionally.